

เตตระแอนไอออนคาบิกซ์[4]เอรีนฟลูออโรฟอร์ที่ละลายน้ำได้สำหรับการตรวจวัด Fe^{2+} และ Fe^{3+}

นางสาวยมลพร ยอดตา

วิทยานิพนธ์นี้เป็นส่วนหนึ่งของการศึกษาตามหลักสูตรปริญญาวิทยาศาสตรมหาบัณฑิต

สาขาวิชาเคมี ภาควิชาเคมี

คณะวิทยาศาสตร์ จุฬาลงกรณ์มหาวิทยาลัย

ปีการศึกษา 2553

ลิขสิทธิ์ของจุฬาลงกรณ์มหาวิทยาลัย

WATER SOLUBLE TETRA-ANIONIC CALIX[4]ARENE FLUOROPHORE FOR
SELECTIVE SENSING OF Fe^{2+} AND Fe^{3+}

Miss Yamonporn Yodta

A Thesis Submitted in Partial Fulfillment of the Requirements
for the Degree of Master of Science Program in Chemistry

Department of Chemistry

Faculty of Science

Chulalongkorn University

Academic Year 2010

Copyright of Chulalongkorn University

Thesis Title WATER SOLUBLE TETRA-ANIONIC CALIX[4]ARENE
FLUOROPHORE FOR SELECTIVE SENSING OF Fe²⁺
AND Fe³⁺
By Miss Yamonporn Yodta
Field of Study Chemistry
Thesis Advisor Associate Professor Mongkol Sukwattanasinitt, Ph.D.

Accepted by the Faculty of Science, Chulalongkorn University in Partial
Fulfillment of the Requirements for the Master's Degree

..... Dean of the Faculty of Science
(Professor Supot Hannongbua, Dr.rer.nat.)

THESIS COMMITTEE

..... Chairman
(Associate Professor Sirirat Kokpol, Ph.D.)

..... Thesis Advisor
(Associate Professor Mongkol Sukwattanasinitt, Ph.D.)

..... Examiner
(Professor Thawatchai Tuntulani, Ph.D.)

..... Examiner
(Assistant Professor Paitoon Rashatasakhon, Ph.D.)

..... External Examiner
(Poonsakdi Ploypradith, Ph.D.)

ยมลพร ยอดตา : เตตระแอนไอออนคาลิกซ์[4]เอรีนฟลูออโรฟออร์ที่ละลายน้ำได้สำหรับการตรวจวัด Fe^{2+} และ Fe^{3+} . (WATER SOLUBLE TETRA-ANIONIC CALIX[4]ARENE FLUOROPHORE FOR SELECTIVE SENSING OF Fe^{2+} AND Fe^{3+}) อ.ที่ปรึกษาวิทยานิพนธ์หลัก : รศ.ดร.มงคล สุขวัฒนาสินธิ์, 72 หน้า.

ได้สังเคราะห์อนุพันธ์ที่ละลายน้ำได้ของ 1,3-อัลเทอเนตคาลิกซ์[4]เอรีนที่ประกอบด้วยเอไทน์นิต เบนโซอิกเอซิด 4 หมู่ ด้วยปฏิกิริยาควบไซโนกาซิทาที่ใช้คอปเปอร์-แพลเลเดียมเป็นตัวเร่งปฏิกิริยาระหว่าง 1,3-อัลเทอเนต เทตระไอโอดคาลิกซ์[4]เอรีน และ 4-เอไทน์นิต เบนโซอิกเอซิด จากนั้นทำการไฮโดรไลซ์หมู่เอสเตอร์ทั้ง 4 หมู่ด้วยเบส ซึ่งสารละลายของสารที่สังเคราะห์ได้ในตัวทำละลายไดเมทิลซัลโฟลค์ไซดีให้ค่าการดูดกลืนแสงและค่าการคายแสงสูงสุดที่ 317 และ 418 นาโนเมตร ตามลำดับ และมีประสิทธิภาพในการเรืองแสงเท่ากับ 0.36 ซึ่งใกล้เคียงกับโมเลกุลตั้งต้นที่มีหมู่เอสเตอร์ทั้ง 4 หมู่ ($\Phi = 0.40$) อย่างไรก็ตาม ในสารละลายฟอสเฟตบัฟเฟอร์ pH 8 สารเตตระคาร์บอกซิลิกมีค่าประสิทธิภาพในการเรืองแสงเพียง 0.006 เนื่องจากกระบวนการไฮเดรชันสามารถทำให้โมเลกุลที่สภาวะกระตุ้นแบบมีการถ่ายเทประจุ (ICT state) มีความเสถียรเพิ่มขึ้นได้ ประสิทธิภาพในการเรืองแสงในน้ำสามารถทำให้เพิ่มขึ้นได้ด้วยการเติมสารลดแรงตึงผิวประเภทที่ไม่มีประจุ Brij 58 เนื่องจากสารลดแรงตึงผิวสามารถลดการเกิดไฮเดรชันได้ ซึ่งสัญญาณการเรืองแสงในระบบที่มี Brij 58 นี้ สามารถตรวจจับได้อย่างจำเพาะด้วยไอออนของ Fe^{2+} และ Fe^{3+} โดยมีค่าคงที่ในการจับสัญญาณมีค่าเท่ากับ $3.5 \times 10^4 M^{-1}$ และ $8.6 \times 10^3 M^{-1}$ ตามลำดับ

ภาควิชา เคมี.....ลายมือชื่อ.....
 สาขาวิชา เคมี.....ลายมือชื่อ.....
 ปีการศึกษา 2553.....

5072595323 : MAJOR CHEMISTRY

KEYWORDS : CALIX[4]ARENE / ION RECOGNITION

YAMONPORN YODTA : WATER SOLUBLE TETRA-ANIONIC CALIX[4]ARENE FLUOROPHORE FOR SELECTIVE SENSING OF Fe^{2+} AND Fe^{3+} . THESIS ADVISOR : ASSOC. PROF. MONGKOL SUKWATTASINITT, Ph.D., 72 pp.

Water soluble 1,3-alternate calix[4]arene containing four ethynylbenzoic acid is synthesized through a Sonogashira copper-palladium catalyzed coupling reaction between 1,3-alternate tetraiodocalix[4]arene and 4-ethynylbenzoate followed by base catalyzed hydrolysis of the four ester groups. In dimethylsulfoxide solution, the synthesized compound exhibit maximum absorption and emission at 317 and 418 nm, respectively, with high quantum efficiency of 0.36 comparable to the tetraester precursor ($\Phi = 0.40$). The tetracarboxylic compound however gives low quantum efficiency of 0.6% in phosphate buffer pH 8 solution due to hydration stabilizing internal charge-transfer (ICT) state. The quantum efficiency in aqueous media can be improved by nonionic surfactant Brij 58 due to reducing hydration around the fluorophores. The fluorescence signal of the phosphate buffer solution of the compound in the presence of Brij 58 is selectively quenched by Fe^{2+} and Fe^{3+} with different Stern-Volmer constant (K_{sv}) of $3.5 \times 10^4 \text{ M}^{-1}$ and $8.6 \times 10^3 \text{ M}^{-1}$, respectively.

Department : Chemistry Student's Signature :

Field of Study : Chemistry Advisor's Signature :

Academic Year : 2010

ACKNOWLEDGEMENTS

I wish to express my deep gratitude to my advisor, Associate Professor Dr. Mongkol Sukwattanasinitt, for his generous assistance, invaluable guidance and encouragement throughout the course of this research.

I would like to gratefully acknowledge the committee, Associate Professor Dr. Sirirat Kokpol, Professor Dr. Thawatchai Tuntulani, Assistant Professor Dr. Paitoon Rashatasakhon and Dr. Poonsakdi Ploypradith for their comments, guidance and extending cooperation over my presentation. I would like to thank Dr. Anawat Ajawachom and Dr. Sumrit Wacharasindhu for his attention and suggestion during our group meeting. I would like to thank Associate Professor Dr. Sanong Ekgasit for permission to use IR instrument.

I would like to express my gratitude to Organic Synthesis Research Unit (OSRU), Department of Chemistry, Faculty of Science, Chulalongkorn University for providing the chemicals and facilities throughout the course of study.

A deep affectionate gratitude is acknowledged to my beloved family for their understanding, encouragement and support throughout the education course. I especially thank Mr. Wutthichai Reainthippayasakul, Dr. Chantana Sae-Lim, Ms. Radeemada Mungkarndee, Ms. Warathip Siripornnoppakhun and Mr. Thirawat Sirijindalert for their suggestion and guidance. I would like to thank Mr. Thanesuan Nuanyai, Mr. Nakorn Niamnont, Ms. Wisuttaya Worawalai and Mr. Nopporn Earmrattana for their technical assistance. I also appreciate and would like to thank Mr. Akachai Khumsri for photophysical property study with spectrofluorometer. I would like to thank all of my friends for their friendship, especially Ms. Pagasukon, Mr. Chaiwat Phollookin, Mr. Thanakrit Chantra and Ms. Suricha Pumtang for their help during the course of my graduate research. Moreover, I would like to thank Mr. Watcharin Ngampueng, Ms. Nattaporn Kimpitak, Ms. Daranee Homrarueng, Ms. Wannapa Yuanboonlim and Ms. Wanwisa Thongmalai for their suggestion and encouragement.

Finally, I would like to thank Center for Petroleum, Petrochemicals and Advanced Materials and my financial support from the TRF-Master Research Grants under Thailand Research Fund (TRF), ADB under the Petroleum & Petrochemical Technology Consortium and 90th anniversary of Chulalongkorn University Fund.

CONTENTS

	Page
ABSTRACT (THAI)	iv
ABSTRACT (ENGLISH)	v
ACKNOWLEDGEMENTS	vi
CONTENTS	vii
LIST OF TABLES	x
LIST OF FIGURES	xi
LIST OF SCHEMES	xv
LIST OF ABBREVIATIONS	xvi
CHAPTER	
I INTRODUCTION	1
1.1 Supramolecular chemistry.....	1
1.2 Calix[4]arene.....	1
1.3 Water soluble calix[4]arene.....	2
1.4 Fluorescence chemosensor.....	5
1.5 Iron sensor.....	14
1.6 Objectives of this research.....	19
II EXPERIMENTAL	20
2.1 Materials and chemicals.....	20
2.2 Analytical instruments.....	20
2.3 Synthesis of 25,26,27,28-tetrabenzoyloxy-4-ethynylbenzoic acid calix[4]arene.....	21
2.3.1 Preparation of <i>p-tert</i> -butyl calix[4]arene.....	21
2.3.2 Preparation of calix[4]arene.....	22
2.3.3 Preparation of 25,26,27,28-tetrabenzoyloxy-calix[4]arene (1).....	23
2.3.4 Preparation of 25,26,27,28-tetrabenzoyloxy-4-iodo calix[4]arene (2).....	24

	Page
2.3.5 Preparation of 25,26,27,28-tetrabenzoyloxy-4-ethynyl benzoic methyl ester calix[4]arene (3).....	25
2.3.6 Preparation of 25,26,27,28-tetrabenzoyloxy-4-ethynyl benzoic acid calix[4]arene (4).....	26
2.4 Photophysical properties study.....	27
2.4.1 UV-Visible spectroscopy.....	27
2.4.2 Fluorescence spectroscopy.....	27
2.4.3 Fluorescence quantum yields.....	27
2.5 Fluorescent sensor study.....	28
2.5.1 Surfactant enhancement.....	28
2.5.2 Metal ion sensor.....	28
2.6 Synthesis of stilbene-bridged calix[4]arene.....	29
2.6.1 Preparation of <i>p</i> -nitrocalix[4]arene (5).....	29
2.6.2 Preparation of 3-(2-bromoethoxy)benzaldehyde (6).....	30
2.6.3 Preparation of <i>m</i> -bisbenzaldehyde- <i>p</i> -nitrocalix[4]arene (7).....	31
2.7 Synthesis of diacetylene calix[4]arene.....	32
2.7.1 Preparation of tetra(propargyloxy)- <i>tert</i> -butyl calix[4]arene (8).....	32
2.7.2 Preparation of methyl-6-iodoheptynoate (9).....	33
2.7.3 Preparation of 25,26,27,28-tetra(methylheptynoate)oxy- <i>tert</i> -calix[4]arene (10).....	34
III RESULTS AND DISCUSSION	35
3.1 Synthesis and characterization of 25,26,27,28-tetrabenzoyloxy-4-ethynylbenzoic acid calix[4]arene (4).....	35
3.2 Photophysical property study.....	40
3.3 Surfactant enhancement of 25,26,27,28-tetrabenzoyloxy-4-ethynylbenzoic acid calix[4]arene (4).....	42
3.4 Metal ion sensor.....	40
3.5 Synthesis attempt of stilbene-bridge calix[4]arene.....	49

	Page
3.6 Synthesis attempt of diacetylene calix[4]arene.....	51
IV CONCLUSION	54
4.1 Conclusion.....	55
4.2 Suggestion for future work.....	55
REFERENCES	56
APPENDIX	62
VITAE	72

LIST OF TABLES

Table		Page
3.1	Elemental (C, H, N) analysis and HRMS mass spectrometry of compound 1-4	39
3.2	Photophysical properties of compound 3 in DMSO and compound 4 in DMSO and 50 mM phosphate buffer pH 8.0.....	41
3.3	Photophysical properties of compound 4 in 50 mM phosphate buffer pH 8.0 in the presence of Brij 58 compared with compound 4 in 50 mM phosphate buffer pH 8.0 in the absence of Brij 58.....	46

LIST OF FIGURES

Figure		Page
1.1	Calix[4]arene conformations.....	2
1.2	Water soluble calix[4]arenes 1 with chromophores (“antenna”) attached to the lower rim.....	3
1.3	Structures of calix[4]arene and thiacalix[4]arene containing hydroxyl, carboxy, sulfato or diethanolamino groups at the para position of the phenolic ring and/or on the benzo-ether moieties.....	3
1.4	Structures of calix[4]arene and thiacalix[4]arene containing sulfonate groups.....	4
1.5	Structures of calix[4]arene derivative containing with carboxylate and sulfonate groups.....	4
1.6	Proposed conformational changes of 1 and 2 upon complex formation with Pb^{2+} and with In^{3+}	6
1.7	Conformational changes of fluorescence chemosensors 11 upon complex formation with Pb^{2+} , Cu^{2+} and K^{+}	7
1.8	Complexation of fluorescence chemosensors 12 with Hg^{2+} <i>via</i> fluorescence resonance energy transfer.....	7
1.9	(a) Structure of calix-di-imine derivative, $R=tert$ -butyl 13 and (b) Relative fluorescence intensity at the metal ion to ligand in the titration of calix-di-imine derivative 13 with different metal ions.....	8
1.10	(a) Structure of the anthracene-anchored 1,3-di-derivatives of lower rim calix[4]arene, $R=tert$ -butyl 14 and (b) Fluorescence spectra of 14 / M^{2+} ratio being 1:50 (excitation wavelength of 340 nm).....	9
1.11	Structure of calix[4]arene-diamide derivative bearing with phenanthroimidazole subunit.....	9
1.12	Complexation of fluorescence chemosensor 16 with metal ion (Cd^{2+} and Zn^{2+}) <i>via</i> excimer formation and extinction mechanism.....	10

Figure	Page
1.13	Structure of bis-(2-picolyl)amine based on calix[4]arene (R= <i>tert</i> -butyl)..... 10
1.14	Structure of an unsymmetrical 1,3-alternate calix[4]biscrown..... 11
1.15	Structure of 1,3-alternate calix[4]arene having bispyrenylamide and carboxylic acid..... 12
1.16	Structure of calix[4]arene derivatives with benzoxazol and benzothiazole units..... 12
1.17	A water soluble fluorescent dendritic compounds exhibited a highly selective fluorescence quenching by Hg ²⁺ ions in aqueous media in the presence of Triton X-100 surfactant..... 13
1.18	Structure of FD1..... 14
1.19	Structure of bis(7-methoxybenzofuran-2-yl)ketoxime (BFK) dye..... 15
1.20	Proposed mechanism of Fe ³⁺ -induced ring opening and fluorescent enhancement..... 15
1.21	Structure of glucose-based derivative..... 16
1.22	Structure of β -aminobisulfonate receptor linked naphthalene fluorophore..... 16
1.23	Structure of calcein blue..... 17
1.24	Structure of calcein..... 17
1.25	Schematic illustration of the interaction between probe I (pyren-TEMPO) and Fe(II)..... 18
1.26	Proposed binding mode and color change of fluoran dye with Fe ²⁺ 18
1.27	Schematic illustration for (a) Fe ²⁺ induced hydroxyl generation and QDs based sensor for Fe ²⁺ detection; (b) The fluorescence quenching mechanism by electron transfer from the QDs to hydroxyl radicals... 19
1.28	The target molecule..... 19
3.1	¹ H NMR spectra of compound 1-4 37
3.2	IR spectra of compound 1-4 38
3.3	Normalized spectral overlap between absorption (dashed line) and emission spectra (solid line) of compound 3 and 4 40
3.4	Proposed electronic energy levels of compound 4 in DMSO and phosphate buffer pH 8.0 41

Figure	Page
3.5	Table of 9 types of surfactants (3 anionic, 3 cationic, and 3 non-ionic) with the structure..... 43
3.6	Fluorescence intensity of compound 4 (1 μ M in 50 mM phosphate buffer pH 8.0) in the presence of 9 surfactants (0.1 mM) 43
3.7	Emission spectra of compound 4 (1 μ M in 50 mM phosphate buffer pH 8.0) with non-ionic surfactants (0.01 mM)..... 44
3.8	Normalized spectral overlap between absorption (dashed line) and emission spectra (solid line) of compound 4 45
3.9	Proposed electronic energy levels of compound 4 in phosphate buffer pH 8.0 in the absence and presence of Brij 58..... 45
3.10	Fluorescence spectra of 4 (1 μ M in 50 mM phosphate buffer pH 8.0) in the presence of metal ion (100 μ M) 46
A.1	^1H NMR of 25,26,27,28-tetrabenzoyloxy-calix[4]arene..... 63
A.2	^{13}C NMR of 25,26,27,28-tetrabenzoyloxy-calix[4]arene..... 63
A.3	^1H NMR of 25,26,27,28-tetrabenzoyloxy-4-iodocalix[4]arene..... 64
A.4	^{13}C NMR of 25,26,27,28-tetrabenzoyloxy-4-iodocalix[4]arene..... 64
A.5	^1H NMR of 25,26,27,28-tetrabenzoyloxy-4-ethynylbenzoic methyl ester calix[4]arene..... 65
A.6	^{13}C NMR of 25,26,27,28-tetrabenzoyloxy-4-ethynylbenzoic methyl ester calix[4]arene..... 65
A.7	^1H NMR of 25,26,27,28-tetrabenzoyloxy-4-ethynylbenzoic acid calix[4]arene..... 66
A.8	^{13}C NMR of 25,26,27,28-tetrabenzoyloxy-4-ethynylbenzoic acid calix[4]arene..... 66
A.9	^1H NMR of <i>m</i> -bisbenzaldehyde- <i>p</i> -nitrocalix[4]arene..... 67
A.10	^1H NMR of <i>p</i> -nitrocalix[4]arene..... 67
A.11	^{13}C NMR of <i>p</i> -nitrocalix[4]arene..... 67
A.12	^1H NMR of methyl-6-iodoheptynoate..... 68
A.13	^{13}C NMR of methyl-6-iodoheptynoate..... 68
A.14	^1H NMR of 25,26,27,28-tetra(methylheptynoate)oxy- <i>tert</i> -calix[4]arene..... 69

Figure		Page
A.15	Mass spectrum (ESI+) of 25,26,27,28-tetrabenzoyloxy-4-iodocalix[4]arene.....	70
A.16	Mass spectrum (ESI+) of 25,26,27,28-tetrabenzoyloxy-4-ethynylbenzoic methyl ester calix[4]arene.....	70
A.17	Mass spectrum (ESI+) of 25,26,27,28-tetrabenzoyloxy-4-ethynylbenzoic acid calix[4]arene.....	71

LIST OF SCHEMES

Scheme		Page
3.1	Synthesis of 25,26,27,28-tetrabenzoyloxy-4-ethynylbenzoic acid calix[4]arene.....	36
3.2	Retrosynthesis of stilbene-bridged calix[4]arene.....	49
3.3	Synthesis of mono-substitution <i>m</i> -benzaldehyde- <i>p</i> -nitro calix[4]arene.....	50
3.4	Retrosynthesis of dicetylene calix[4]arene.....	51
3.5	Synthesis of 25,26,27,28-tetra(methylheptynoate)oxy- <i>tert</i> -calix[4]arene.....	52

LIST OF ABBREVIATIONS

Ar	aromatic
calcd	calculated
^{13}C NMR	carbon-13 nuclear magnetic resonance
CDCl_3	deuterated chloroform
$\text{DMSO-}d_6$	deuterated dimethyl sulfoxide
DMSO	dimethylsulfoxide
d	doublet (NMR)
dd	doublet of doublet (NMR)
ESIMS	electrospray ionization mass spectrometry
equiv	equivalent (s)
FT-IR	fourier transform infrared spectroscopy
g	gram (s)
^1H NMR	proton nuclear magnetic resonance
Hz	Hertz
HRMS	high resolution mass spectrum
h	hour (s)
IR	infrared
<i>J</i>	coupling constant
mg	milligram (s)
mL	milliliter (s)
mmol	millimole (s)
<i>m/z</i>	mass per charge
m	multiplet (NMR)
M.W.	molecular weight
M	molar
MHz	megaHerz
rt	room temperature
s	singlet (NMR)
THF	tetrahydrofuran
TLC	thin layer chromatography
UV	ultraviolet

δ	chemical shift
$^{\circ}\text{C}$	degree Celsius
μL	microliter (s)
μM	micromolar (s)
Φ	quantum yield
% yield	percentage yield

CHAPTER I

INTRODUCTION

1.1 Supramolecular chemistry

Supramolecular chemistry is a study of new molecular systems in the field of noncovalent interactions between host and guest molecules as defined by Jean-Marie Lehn [1]. By tradition, chemists have focused primarily on understanding the behavior of molecules and their construction from constituent atoms. At the present, researchers in supramolecular chemistry are interested in the weaker and reversible noncovalent interactions, such as hydrogen bonding, dative bonding, hydrophobic forces, (London) dispersion forces, π - π stacking interactions, and electrostatic effects [2] involving in molecular self-assembly, molecular folding, molecular recognition, host-guest chemistry, mechanically-interlocked molecular architectures, and dynamic covalent chemistry [3]. Supramolecular chemistry has proved useful for the development of new materials, pharmaceuticals, drug delivery systems, high-tech sensors, and contrast agents for CAT scans. It is also useful for the design of catalysts, solid-state reactions, and treatments of radioactive wastes [4-7]. In addition, the study of noncovalent interactions is crucial to understanding many biological forms and processes, including cell structure and vision. The desire to study biological systems often provides the motivation behind supramolecular chemical research [8-9].

1.2 Calix[4]arene

Calix[4]arene is one of the most established molecular scaffolds in the design of artificial receptors because of its tunable and unique three-dimensional structures with many interesting properties together with the ease of functionalization for encapsulation and recognition properties [10-11]. The structure of calix[4]arene consists of four phenol rings linked together with four methylene units in a circular fashion producing a basket like architecture. Flipping of one or more phenyl rings around the flexible methylene linkages allows calix[4]arene to exist in one or more of the four main conformers viz. cone, partial cone, 1,2-alternate and 1,3-alternate with idealized structures having C_{4v} , C_s , C_{2h} , D_{2d} symmetry, respectively, as shown in

Figure 1.1. Furthermore, the structures of these conformers can be easily distinguished by the characteristic ^1H NMR patterns arising from the ArCH_2Ar methylene protons judging from the symmetry of each conformer, cone, partial cone, 1,2-alternate, and 1,3-alternate will appear as a pair of doublets, two pairs of doublets, one singlet and pair of doublets, and one singlet, respectively [13-14].

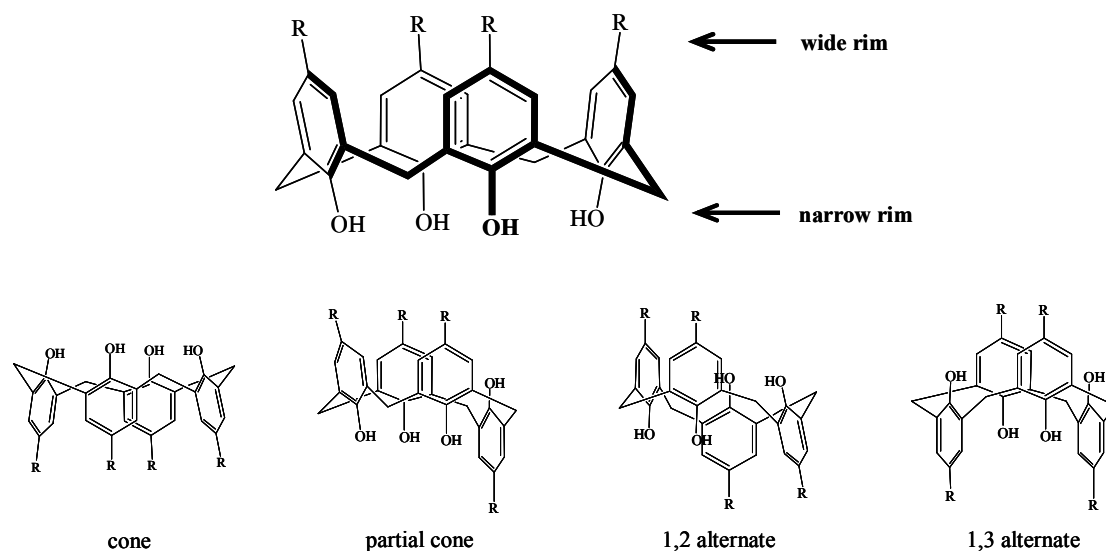


Figure 1.1 Calix[4]arene conformations [12].

1.3 Water soluble calix[4]arene

Calix[4]arene are generally soluble in organic solvents; however water soluble ones are also synthesized and reported by many authors. Several derivatives of water soluble calix[4]arenes were synthesized and used in many applications. In 1997, Steemers and coworkers reported the synthesis of water soluble calix[4]arenes **1** with chromophores (“antenna”) attached to the lower rim [15]. The neutral lanthanide complexes of **1** showed that photoexcitation of the antenna can induce lanthanide emission *via* intramolecular energy transfer.

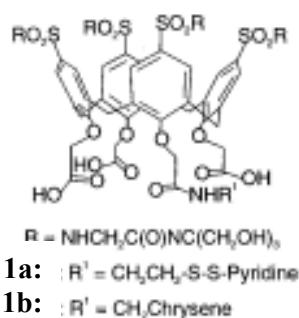


Figure 1.2 Water soluble calix[4]arenes **1** with chromophores (“antenna”) attached to the lower rim.

In 2003, Rostaing and coworkers reported the synthesis of the water soluble receptors **2**, **3** and **4** by introducing hydroxy, sulfato or diethanolamino groups at the *para* position of the phenolic ring and/or on the benzo-ether moieties [16] and studied of the complexation properties of these ionophores for all alkali cations in methanolic and aqueous media by UV-Vis spectroscopy. The results showed that compounds **2**, **3** and **4** represented selective ligands for Cs^+ cation in a moderate salted medium ($[\text{NaNO}_3] = 85 \text{ g/L}$).

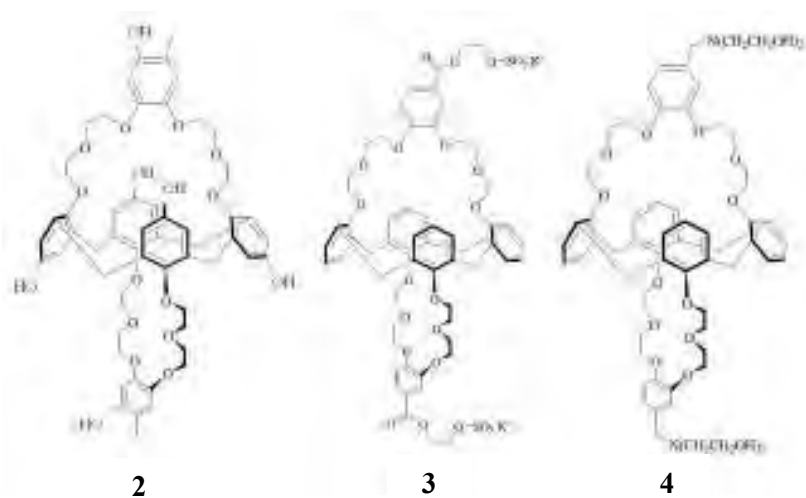


Figure 1.3 Structures of calix[4]arene and thiacalix[4]arene containing hydroxy, sulfato or diethanolamino groups at the *para* position of the phenolic ring and/or on the benzo-ether moieties.

In 2004, Liu and coworkers reported the derivatives of calix[4]arene and thiacalix[4]arene containing sulfonate groups **5**, **6**, and **7** which were soluble in acidic aqueous solution [17] and displayed binding abilities for lanthanoid(III) nitrates but *p*-sulfonatothiacalix[4]arene **7** gave not only the lower binding constants for all of lanthanoid(III) ions but also lower cations selectivity.

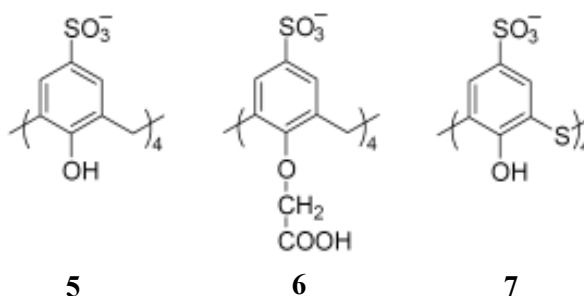


Figure 1.4 Structures of calix[4]arene and thiacalix[4]arene containing sulfonate groups.

In 2010, Okur and coworkers reported the optimization and characterization of a water soluble calix[4]arene derivative containing carboxylate and sulfonate groups **8** [18] and studied the capability in humidity sensor of this compound based on quartz crystal microbalance technique by investigating the moisture of adsorption and desorption kinetics and monitoring with increasing relative humidity (RH). The experimental results showed that the calix[4]arene films have strong affinity to water vapor between 29% and 80% RH. Hence, this water soluble calix[4]arene films had a great potential for humidity sensing applications at room temperature operations.

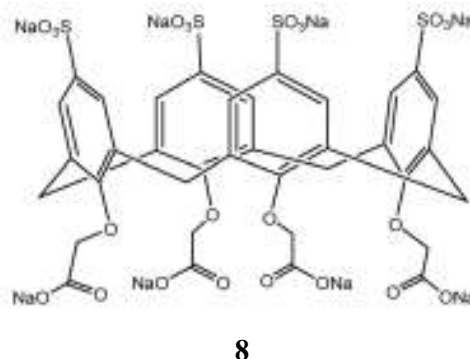


Figure 1.5 Structure of calix[4]arene derivative containing carboxylate and sulfonate groups.

1.4 Fluorescence chemosensor

Fluorescence is used as a detection method in many chemistry, biology and medicine for sensing or detecting. Fluorescence has the principle advantage over other light-based methods such as simplicity, high selectivity, and sensitivity. Nowadays, ion recognition plays an important role in a wide range of chemical reactions, including biological metabolism. For the purpose of detection and quantitative determination of ions, much effort has been devoted to develop the appropriate chemosensors. The most important design of effective chemosensors is the association of a selective molecular recognition resulting in a physical signal highly sensitive to its occurrence. Most of the fluorescent chemosensors are composed of an ion recognition unit (ionophore) for selective binding of the substrate, while the fluorogenic unit (fluorophore) provides the means of signaling this bonding, whether by fluorescence quenching or enhancement. The combination of these two words is also called for “fluoroionophore”. The mechanism which controls the response of a fluoroionophore to substrate binding includes photoinduced electron transfer (PET), photoinduced charge transfer (PCT), fluorescence (Förster) resonance energy transfer (FRET), and excimer/excimer formation or extinction [19-21] for example, Kim and coworkers reported the synthesis of calix[4]arenes **9** and **10** bearing two facing amide groups linked to pyrene units in 2005 [22]. These fluorescence chemosensors were selective for In^{3+} and Pb^{2+} over other metal ions in CH_3CN . By changing the conformation between **9** and **10**, they gave the difference in quenching mechanism. Compound **9** enhances the excimer emission with quenching of the monomer emission because In^{3+} -induced deprotonation of the phenolic OH groups, leading to strong face-to-face π -stacking of the two pyrene units. However, when Pb^{2+} was added to **9**, the fluorescence emission was strongly quenched because of the reverse PET from the pyrene units to the amide groups, as well as a heavy-metal ion effect. For **10**, addition of Pb^{2+} or In^{3+} quenched the excimer emission due to a conformational change caused by binding metal ion of amide carbonyl groups. In the resulting conformation, face-to-face π -stacking of the two pyrene units is destroyed as shown in Figure 1.6.

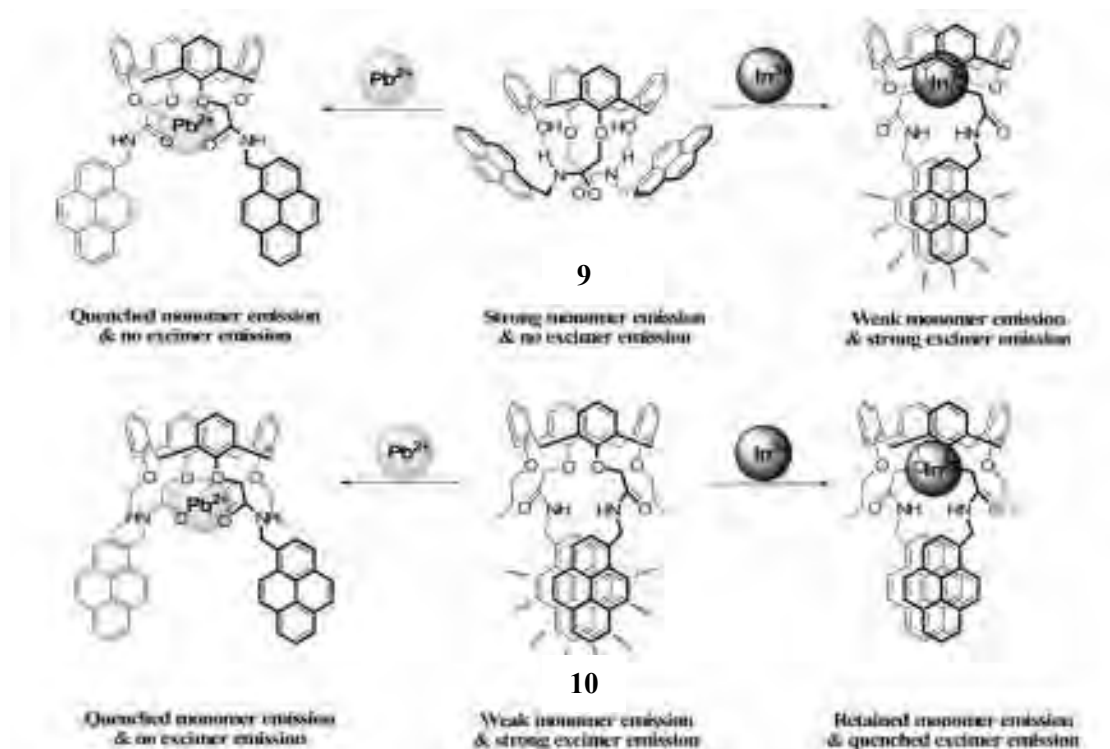


Figure 1.6 Proposed conformational changes of **9** and **10** upon complex formation with Pb^{2+} and In^{3+} .

In 2006, Choi and coworkers synthesized 1,3-alternate calix[4]crown fluoroionophore containing two cation recognition sites, a crown ether ring and two facing pyreneamide groups **11** [23]. The molecule was used as a fluorescence chemosensor for transition metal ions (Pb^{2+} and Cu^{2+}) and an alkali metal cation (K^+) in CH_3CN . The experimental data indicated that Pb^{2+} and K^+ interacted with the two pyrenylamide groups and the crown-5 ring, respectively, *via* excimer formation and extinction mechanism while Cu^{2+} interacted with the nitrogen atoms of the amide group by a PCT mechanism as shown in Figure 1.7.

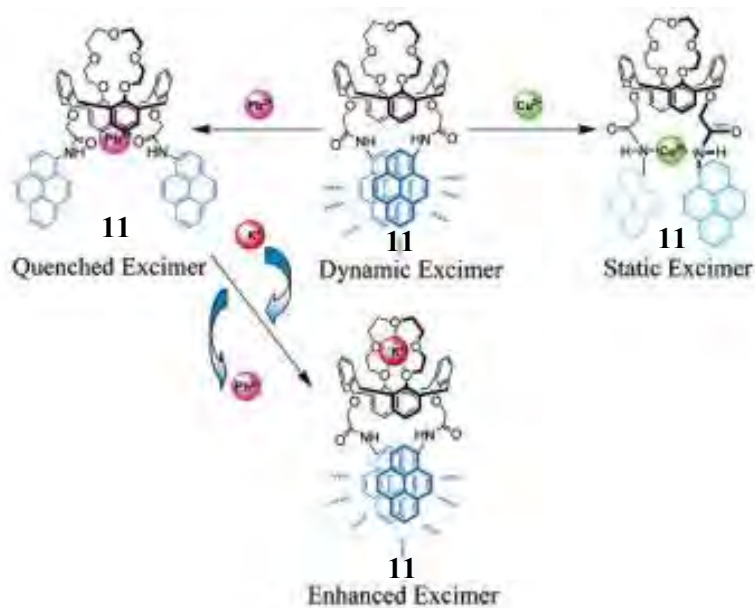
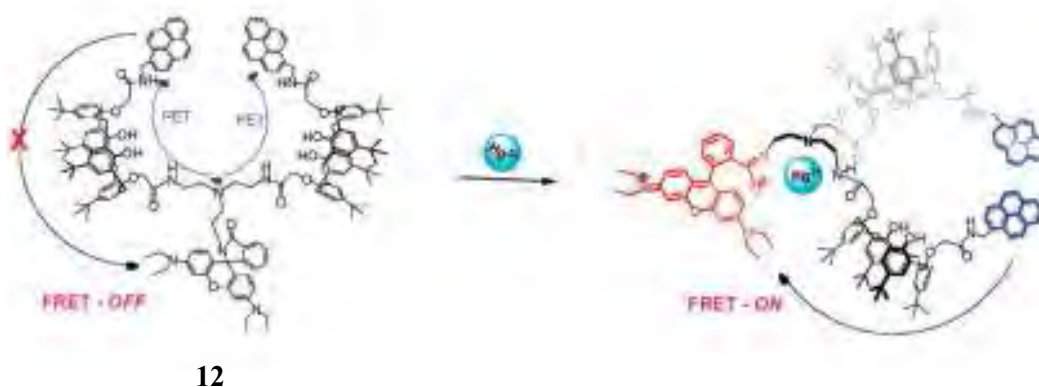


Figure 1.7 Conformational changes of fluorescence chemosensors **11** upon complex formation with Pb^{2+} , Cu^{2+} and K^+ .

In 2007, calixarene-based FRET chemosensor containing two pyrenyl groups (energy donor) and a rhodamine group (energy acceptor) **12** was synthesized and reported by Othman and coworkers [24]. Addition of Hg^{2+} in CH_3CN solution of this fluorescence chemosensors gave a significantly enhanced fluorescence emission *via* energy transfer (FRET-ON) from the pyrenyl excimer to a ring-opened rhodamine moiety as shown in Figure 1.8.



12

Figure 1.8 Complexation of fluorescence chemosensor **12** with Hg^{2+} *via* fluorescence resonance energy transfer.

Furthermore, many publications reported the use of calix[4]arene platforms for designing the fluorescence chemosensor, especially calix[4]arene in 1,3-di-derivative. The 1,3-di-derivative of calix[4]arenes have received increasing attention and become promising candidates for fluorescence sensing probes because they are in a certain preorganized framework to easily accommodate metal ions or neutral molecules.

In 2005, Dessingou and coworkers synthesized the fluorescence-sensitive 1,3-di-derivative of calix[4]arene bearing 2-hydroxy-1-naphthaldehyde moieties **13** [25] and used this derivative as a fluorescence-on chemosensor for Zn^{2+} in CHCl_3 and MeOH. Literature reports on high selectivity and sensitivity for Zn^{2+} recognition at concentrations ≤ 60 ppb by enhancement fluorescence intensity involving an energy transfer mechanism between β -hydroxy groups and naphthylidene moieties.

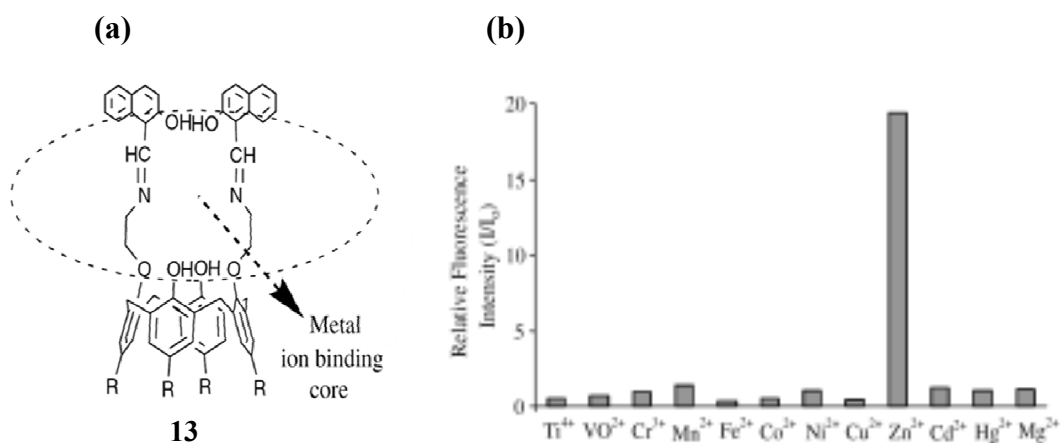


Figure 1.9 (a) Structure of calix-di-imine derivative, R=*tert*-butyl **13** and (b) Relative fluorescence intensity at the metal ion to ligand in the titration of calix-di-imine derivative **13** with different metal ions.

In 2006, Kumar and coworkers reported the synthesis of anthracene-anchored 1,3-di-derivatives of lower rim calix[4]arene **14** [26] and the binding studies revealed that the complexation of this calix[4]arene derivative in the presence of Fe^{2+} and Cu^{2+} gave high enhancement fluorescence intensity which occurred by the lone pair present on the imine-nitrogen atom, resulting in the photo-induced electron transfer.

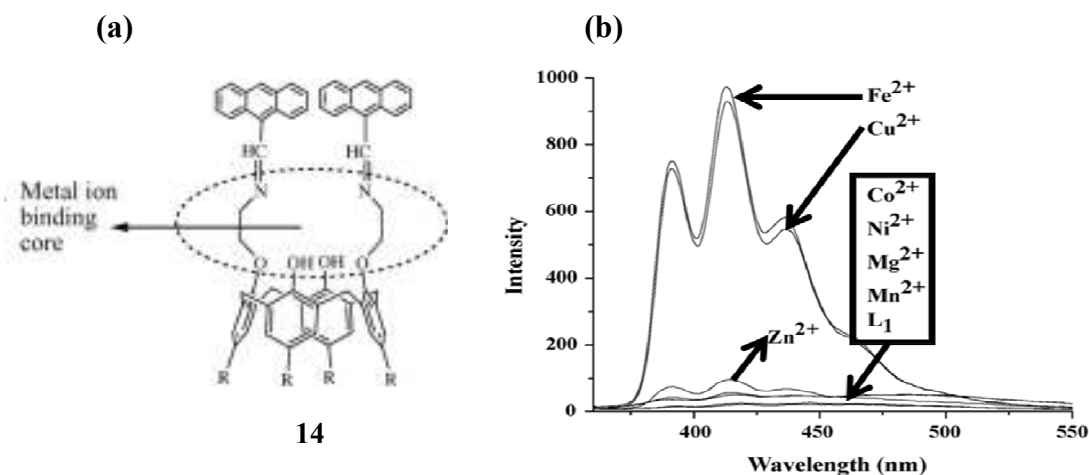


Figure 1.10 (a) Structure of the anthracene-anchored 1,3-di-derivatives of lower rim calix[4]arene, R=*tert*-butyl **14** and (b) Fluorescence spectra of **14**/ M^{2+} ratio being 1:50 (excitation wavelength of 340 nm).

In 2007, The subunit of phenanthroimidazole was introduced into the calix[4]arene-diamide **15** for the purpose of utilizing fluorescence-off chemosensor in 95% aqueous DMSO solution as reported by Song and coworkers [27]. The compound exhibited a large Mg^{2+} induced red-shifted emission, which is appropriate for ratiometric chemosensing of Mg^{2+} ions in semi-aqueous solutions.

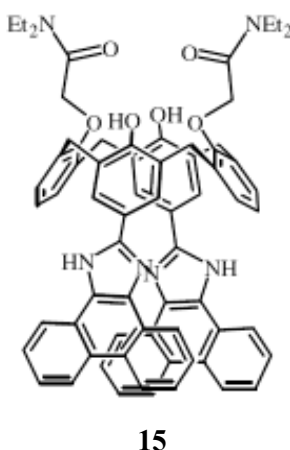


Figure 1.11 Structure of calix[4]arene-diamide derivative bearing with phenanthroimidazole subunit.

In 2008, Park and coworkers reported the synthesis and evaluation of calix[4]arene-based two pyrenyl groups linked to 1,2,3-triazole **16** [28]. This research revealed the binding mode of fluorescence-off chemosensor for Cd^{2+} and Zn^{2+}

in CH₃CN which observed the induced conformational changes of the triazole units by 1:1 complexation *via* the π - π interaction for excimer emission as shown in Figure 1.12.

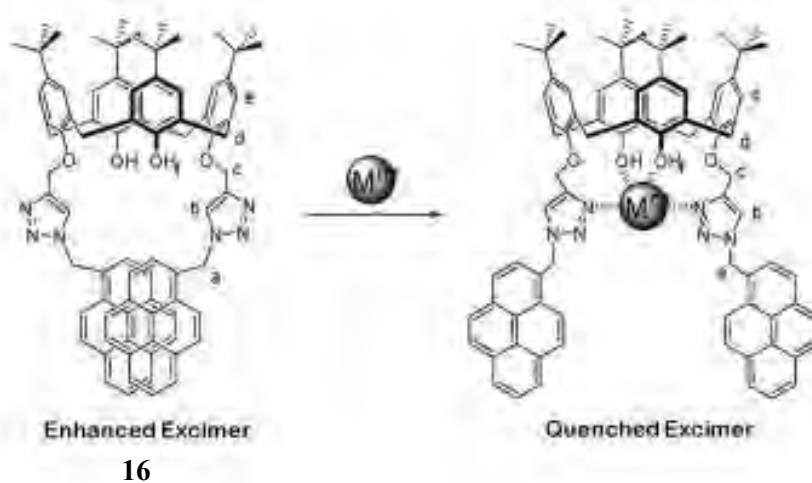


Figure 1.12 Complexation of fluorescence chemosensor **16** with metal ion (Cd^{2+} and Zn^{2+}) *via* excimer formation and extinction mechanism.

In 2009, a highly selective fluorescence switch on Cu^{2+} sensor in 1:1 aqueous methanol was synthesized by introducing a bis-(2-picoly)amine moiety at the lower rim of a calix[4]arene platform *via* amide linkage **17** which was reported by Joseph and coworkers [29].

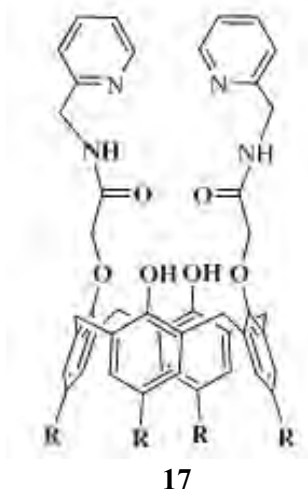


Figure 1.13 Structure of bis-(2-picoly)amine based on calix[4]arene ($\text{R} = \text{tert-butyl}$).

Moreover, the 1,3-alternate conformation has proved particularly useful as the basis for constructing highly sophisticated molecules with practical applications and is a “smart” conformation of calix[4]arenes [30]. In addition, calix[4]arene derivatives in the 1,3-alternate conformation are interesting receptors because 1,3-alternate calix[4]arene presents two individual binding sites of symmetrically or unsymmetrically calix[4]arene platforms leading to higher sensitivity and selectivity for metal ion sensor.

In 2006, Bok and coworkers synthesized an unsymmetrical 1,3-alternate calix[4]biscrown chemosensor **18** [31] which acted as a fluorescence-off chemosensor for Cd^{2+} and Zn^{2+} in CH_3CN by chelation-enhanced fluorescence (CHEF)-type effect and quenching metal effect.

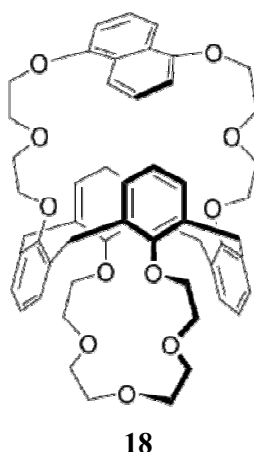


Figure 1.14 Structure of an unsymmetrical 1,3-alternate calix[4]biscrown.

Moreover, Kim and coworkers reported the synthesis of 1,3-alternate calix[4]arene having bispyrenylamide on the two lower rims and two carboxylic acids on the other two lower rims **19** [32] which acted as fluorescence-off chemosensor for Pb^{2+} in CH_3CN .

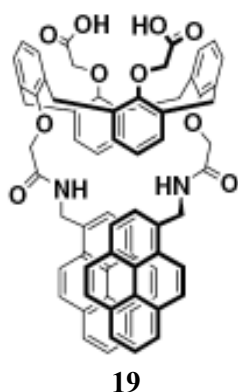


Figure 1.15 Structure of 1,3-alternate calix[4]arene having bispyrenylamide and carboxylic acid.

In 2009, Wang and coworkers synthesized calix[4]arene derivatives **20** with benzoxazole or benzothiazole units in 1,3-alternate conformation [30]. Their complexation properties to different heavy and transition metal ions have been studied by UV–Vis spectroscopy and fluorescence spectrometer. Compounds **20** showed selective recognition to Fe^{3+} and Cr^{3+} , respectively.

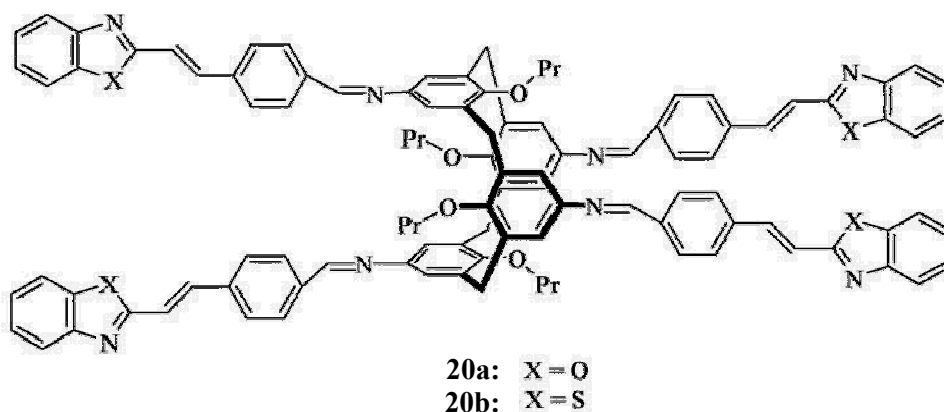


Figure 1.16 Structure of calix[4]arene derivatives with benzoxazole or benzothiazole units.

Finally, there are a few reports in the synthesis of water soluble calix[4]arene for fluorescence metal ion sensor. Previously, some selective fluorescent chemosensors for metal ions have been reported based on structural moieties in organic solvents. Most of them have some disadvantages in practical use, such as low water solubility, interference from other metal ions, strict reaction condition or

complicated synthetic route. Therefore, development of simple fluorescence chemosensor that can selectively sense for metal ions in aqueous media is significant [33-35]. Some reports have added surfactants or polyelectrolytes to enhance the fluorescence intensity [36] and reduce aggregation problem in aqueous media.

In 2009, Niamnont and coworkers reported the synthesis and study sensor properties of water soluble fluorescent dendritic compounds which were composed of phenylene-ethynylene repeating units and anionic carboxylate or cationic ammonium peripheral groups without and with a surfactant [37]. The fluorescent dendrimer containing nine phenylene-ethynylene units and six carboxylate peripheral groups showed low fluorescence quantum yield and no significant selectivity in metal ion sensor. After adding Triton X-100, the signals exhibited a highly selective fluorescence quenching by Hg^{2+} ions in aqueous media with the presence of Triton X-100 as surfactant as shown in Figure 1.17.

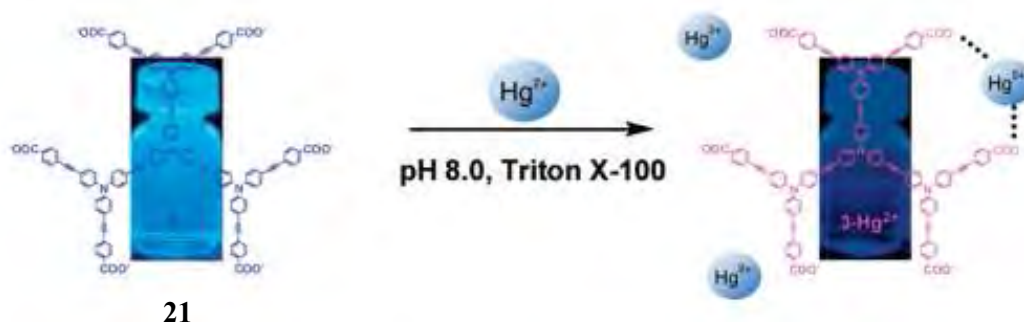


Figure 1.17 Water soluble fluorescent dendritic compounds exhibited a highly selective fluorescence quenching by Hg^{2+} ions in aqueous media in the presence of Triton X-100 surfactant.

1.5 Iron sensor

Iron is a fundamental element found in both industrial applications and biological systems, especially for its presence in the structures of numerous enzymes and proteins. At the cellular level, it is an essential element for the formation of hemoglobin of red blood cells and plays an important role in oxygen metabolism and electron transfer processes to DNA and RNA syntheses [38] and enzymes including in hydroxylases, peroxidases and dismutases. Moreover, iron is indispensable for most

organisms, and both its shortage and excess can stimulate various disorders. Iron metabolism disorders have been reported to cause anemia as well as liver and kidney damage (hemochromatosis) which might ultimately cause liver cancer, liver cirrhosis, arthritis, diabetes or heart failure [39]. Up to date studies have linked neurodegenerative disorders such as Parkinson's disease [40] and Alzheimer's disease to elevated iron levels [41]. Iron also ties to some important infectious diseases such as malaria [42]. Therefore, the improvement of trustworthy sensing techniques for iron ions is considerable significance for health diagnosis and environmental analysis. Over the past few years, there are several literatures reported the analytical techniques developed for the iron(II) determinations including electron spin resonance method (the method is very expensive and inconvenience in operation), UV-Vis spectrometry, controlled-potential coulometry and direct potentionmetry, high-performance liquid chromatographic method, luminescence based analysis, capillary electrophoresis, and fluorometric analysis [43].

In 2007, Zhang and coworkers reported turn-on fluorescent sensor of FD1 [44] based on the well-known spirolactam (nonfluorescence) **22** to ring-open amide (fluorescence) equilibrium of rhodamine for imaging of iron(III) ion in biological samples. FD1 exhibited high selectivity and sensitivity for Fe^{3+} over Cu^{2+} , Na^+ , K^+ , Cu^+ , Ag^+ , Ca^{2+} , Cd^{2+} , Co^{2+} , Cr^{2+} , Zn^{2+} , Mg^{2+} , Mn^{2+} , Ni^{2+} , Pb^{2+} , and Fe^{2+} . Moreover, fluorescent microscopy experiments further established that FD1 could be used for sensing Fe^{3+} within living cells.

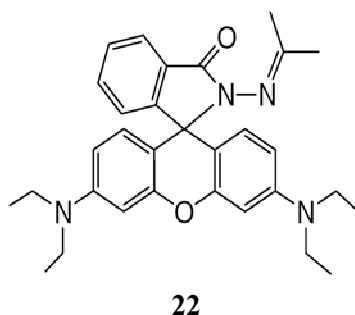


Figure 1.18 Structure of FD1.

Oter and coworkers utilized a fluorescent *benzofuran* derivative bis(7-methoxy-benzofuran-2-yl)ketoxime (BFK) **23** in construction of poly vinyl chloride (PVC)-based fiber optic for Fe^{3+} sensor. The optical sensor exhibited a selective fluorescence quenching response in the presence of Fe^{3+} [45].

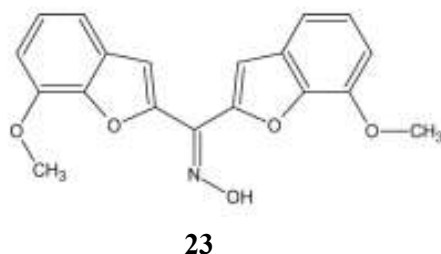


Figure 1.19 Structure of bis(7-methoxybenzofuran-2-yl)ketoxime (BFK) dye.

In 2009, Zhang and coworkers synthesized a fluorescent chemosensor [46] based on rhodamine 6G derivatives **24** which exhibited considerable fluorescence enhancement induced by Fe^{3+} (Figure 1.20).

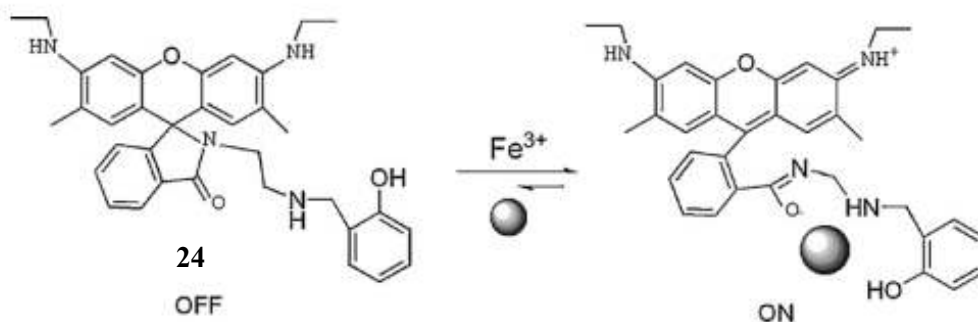


Figure 1.20 Proposed mechanism of Fe^{3+} -induced ring opening and fluorescent enhancement.

Mitra and coworkers synthesized a new glucose-based C2-derivatized colorimetric chemo-sensor by a one-step condensation of glucosamine and 2-hydroxy-1-naphthaldehyde **25** [47]. The recognition of transition metal ions results in visual color change only in the presence of Fe^{2+} , Fe^{3+} and Cu^{2+} in methanol. However, in an aqueous HEPES buffer (pH 7.2) it is only the Fe^{3+} that gives a distinct visual color change even in the presence of other metal ions, up to a concentration of 280 ppb.

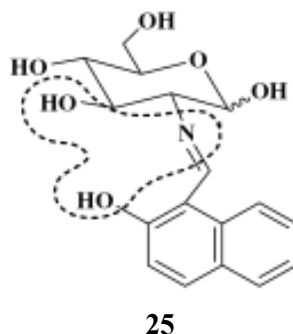


Figure 1.21 Structure of glucose-based derivative.

Singh and coworkers synthesized a novel aminobisulfonate receptor joined to a naphthalene fluorophore *via* a methylene spacer in a fluorophore-spacer-receptor structure **26** [39] and developed this fluorescent sensor for the determination of Fe^{3+} in an aqueous solution at pH 7.0. The fluorescence emission of the sensor was quenched upon addition of Fe^{3+} , most likely due to electron/energy transfer between Fe^{3+} and the excited naphthalene. The sensor displayed good selectivity for Fe^{3+} over other physiologically relevant metal ions.

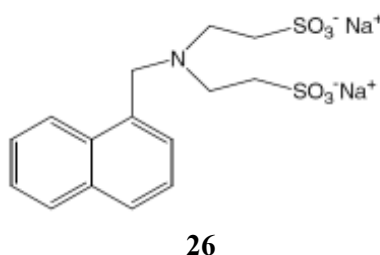


Figure 1.22 Structure of β -aminobisulfonate receptor linked naphthalene fluorophore.

Although there are a number of papers that deal with organic dye-based chemosensors for Fe(III), only a few have reported the Fe(II) detection. In 1995, Noiré and coworkers reported the preparation of Fe(II) optical sensor by adsorbing calcein blue (CB) **27** on a hydrophobic support incorporated in a flow cell [48]. The sensor based on the fluorescence quenching of CB at pH = 2.2 is sensitive to ferrous ions over a wide range of analytical interest (1-500 μM), with a linear and efficient quenching region at the iron concentrations of 10^{-6} to 10^{-5} M.

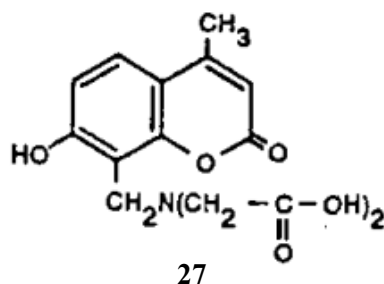


Figure 1.23 Structure of calcein blue.

In 2003, Hasinoff reported the study of fluorescent metal chelating dye, calcein **28** [49]. The experimental results indicated that Fe(II) catalyzed the degradation of calcein through both hydrogen peroxide, and to a lesser extent, non-hydrogen peroxide-dependent pathways. The iron-calcein complexes that were responsible for the degradation of calcein were likely high valence oxidizing iron-oxo species such as perferryl or ferryl complexes that were redox cycled by ascorbic acid. Thus, the use of calcein as an intracellular iron-sensing indicator may yield misleading results due to its degradation under certain conditions.

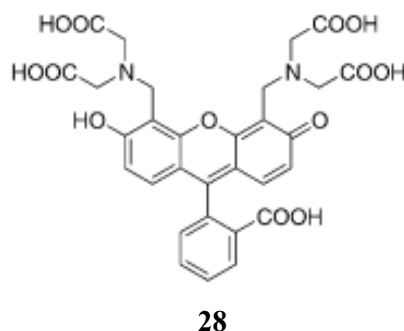


Figure 1.24 Structure of calcein.

In 2006, Chen and coworkers proposed a novel fluorescence method for the determination of Fe(II) with a high selectivity and sensitivity based on the enhancement of fluorescence signals resulting from specific redox reaction between synthesized fluorescence probe pyrene-tetramethylpiperidinyl (TEMPO) and Fe(II) as shown in Figure 1.25 [50].

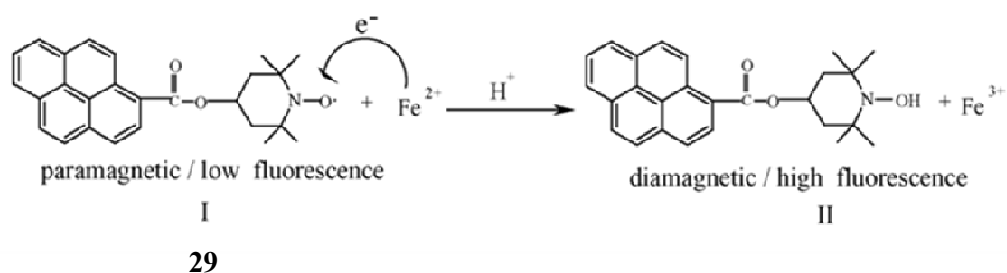


Figure 1.25 Schematic illustration of the interaction between probe I (pyren-TEMPO) and Fe(II).

In 2010, Wang and coworkers designed and synthesized a colorimetric chemosensor based on fluoran dye **30** [51]. The results showed a good selectivity and sensitivity for Fe²⁺ at 100 μ M and observed the color change from colorless to greenish black by the naked eyes as shown in Figure 1.26.

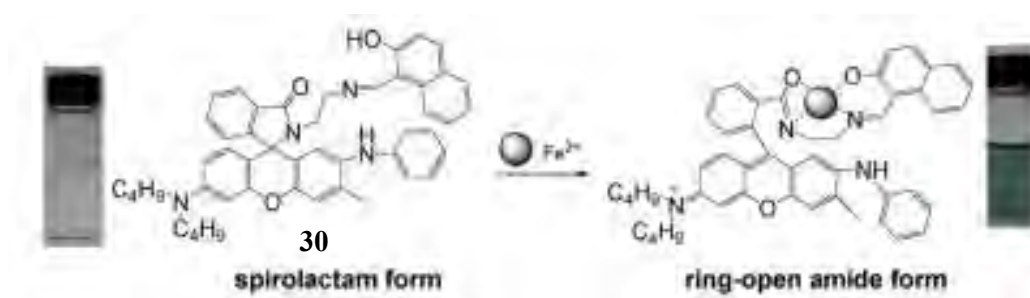


Figure 1.26 Proposed binding mode and color change of fluoran dye with Fe²⁺.

Moreover, Wu and coworkers reported the development method for discriminating Fe²⁺ and Fe³⁺ based on their quenching kinetics for the fluorescence of GSHCdTe QDs and also proposed a GSH-CdTe QDs-Fenton hybrid system for sensitive and selective determination of trace Fe²⁺ based on the fact that Fe²⁺ can catalytically induce the generation of hydroxyl radicals from H₂O₂ and hydroxyl radicals can quench the fluorescence of GSH-CdTe QDs more effectively than individual Fe²⁺ or H₂O₂ as shown in Figure 1.27 [52].

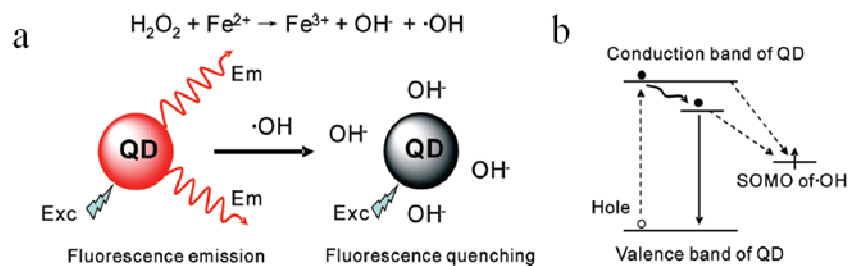


Figure 1.27 Schematic illustration for (a) Fe^{2+} induced hydroxyl generation and QDs based sensor for Fe^{2+} detection; (b) The fluorescence quenching mechanism by electron transfer from the QDs to hydroxyl radicals.

1.6 Objectives of this research

The target of this work has been focused on the synthesis of water soluble 1,3-alternate calix[4]arene containing diphenylacetylene with carboxylic group as a fluoroionophore and study of photophysical properties of this compound for metal ion sensor in aqueous media. Moreover, the selective binding affinity of this fluorophore toward certain types of metal ions is expected.

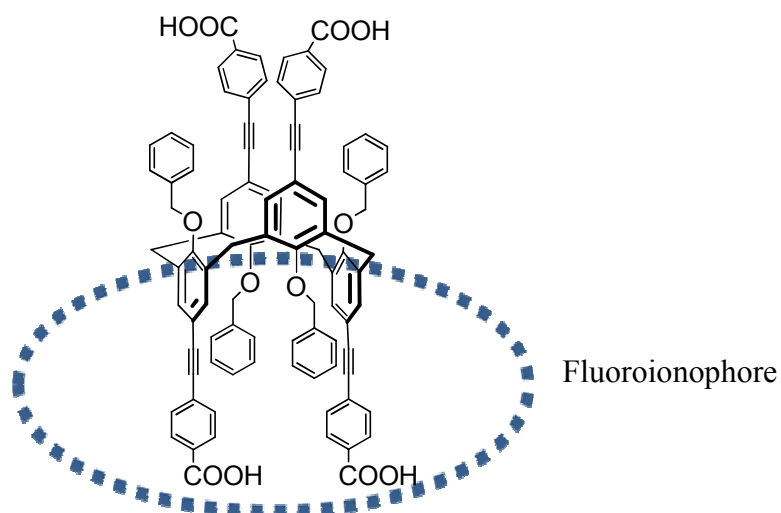


Figure 1.18 The target molecule.

CHAPTER II

EXPERIMENTAL

2.1 Materials and chemicals

All reagents were purchased from Sigma-Aldrich, Fluka[®] (Switzerland) and Merck[®] (Germany). *p-tert*-Butylcalix[4]arene was prepared according to the literature procedures [53]. For general reactions, solvents such as methylene chloride and acetonitrile were reagent grade stored over molecular sieves. In anhydrous reactions, solvents such as THF and toluene were dried and distilled before use according to the standard procedures. All column chromatography were operated using silica gel 60 (70-230 mesh), Merck[®]. Thin layer chromatography (TLC) was performed on silica gel plates (Merck F₂₄₅). Solvents such as methylene chloride, hexane, ethyl acetate and methanol used for extraction and chromatography were commercial grade and distilled before use. Diethyl ether and chloroform used for extraction was reagent grade. Deionized water was used in all experiments unless specified otherwise. All reactions were carried out under positive pressure of N₂ filled in rubber balloons.

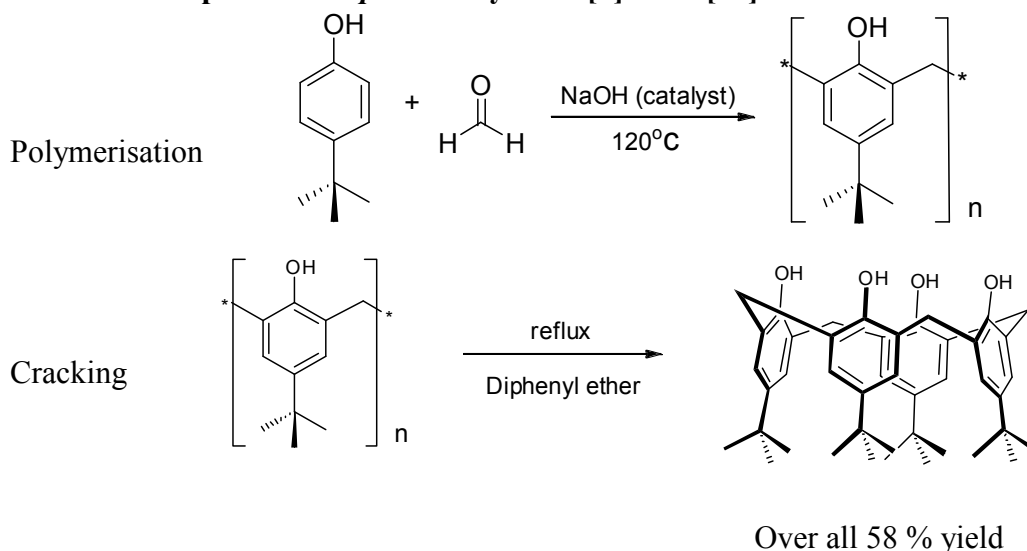
2.2 Analytical instruments

The products were characterized by a melting point apparatus (Electrothermal 9100, Fisher Scientific, USA). Elemental (C, H, N) analysis was performed on PE 2400 series II (Perkin-Elmer, USA). The HRMS spectra were measured on an electrospray ionization mass spectrometer (micrOTOF, Bruker Daltonics). Fourier transform infrared spectra were acquired on Nicolet 6700 FT-IR spectrometer equipped with a mercury-cadmium telluride (MCT) detector (Nicolet, USA). ¹H-NMR spectra were recorded on Varian Mercury 400 MHz NMR spectrometer (Varian, USA) using CDCl₃ and DMSO-*d*₆. ¹³C-NMR spectra were recorded at 100 MHz on Bruker 400 MHz NMR spectrometer using the same solvent. The UV-Visible spectra were obtained from a Varian Cary 50 UV-Vis spectrophotometer (Varian, USA) using water, CHCl₃ and DMSO as a solvent. Fluorescence emission spectra were acquired by using Perkin Elmer precisely LS 45 Luminescence Spectrometer (PerkinElmer, UK) for metal ion sensor and using

a Varian Cary Eclipse spectrofluorometer (Varian, USA) for photophysical property study.

2.3 Synthesis of 25,26,27,28-tetrabenzoyloxy-4-ethynylbenzoic acid calix[4]arene

2.3.1 Preparation of *p*-*tert*-butyl calix[4]arene [53]



First step: polymerisation

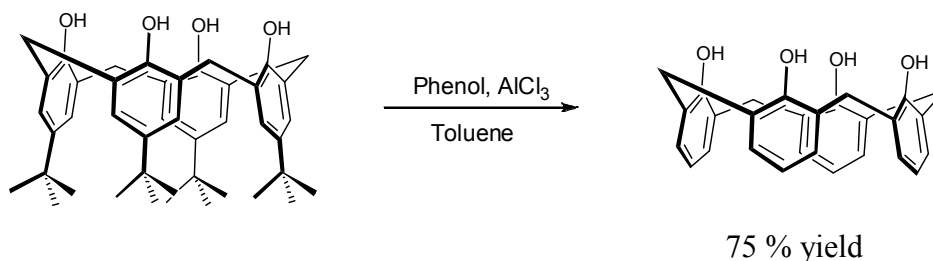
In a 1 L round-bottomed flask equipped with a magnetic stirring bar, a mixture of *p*-*tert*-butylphenol (25.00 g, 0.17 mol), 37% formaldehyde in ethanol (15.50 mL, 0.20 mol) and sodium hydroxide (0.30 g 7.50 mmol) was stirred and heated at 100-120°C on a heating mantle. The flask was left open to allow the water by-product to escape from the reaction mixture. The stirring and heating was continued until a colourless liquid turned into a spongy crispy yellow solid as the water evaporated. The reaction was then allowed to cool to room temperature. Over heating resulted in low yield of the desired product in the following step due to the formation of green polymeric materials. The small amount of green polymer by-product, if formed, was disposed and only the yellow part of the precursor was brought to the next step, cracking. The precursor prepared should be used within one or two days to assure the high yield of *p*-*tert*-butylcalix[4]arene.

Second step: cracking

Two batches of the yellow polymer formed in the first step were crushed into powder. In a 2 L two-necked round-bottomed flask equipped with a magnetic stirring bar, condenser and a Dean-Stark trap, the precursor from polymerisation process (25.00 g) was stirred in diphenyl ether (250 mL). The reaction flask and

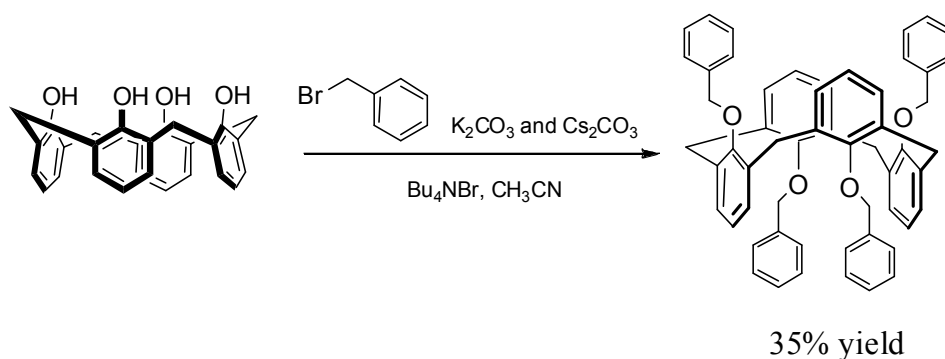
the Dean-Stark side arm were wrapped with a heating jacket and cotton wool in aluminium foil in order to maintain the temperature. The mixture was refluxed on a heating mantle. The “pop” sound was produced indicating the removal of water from the reaction. When the “pop” sound was completely subsided, the reaction was allowed to cool to room temperature (around 2.5 hours). The pale brown product was precipitated out by addition of ethyl acetate (400 mL). The product was filtered and washed with ethyl acetate (400 mL) and 25% acetic acid in ethyl acetate (300 mL) yielding a white solid. The *p-tert*-butylcalix[4]arene was further purified by crystallisation in toluene giving a white crystal as a product in 58% yield.

2.3.2 Preparation of calix[4]arene [54]



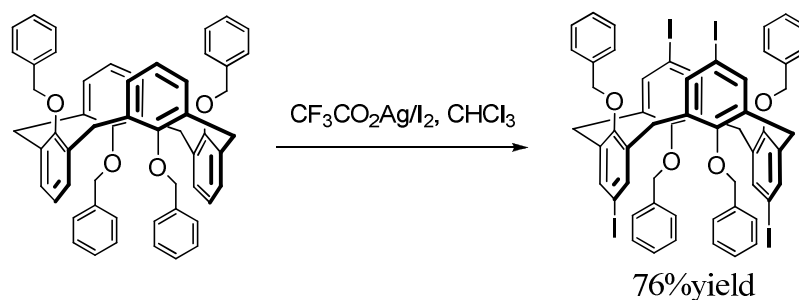
In a 500 mL round-bottomed flask equipped with a magnetic stirring bar, a mixture of *p-tert*-butylcalix[4]arene (13.24 g, 0.02 mol), phenol (9.60 g, 0.10 mol) in anhydrous toluene (200 mL) was cooled to 0°C in an ice bath. AlCl₃ (14.00 g, 0.10 mol) was slowly added to the reaction mixture. The reaction mixture was allowed to warm to room temperature and stirred for 1 hour. HCl (3 M, 100 mL) was added to the reaction mixture at 0°C and extracted with water (2x30 mL). The organic phase was separated and dried over anhydrous Na₂SO₄. The solvent was evaporated under reduced pressure until the white solid was precipitated and methanol (100 mL) was poured into the residue. The product was precipitated out as a white solid. The precipitate was filtered and washed with cold toluene and methanol. The calix[4]arene was further purified by crystallization in toluene giving a white solid as a product in 75 % yield.

2.3.3 Preparation of 25,26,27,28-tetrabenzoyloxy-calix[4]arene (**1**)



A mixture of calix[4]arene (0.31 g, 0.73 mmol), K_2CO_3 (0.49 g, 3.55 mmol), tetrabutylammonium bromide (0.05 g, 0.15 mmol) and CH_3CN (25 mL) was stirred for 30 min, and then benzylbromide (0.32 g, 1.87 mmol) was added dropwise into the stirred mixture. The reaction mixture was refluxed for 2 days, allowed to cool to room temperature and filtered. The filtrate was added with Cs_2CO_3 (1.11 g, 3.40 mmol) and tetrabutylammonium (0.12 g, 0.37 mmol) and stirred for 30 min. Another portion of benzylbromide (1.01 g, 5.91 mmol) was added. The reaction mixture was refluxed for 2 days, allowed to cool to room temperature and filtered. The filtrate was evaporated under reduced pressure and the resulting residue was dissolved in CH_2Cl_2 (25 mL) and extracted with aqueous HCl (2 M, 2 x 25 mL). The organic phase was separated, dried over anhydrous $MgSO_4$, filtered and evaporated by rotary evaporator. The crude product was crystallized from CH_2Cl_2/CH_3OH yielding the desired product as a white solid (0.20 g, 35% yield). 25,26,27,28-tetrabenzoyloxy-calix[4]arene (**1**): mp: 198-200 °C; 1H NMR (400 MHz, $CDCl_3$) δ (ppm): 7.47-7.35 (m, 12H, $H_{para-Ar}$ and $H_{meta-Ar}$), 7.20 (d, 8H, $J = 7.0$ Hz, $H_{ortho-Ar}$), 6.69 (d, 8H, $J = 7.5$ Hz, Ar-H), 6.47 (t, 4 H, $J = 7.5$ Hz, Ar-H), 4.88 (s, 8H, OCH_2Ar), 3.60 (s, 8H, $ArCH_2Ar$). ^{13}C -NMR (100 MHz, $CDCl_3$) δ (ppm): 155.8, 138.1, 133.9, 131.2, 127.8, 127.0, 126.8, 122.2, 71.8, 37.2. Anal. found: C 85.46%, H 5.95% (calcd. For $C_{56}H_{48}O_4$: C 85.68%, H 6.16%).

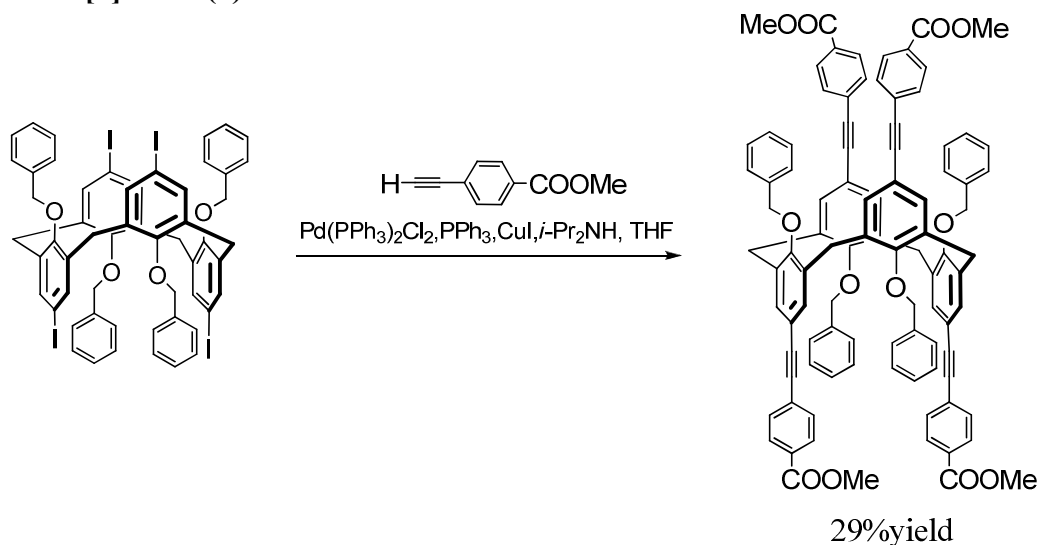
2.3.4 Preparation of 25,26,27,28-tetrabenzoyloxy-4-iodocalix[4]arene (2)



A mixture of **1** (0.11 g, 0.14 mmol), CF₃COOAg (0.20 g, 0.91 mmol) and CHCl₃ (20 mL) was stirred and refluxed for 15 min and then the temperature was reduced to 50-60°C and stirred for another 15 min period. Iodine (0.50 g, 1.97 mmol) was added and the stirring was continued at 50-60°C for 3 hours. The reaction mixture was allowed to cool to room temperature and filtered over Celite[®]. The filtrate was extracted with 20% aqueous NaHSO₃ (25 mL) and H₂O (25 mL). The organic phase was separated, dried over anhydrous MgSO₄, filtered and evaporated to dryness by rotary evaporator. The crude product was crystallized from CH₂Cl₂/CH₃OH yielding the desired product as a white solid (0.14 g, 76% yield).

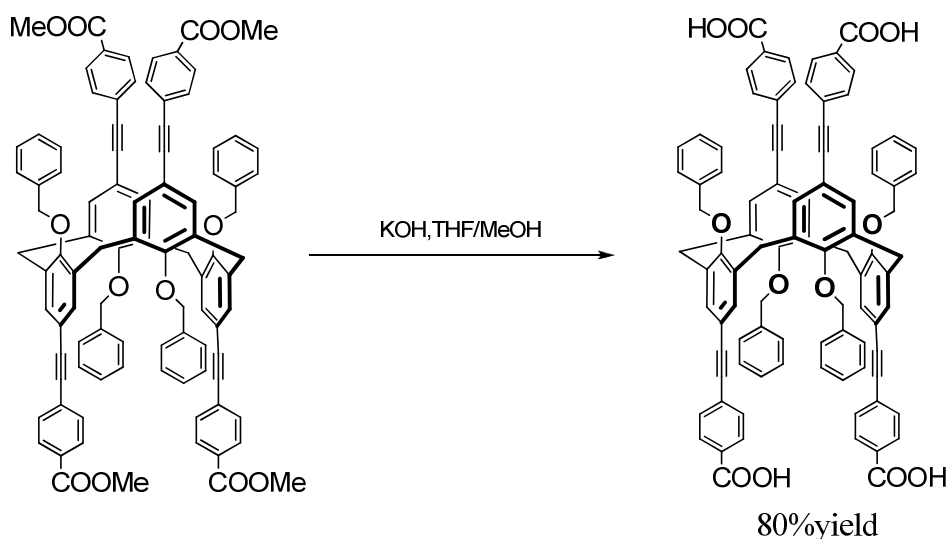
25,26,27,28-tetrabenzoyloxy-4-iodocalix[4]arene (2): mp: >225 °C decomposed; ¹H NMR (400 MHz, CDCl₃) δ (ppm): 7.65 (t, 8H, *J* = 7.6 Hz, H_{meta-Ar}), 7.52-7.37 (m, 12H, H_{para-Ar} and H_{ortho-Ar}), 7.21 (s, 8H, Ar-H), 4.86 (s, 8H, OCH₂Ar), 3.37 (s, 8H, ArCH₂Ar). ¹³C-NMR (100 MHz, CDCl₃) δ (ppm): 155.8, 139.6, 137.3, 135.2, 129.4, 127.4, 126.3, 86.3, 73.8, 35.1. Anal. found: C 50.47%, H 3.33% (calcd. for C₅₆H₄₄I₄O₄: C 52.20%, H 3.44%); HRMS (ESI) found: 1310.9415 [M + Na⁺]. (calcd. for C₅₆H₄₄I₄O₄Na 1310.9316).

2.3.5 Preparation of 25,26,27,28-tetrabenzoyloxy-4-ethynylbenzoic methyl ester calix[4]arene (**3**)



A mixture of **2** (0.15 g, 0.12 mmol), 4-ethynylbenzoic methyl ester (0.18 g, 1.12 mmol), $(\text{PPh}_3)_2\text{PdCl}_2$ (0.02 g, 0.03 mmol), Ph_3P (6.20 mg, 0.02 mmol), di-*iso*-propylamine (1 mL, 7.14 mmol) and tetrahydrofuran (10 mL) was degassed and stirred for 1 hour at room temperature. Then CuI (7.00 mg, 0.04 mmol) was added and the mixture was degassed again and stirred under N_2 for 24 hours. The reaction mixture was then evaporated by rotary evaporator. The residue was purified by column chromatography using CH_2Cl_2 as an eluent yielding the desired product as a white solid (0.05 g, 29% yield). *25,26,27,28-tetrabenzoyloxy-4-ethynylbenzoic methyl ester calix[4]arene (3)*: mp: >268 °C decomposed; ^1H NMR (400 MHz, CDCl_3) δ (ppm): 7.91 (d, 8H, $J = 8.2$ Hz, $\underline{\text{H}}_{\text{ortho-Ar C=O}}$), 7.45 (m, 16H, $\underline{\text{H}}_{\text{meta-Ar}}$ and $\underline{\text{H}}_{\text{ortho-Ar}}$), 7.36 (d, 8H, $J = 8.2$ Hz, $\underline{\text{H}}_{\text{meta-Ar C=O}}$), 7.22 (s, 4H, $\underline{\text{H}}_{\text{para-Ar}}$), 7.03 (s, 8H, $\underline{\text{Ar-H}}$), 5.00 (s, 8H, $\underline{\text{OCH}_2\text{Ar}}$), 3.98 (s, 12H, $\underline{\text{OCH}_3}$), 3.59 (s, 8H, $\underline{\text{ArCH}_2\text{Ar}}$). ^{13}C -NMR (100 MHz, CDCl_3) δ (ppm): 166.6, 156.6, 137.2, 135.1, 133.5, 131.2, 129.3, 128.9, 128.6, 126.9, 126.2, 116.4, 93.2, 87.6, 72.7, 52.2, 36.2. Anal. found: C 81.30%, H 5.11% (calcd. For $\text{C}_{96}\text{H}_{72}\text{O}_{12}$: C, 81.34%; H, 5.12%); HRMS (ESI) found: 1440.4862 [$\text{M} + \text{Na}^+$] calcd for $\text{C}_{96}\text{H}_{72}\text{O}_{12}\text{Na}$: 1440.4955).

2.3.6 Preparation of 25,26,27,28-tetrabenzoyloxy-4-ethynylbenzoic acid calix[4]arene (**4**)



A mixture of **3** (0.04 g, 0.03 mmol), saturated aqueous KOH (1 mL) and THF/MeOH (30/5 mL) was stirred and refluxed for 1 day before the reaction mixture was allowed to cool to room temperature. The organic solvent was evaporated and deionized water (20 mL) was added. The aqueous HCl (2 M) until pH=4. The precipitate was washed with deionized water (5 x 20 mL) and dried *in vacuo* to yield **4** as yellowish brown solid (0.01 g, 80% yield). 25,26,27,28-tetrabenzoyloxy-4-ethynylbenzoic acid calix[4]arene (**4**): mp: >263 °C decomposed; ^1H NMR (400 MHz, DMSO- d_6) δ (ppm): 7.91 (d, 8H, $J = 7.9$ Hz, $\text{H}_{\text{ortho-Ar C=O}}$), 7.38 (m, 24H, $\text{H}_{\text{meta-Ar}}$, $\text{H}_{\text{ortho-Ar}}$ and $\text{H}_{\text{meta-Ar C=O}}$), 7.17 (br, 4H, $\text{H}_{\text{para-Ar}}$), 6.93 (s, 8H, Ar-H), 5.00 (s, 8H, OCH_2Ar), 3.68 (s, 1H, ArCH_2Ar). ^{13}C -NMR (100 MHz, DMSO- d_6) δ (ppm): 166.6, 156.6, 137.5, 134.3, 133.7, 130.8, 129.3, 128.2, 127.3, 126.1, 115.1, 92.9, 86.8, 71.8, 35.3. Anal. found: C 78.26%; H 4.99% (calcd. for $[\text{C}_{92}\text{H}_{64}\text{O}_{12} + 3\text{H}_2\text{O}]$): C 78.06%, H 4.98%. HRMS (ESI) found: 1399.3753 $[\text{M} + \text{K}^+]$ (calcd for $\text{C}_{92}\text{H}_{64}\text{O}_{12}\text{K}$: 1399.4035).

2.4 Photophysical property study

The stock solutions of ester **3** (~10 μM) in DMSO and carboxylic acid **4** (~7.5 μM) in phosphate buffer (PB, 50 mM) pH 8.0 were prepared.

2.4.1 UV-Visible spectroscopy

The UV-Visible absorption spectra of the stock solutions of 25,26,27,28-tetrabenzoyloxy-4-ethynylbenzoic methyl ester calix[4]arene (**3**) and 25,26,27,28-tetrabenzoyloxy-4-ethynylbenzoic acid calix[4]arene (**4**) were recorded from 250 nm to 700 nm at ambient temperature.

2.4.2 Fluorescence spectroscopy

The stock solutions of **3** and **4** were diluted to ~0.4 and 1 μM , respectively, with their respective solvents. The emission spectra of **3** and **4** were recorded from 325 nm to 700 nm at ambient temperature using an excitation wavelength at 317 and 300 nm, respectively.

2.4.3 Fluorescence quantum yields

The fluorescence quantum yield of **3** and **4** were performed in DMSO and PB phosphate buffer (PB, 50 mM) pH 8.0 by using 2-aminopyridine in 0.1 M H_2SO_4 ($\Phi = 0.60$) as a reference. The UV-Visible absorption spectra of five analytical samples and five reference samples at varied concentrations were recorded. The maximum absorbance of all samples should never exceed 0.1. The fluorescence emission spectra of the same solutions using appropriate excitation wavelengths selected were recorded based on the absorption maximum wavelength (λ_{max}) of each compound. Graphs of integrated fluorescence intensities were plotted against the absorbance at the respective excitation wavelengths. Each plot should be a straight line with 0 interception and gradient m .

In addition, the fluorescence quantum yield (Φ_{F}) was obtained from plotting of integrated fluorescence intensity vs absorbance represented into the following equation:

$$\Phi_{\text{X}} = \Phi_{\text{ST}} \left(\frac{\text{Grad}_{\text{X}}}{\text{Grad}_{\text{ST}}} \right) \left(\frac{\eta_{\text{X}}^2}{\eta_{\text{ST}}^2} \right)$$

The subscripts Φ_{ST} denote the fluorescence quantum yield of a standard reference which used 2-aminopyridine in 0.1 M H_2SO_4 ($\Phi = 0.60$) and Φ_X is the fluorescence quantum yield of sample and η is the refractive index of the solvent.

2.5 Fluorescent sensor study

2.5.1 Surfactant enhancement

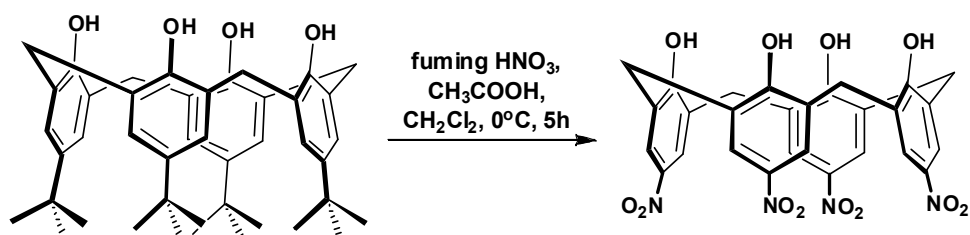
The stock solution of **4** was diluted to ~ 0.1 to $1 \mu M$ in phosphate buffer (PB, 50 mM) pH 8.0 were prepared. The emission spectrum of **4** was recorded from 325 nm to 700 nm at ambient temperature using an excitation wavelength at 300 nm and the photophysical properties were studied for 9 surfactants such as anionic, cationic and non-ionic surfactants. The stock surfactants were prepared in phosphate buffer (PB, 50 mM) pH 8.0. Concentrations of all stock surfactants were adjusted to 0.1 mM and were added with the desired volumes (0-500 μL) to the fluorophore solutions. The final volumes of the mixtures were adjusted to 5 mL.

2.5.2 Metal ion sensor

The stock solution of **4** were diluted to ~ 0.1 to $1 \mu M$ in phosphate buffer (PB, 50 mM) pH 8.0 were prepared. The emission spectrum of **4** was recorded from 325 nm to 700 nm at ambient temperature using an excitation wavelength at 300 nm and the photophysical properties were studied for metal ion sensor with and without non-ionic surfactants. Metal acetate and sulfate solutions were prepared in Milli-Q water. Concentrations of all stock metal acetate and sulfate solutions were adjusted to 100 μM and were added with the desired volumes (0-500 μL) to the fluorophore solutions. The final volumes of the mixtures were adjusted to 5 mL.

2.6 Synthesis of stilbene-bridged calix[4]arene

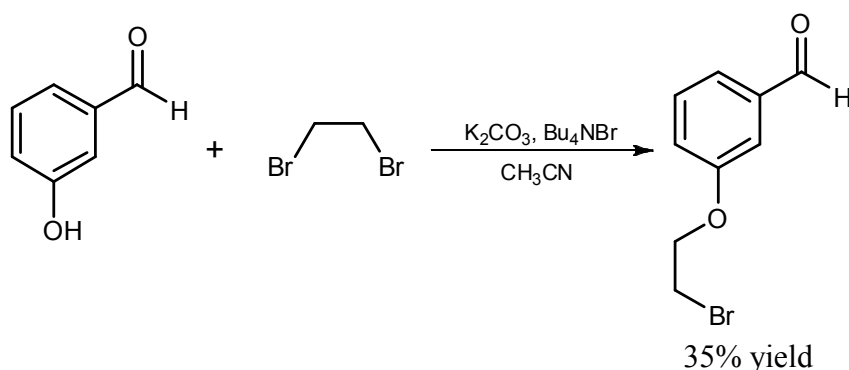
2.6.1 Preparation of *p*-nitrocalix[4]arene (5)



93% yield

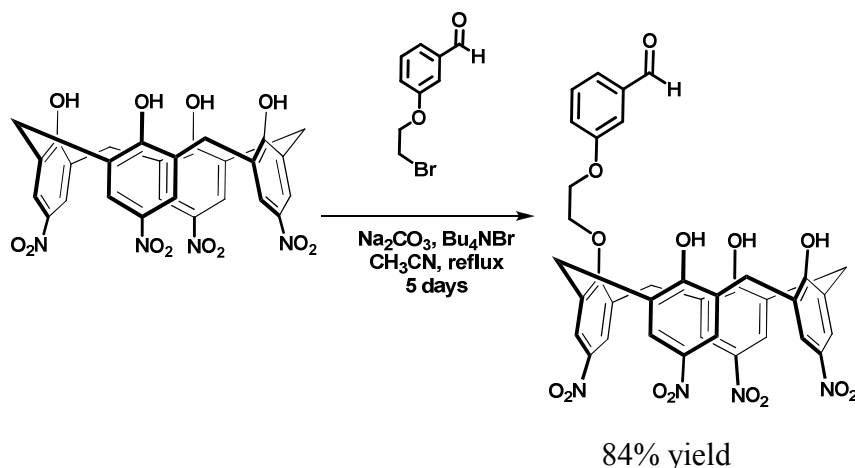
Glacial acetic acid 10 mL and fuming HNO₃ (4.2 mL, 66.7 mmol) was slowly added to a round bottom flask. *p*-*tert*-butyl calix[4]arene (0.50 g, 0.77 mmol) was taken separately in CH₂Cl₂ 10 mL and cooled to 0°C. This solution was slowly added to the round bottom flask containing nitric acid solution while keeping the mixture temperature below 0°C. The mixture was stirred at this temperature for 5 hours and then this mixture was added into cold water (100 mL). The precipitated solid was filtered and washed with cold water, refiltered again with hot acetone and dried *in vacuo* to yield **5** as pale yellow solid (0.45 g, 93% yield). *p*-nitrocalix[4]arene (**5**): ¹H NMR (400 MHz, DMSO-*d*₆) δ (ppm): 8.15 (s, 8H, ArH), 5.75 (s, 4H, OH), 4.23 (s, 4H, ArCH₂Ar), 3.73 (s, 8H, ArCH₂Ar). ¹³C-NMR (100 MHz, DMSO-*d*₆) δ (ppm): 162.0, 137.7, 129.0, 124.2, 30.1.

2.6.2 Preparation of 3-(2-bromoethoxy)benzaldehyde (6)



A mixture of 3-hydroxybenzaldehyde (24.42 g, 0.20 mol), K_2CO_3 (30.43 g, 0.22 mol) and Bu_4NBr (6.40 g, 0.02 mol) in CH_3CN (800 mL) was stirred for 30 minutes at room temperature and dibromoethane (78 mL, 1.60 mol) was then added all at once to avoid the disubstitution by-product. The reaction mixture was refluxed for 48 hours at $90^\circ C$ and then allowed to cool to room temperature. The mixture was filtered and washed with CH_2Cl_2 (300 mL). The combined organic layers were evaporated under reduced pressure. The resulting residue was dissolved in CH_2Cl_2 (150 mL) and then extracted with aqueous NaOH (4 M, 4 x 25 mL). The organic phase was separated, dried over anhydrous $MgSO_4$, filtered and evaporated by rotary evaporator. The product was further purified by column chromatography using 10% ethyl acetate in hexane as an eluent yielding a yellow liquid (0.20 g, 35% yield). 3-(2-bromoethoxy)benzaldehyde (6): 1H NMR (400 MHz, $CDCl_3$) δ (ppm): 9.95 (s, 1H, ArCHO), 7.47-7.13 (m, 4H, ArH), 4.33 (t, 2H, $J = 6.0$ Hz, $\underline{CH_2OAr}$), 3.65 (t, 2H, $J = 6.0$ Hz, $\underline{CH_2Br}$).

2.6.3 Preparation of *m*-bisbenzaldehyde-*p*-nitrocalix[4]arene (7)

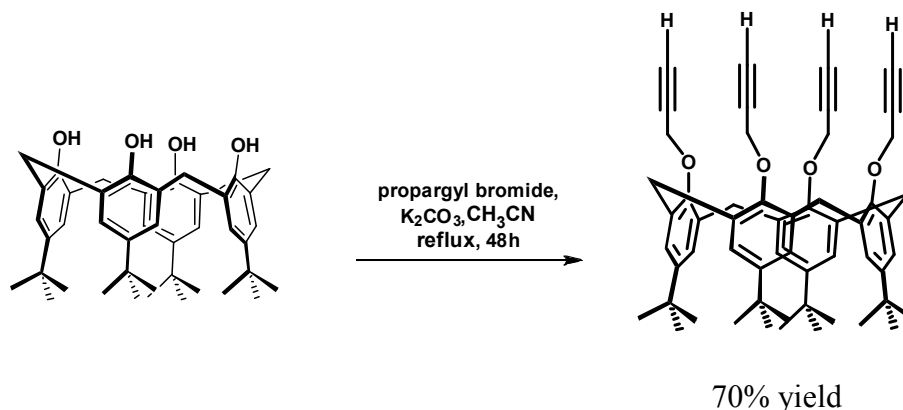


A mixture of **5** (0.38 g, 0.63 mmol), Na₂CO₃ (1.35 g, 6.40 mmol) and Bu₄NBr (0.04 g, 0.1 mmol) in CH₃CN (50 mL) was stirred for 30 minutes at room temperature and 3-(2-bromoethoxy)benzaldehyde (**6**) (0.50 g, 1.70 mmol) was then added dropwise. The reaction mixture was refluxed for 5 days at 90°C and then allowed to cool to room temperature. The mixture was filtered and washed with acetone (50 mL) and CH₂Cl₂ (50 mL). The combined organic layers were evaporated under reduced pressure. The resulting residue was dissolved in CH₂Cl₂ (150 mL) and then extracted with aqueous HCl (2 M, 4 x 25 mL). The organic phase was separated, dried over anhydrous MgSO₄, filtered and evaporated by rotary evaporator. The product was purified by column chromatography using 80% ethyl acetate in hexane as an eluent and was further purified by crystallization in acetone and CHCl₃ yielding a yellow solid (0.40 g, 84% yield) which was a mono-substitution product.

m-bisbenzaldehyde-*p*-nitrocalix[4]arene (**7**): ¹H NMR (400 MHz, DMSO-*d*₆) δ (ppm): 10.28 (s, 1H, ArCHO), 8.50-7.77 (m, 12H, aldehyde-ArH and calix-ArH), 7.61 (s, 3H, OH), 4.98 (d, 2H, *J* = 12.5 Hz, ArCH₂Ar), 4.72 (d, 4H, *J* = 13.7 Hz, OCH₂CH₂O), 4.47 (d, 2H, *J* = 12.8 Hz, ArCH₂Ar), 3.81 (m, 2H, ArCH₂Ar).

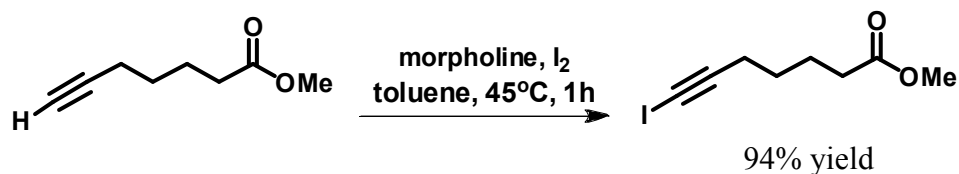
2.7 Synthesis of diacetylene calix[4]arene

2.7.1 Preparation of tetra(propargyloxy)-*tert*-butylcalix[4]arene (**8**)



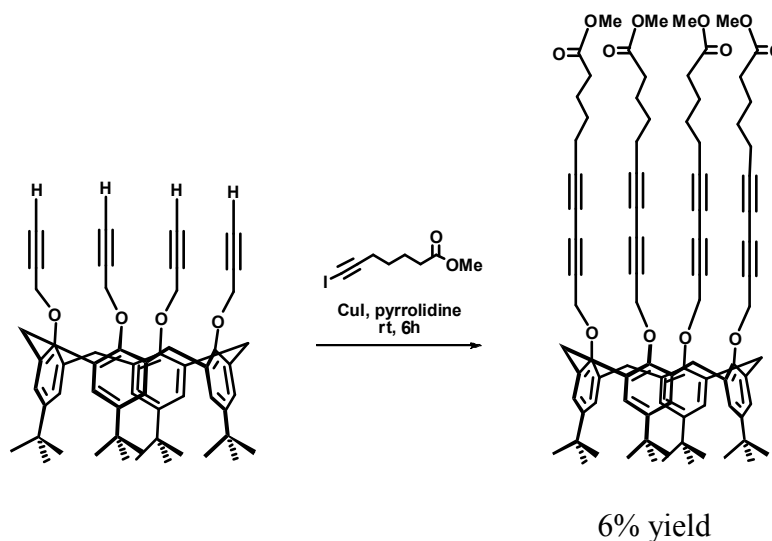
A mixture of *p-tert*-butyl calix[4]arene (10.00 g, 15.00 mmol), K_2CO_3 (43.37 g, 0.31 mol) in CH_3CN (300 mL) was stirred for 30 minutes at room temperature. A solution of propargyl bromide (23.33 g, 0.15 mol) was added dropwise over 30 minutes. The reaction mixture was refluxed for 5 days at $90^\circ C$ and then allowed to cool to room temperature. The mixture was filtered and washed with CH_2Cl_2 200 mL. The reaction mixture was quenched with aqueous HCl (2 M, 100 mL), extracted with CH_2Cl_2 (3 x 100 mL), and the combined organic layers were washed with brine (100 mL), dried over anhydrous $MgSO_4$, filtered and evaporated by rotary evaporator. The crude mixture was purified by crystallization in $CHCl_2/MeOH$ to afford a white solid (8.64 g, 70% yield). *tetra(propargyloxy)-tert-butylcalix[4]arene* (**8**): 1H NMR (400 MHz, $CDCl_3$) δ (ppm): 6.78 (s, 8H, Ar-H), 4.80 (s, 8H, OCH_2), 4.60 (d, 4H, $J = 13.2$ Hz, $ArCH_2Ar$), 3.16 (d, 4H, $J = 13.2$ Hz, $ArCH_2Ar$), 2.48 (t, 3H, $J = 2.4$ Hz, CCH), 1.07 (s, 36H, $(CH_3)_3$). ^{13}C -NMR (100 MHz, $CDCl_3$) δ (ppm): 152.4, 145.5, 134.3, 124.9, 81.2, 74.3, 61.0, 33.9, 32.3, 31.3.

2.7.2 Preparation of methyl-6-iodoheptynoate (9)



To a solution morpholine (27.88 mL, 0.32 mol) in toluene (300 mL) was added iodine (12.24 g, 48.00 mmol) and the mixture was shielded from light and stirred at 45°C for 1 hour. 6-Heptynoic acid (3.31 g, 0.02 mol) in toluene (10 mL) and the reaction mixture was stirred at 45°C for 1 hour. The reaction mixture was cooled to room temperature. The mixture was filtered and washed with diethylether (100 mL) and extracted with a saturated aqueous solution of Na₂S₂O₃ (100 mL), dried over anhydrous MgSO₄, filtered and evaporated by rotary evaporator. The crude mixture was purified by column chromatography using 10% ethyl acetate in hexane as an eluent yielding a yellow liquid (5.89 g, 94% yield). *methyl-6-iodoheptynoate (9)*: ¹H NMR (400 MHz, CDCl₃) δ (ppm): 3.64 (s, 3H, C=OOCH₃), 2.36 (t, 2H, *J* = 7.0 Hz, C=OCH₂), 2.30 (t, 2H, *J* = 7.4 Hz, ICCCH₂), 1.73-1.66 (m, 2H, C=OCH₂CH₂), 1.56-1.48 (m, 2H, ICCCH₂CH₂). ¹³C-NMR (100 MHz, CDCl₃) δ (ppm): 173.7, 93.9, 51.5, 33.4, 27.8, 23.9, 20.4.

2.7.3 Preparation of 25,26,27,28-tetra(methylheptynoate)oxy-*tert*-calix[4]arene (**10**)



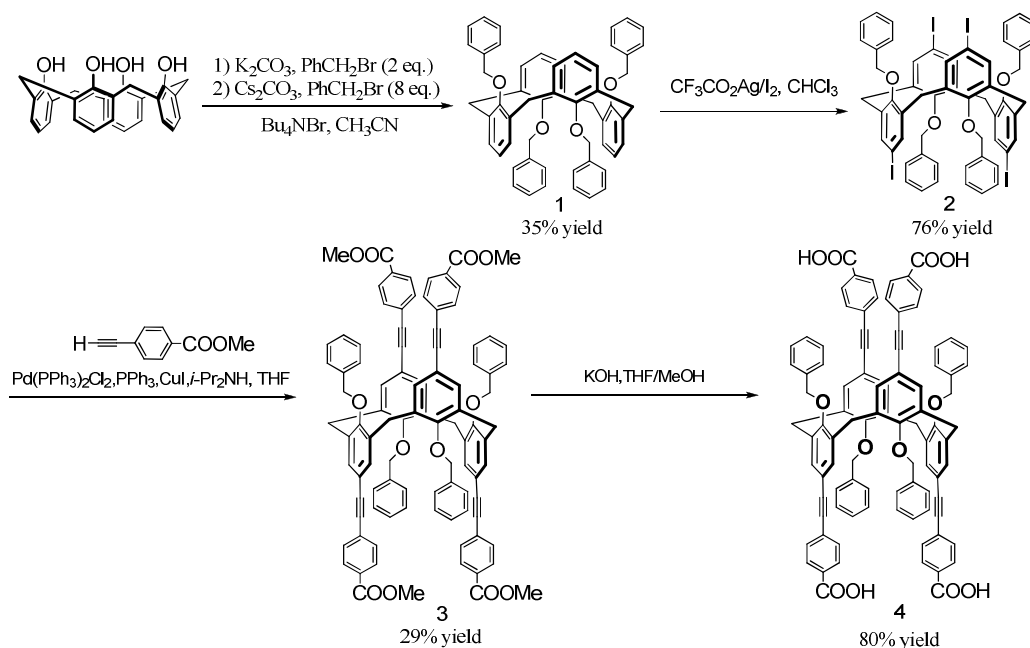
To a mixture of **8** (0.45 g, 0.57 mmol), methyl-6-iodoheptynoate (1.78 g, 6.69 mmol) in pyrrolidine (3 mL, 0.04 mol) was added copper(I)iodide (0.07 g, 0.35 mmol). After stirring at room temperature for 6 hours, the reaction mixture was then added with a saturated aqueous of NH_4Cl (50 mL) and extracted with diethylether (3 x 50 mL). The combined organic layers were dried over anhydrous MgSO_4 , filtered and evaporated by rotary evaporator. The crude mixture was purified by column chromatography using 10% methanol in ethyl acetate as an eluent yielding a yellow liquid (0.05 g, 6% yield). 25,26,27,28-tetra(methylheptynoate)oxy-*tert*-calix[4]arene (**10**): ^1H NMR (400 MHz, CDCl_3) δ (ppm): 6.67 (s, 8H, ArH), 4.83 (s, 8H, ArOCH₂), 4.54 (d, 4H, $J = 12.9$ Hz, ArCH₂Ar), 3.66 (s, 12H, C=OCH₃), 3.17 (d, 4H, $J = 12.9$ Hz, ArCH₂Ar), 2.36 (m, 4H, CH₂(CH₂)₃C=OOCH₃ and CH₂C=OOCH₃), 1.78-1.71 (m, 2H, CH₂CH₂C=OOCH₃), 1.63-1.55 (m, 2H, CH₂(CH₂)₂C=OOCH₃), 1.06 (s, 36H, (CH₃)₃).

CHAPTER III

RESULTS AND DISCUSSION

3.1 Synthesis and characterization of 25,26,27,28-tetrabenzoyloxy-4-ethynylbenzoic acid calix[4]arene (**4**)

The synthetic route for 25,26,27,28-tetrabenzoyloxy-4-ethynylbenzoic acid calix[4]arene (**4**) is presented in Scheme 3.1. The synthesis began with a nucleophilic substitution reaction on the phenolic oxygen of calix[4]arene with benzylbromide using K_2CO_3 and Cs_2CO_3 base, consecutively, to give 1,3 alternate tetrabenzyl *O*-substituted calix[4]arene **1** in moderate yield (35%) because of steric effect and the mixture of mono-, di- and tri-substitution. Previously works have shown that the reaction of calix[4]arenes with alkylating agent in CH_3CN in the presence of K_2CO_3 and Cs_2CO_3 is a well established method to obtain tetraalkoxycalix[4]arenes fixed in the 1,3-alternate conformation [55-58]. The iodination at the *para* position of the phenol rings of calix[4]arene **1** with CF_3CO_2Ag/I_2 in $CHCl_3$ gave the corresponding tetraiodocalix[4]arene **2** in good yield of 76%. The next step was a Sonogashira copper-palladium catalyzed cross-coupling reaction between compound **2** and methyl 4-ethynylbenzoate to give compound **3** in 29% yield. The low yield occurred with homo-coupling of methyl 4-ethynylbenzoate and steric effect. The desired product **4** was obtained in high yield (80%) from basic hydrolysis of **3** to convert the methyl ester to carboxylic acid. All new compounds were characterized by 1H NMR spectroscopy, IR spectroscopy, elemental (C, H, N) analysis and high resolution mass spectrometry (HRMS).



Scheme 3.1 Synthesis of 25,26,27,28-tetrabenzoyloxy-4-ethynylbenzoic acid calix[4]arene.

The 1H NMR spectra of compound 1-4 in $CDCl_3$ and $DMSO-d_6$ are shown in Figure 3.1. All the signals can be assigned to all the protons in each corresponding structure. The methylene bridge protons ($ArCH_2Ar$) of calix[4]arene appeared around 3.6-3.8 ppm as a singlet peak characteristic for the 1,3 alternate conformation. Upon iodination of 1, the triplet and doublet aromatic signals of calix[4]arene phenyl ring around 6.5-6.7 ppm was changed to a singlet peak at 7.2 ppm signifying a full substitution at the *para* position of all four phenyl rings of calix[4]arene that is in good agreement with the structure of tetraiodocalix[4]arene 2. The Sonogashira coupling of 2 with methyl 4-ethynylbenzoate afforded compound 3 which showed signal of methyl ester protons as a singlet at 3.98 ppm and two new doublet signals at 7.3 ppm and 7.9 ppm corresponding to the aromatic protons of the four newly mounted *p*-substituted benzoate moieties. The complete hydrolysis of 3 to tetracarboxylic acid 4 was evidenced by the total disappearance of the methyl ester proton signal at 3.98 ppm.

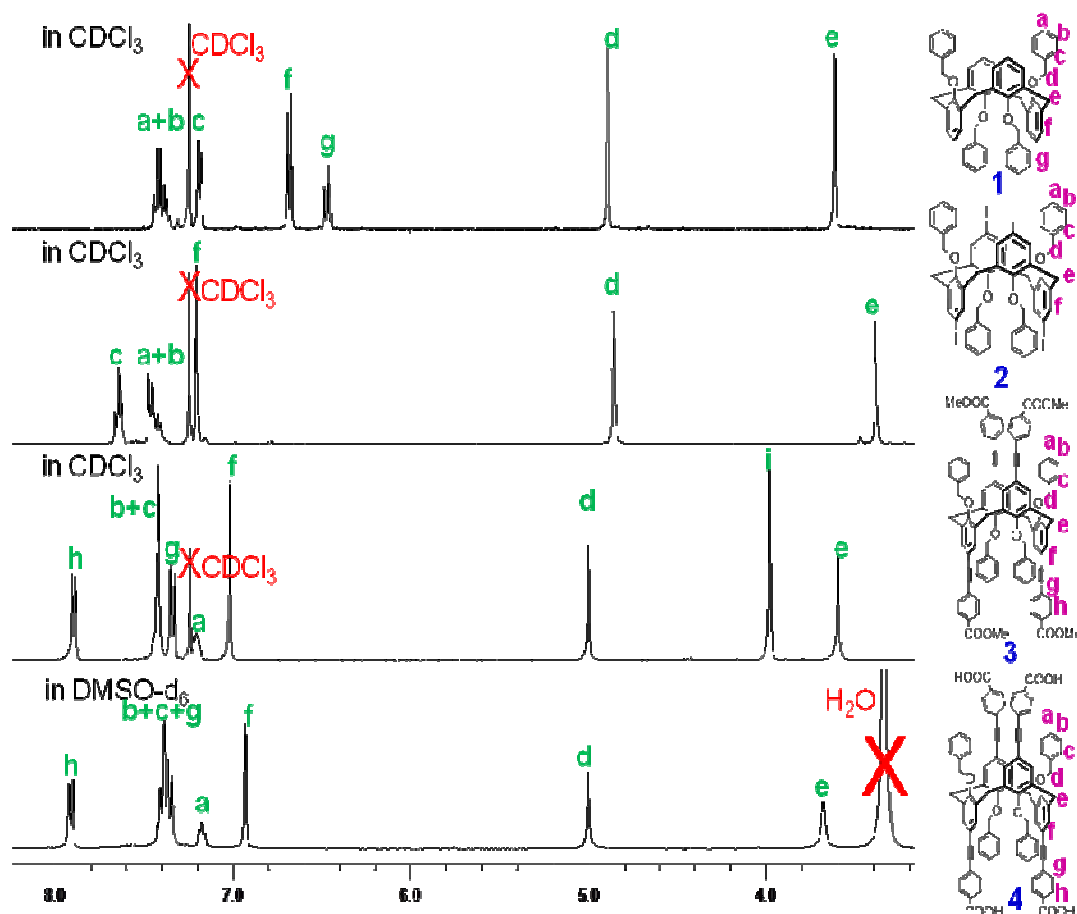


Figure 3.1 ¹H NMR spectra of compound 1-4.

The IR spectra of compound 2-4 are shown in Figure 3.2. Going from compound 2 to compound 3, the IR-spectra showed additional peak at 1700 cm⁻¹ and 2200cm⁻¹ corresponding to C=O and C≡C stretching vibrations, respectively, of the 4-ethynylbezoate units. For compound 4, a new broad OH stretching band appearing at 3600-3000 cm⁻¹ and a shift of C=O stretching band to lower energy, 1690 cm⁻¹ concurred well with the successful hydrolysis of the ester groups to the carboxylic groups.

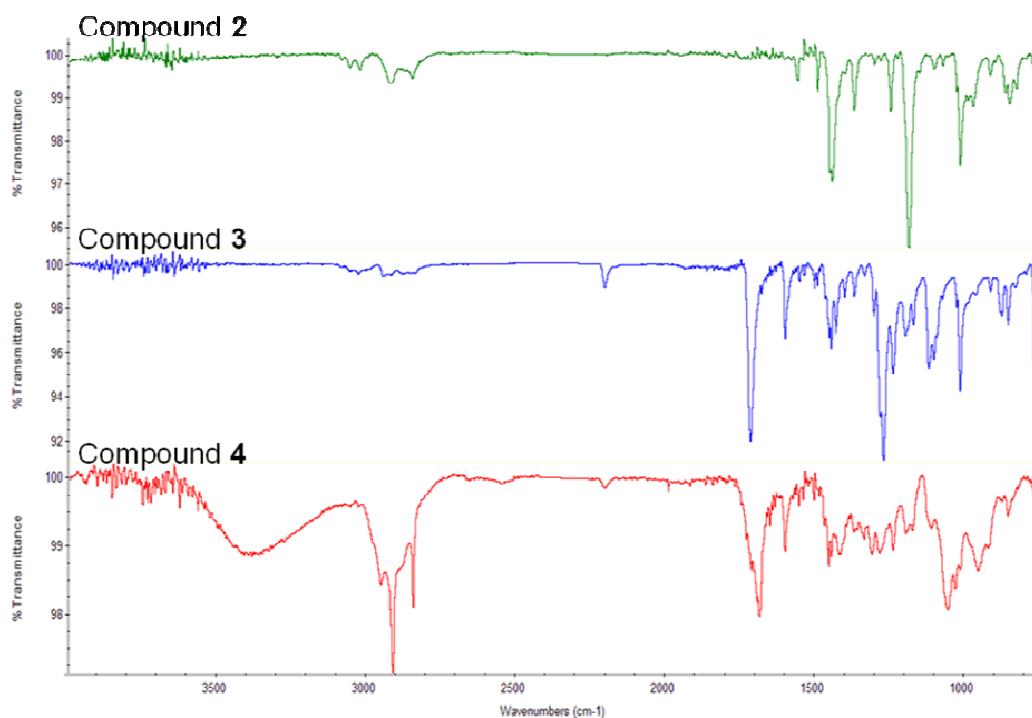






Figure 3.2 IR spectra of compound 2-4.

Other techniques used to confirm the new products are elemental analysis and the HRMS of which results are shown in Table 3.1. The observed elemental percentage and molecular ion mass were consistent with the values calculated from the formula associated with each molecular formula of compound 1-4.

Table 3.1 Elemental (C, H, N) analysis and HRMS mass spectrometry of compound 1-4

Structure	Analytical found C:H	Calculation C:H	HRMS (ESI) found	Calculation Mass
 1	85.46 : 5.95	85.68 : 6.16 $C_{56}H_{48}O_4$	-	-
 2	50.47 : 3.33	52.20 : 3.44 $C_{56}H_{44}I_4O_4$	1310.9415 [2 + Na ⁺]	1310.9316 $C_{56}H_{44}I_4O_4Na$
 3	81.30 : 5.11	81.34 : 5.12 $C_{96}H_{72}O_{12}$	1440.4862 [3 + Na ⁺]	1440.4955 $C_{96}H_{72}O_{12}Na$
 4	78.26 : 4.99	78.06 : 4.98 $C_{92}H_{64}O_{12} + 3H_2O$	1399.3753 [4 + K ⁺]	1399.4035 $C_{92}H_{64}O_{12}K$

3.2 Photophysical property study

The normalized electronic absorption and fluorescence spectra of compound **3** and **4** are presented in Figure 3.3 and their photophysical data are presented in Table 3.2. The tetraester **3** was insoluble in water and thus its absorption and emission spectra were acquired from its dimethylsulfoxide (DMSO) solution. The maximum absorption was observed at 317 nm (λ_{max}) corresponding to the π - π^* transition of the alkoxyphenylethynylbenzoate chromophore [59] with molar extinction coefficient of $6.8 \times 10^4 \text{ M}^{-1}\text{cm}^{-1}$. The solution showed a maximum emission at 421 nm (λ_{em}) upon excitation at 317 nm with quantum efficiency of 0.40.

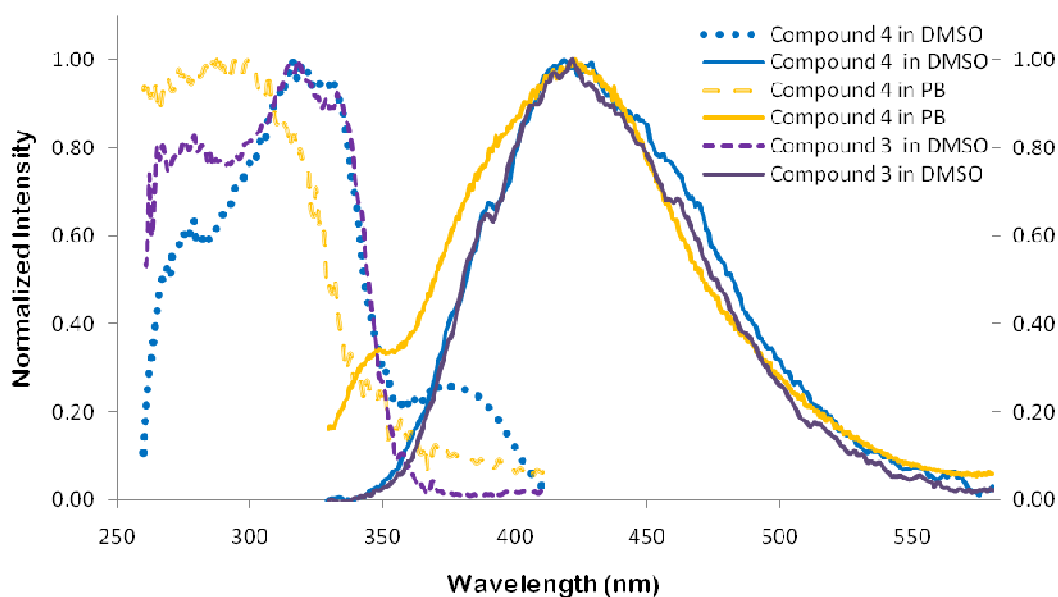


Figure 3.3 Normalized spectral overlap between absorption (dashed line) and emission spectra (solid line) of compound **3** and **4**.

Table 3.2 Photophysical properties of compound **3** in DMSO and compound **4** in DMSO and 50 mM phosphate buffer pH 8.0

Compound	Solvent	Absorption		Fluorescence	
		λ_{\max} (nm)	ε ($M^{-1} \text{ cm}^{-1}$)	λ_{\max} (nm)	Φ_F
3	DMSO	317	6.8×10^4	421	0.40
4	DMSO	317	8.9×10^4	418	0.36
	PB	300	5.4×10^4	425	0.006

The tetracarboxylic acid **4** in DMSO gave the λ_{\max} and λ_{em} at 317 and 418 nm, respectively. Since the absorption and emission spectra of **3** and **4** in DMSO were not significantly different, it is likely that their energy levels in ground state and excited state were quite similar. In the aqueous medium of phosphate buffer pH 8.0, **4** exhibited a hypsochromic shift to give the λ_{\max} at 300 nm. Despite the difference in the absorption spectra, the emission spectra of **4** in DMSO and the buffer solution closely resembled to each other. This observation may be explained according to the schematic presentation shown in Figure 3.4a and b. In the basic aqueous system, the ground state of **4** mostly exists in the carboxylate form stabilized by hydration. Upon excitation, **4** should adopt a higher charged form, internal charge-transfer (ICT) state, which would be further stabilized by the hydration process.

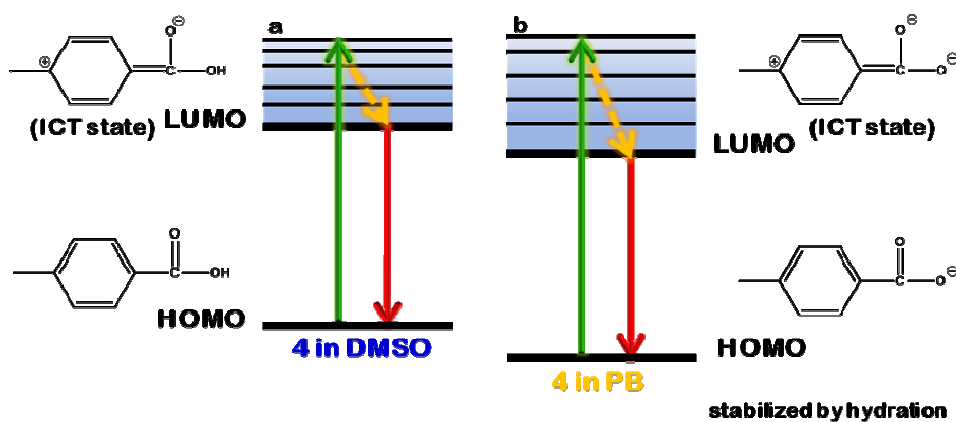


Figure 3.4 Proposed electronic energy levels of compound **4** in DMSO and phosphate buffer pH 8.0.

The molar extinction coefficient of compound **4** in DMSO and in phosphate buffer pH 8.0 are $8.9 \times 10^4 \text{ M}^{-1}\text{cm}^{-1}$ and $5.4 \times 10^4 \text{ M}^{-1}\text{cm}^{-1}$, respectively. The slightly lower molar extinction coefficient of compound **4** in aqueous media is probably due to the smaller dipole moment change upon the excitation of **4** in the carboxylate form. The quantum efficiencies of **4** in DMSO and phosphate buffer were 0.36 and 0.006, respectively. The poor quantum efficiency of **4** in the aqueous medium may be attributed to the decrease of emissive rate (Γ) of the ICT state which is stabilized by water molecules.

3.3 Surfactant enhancement of 25,26,27,28-tetrabenzoyloxy-4-ethynylbenzoic acid calix[4]arene (4)

From literature reviews, the quantum yield of a fluorescence compound can be improved by using surfactants that reduce either its aggregation or its environmental polarity [38, 60-61]. In this study, 9 types of surfactants (3 anionic, 3 cationic and 3 non-ionic) with the structures shown in Figure 3.5 were investigated for their fluorescence enhancement on compound **4**. The fluorescence spectra obtained from the solutions of **4** ($1 \mu\text{M}$ in 50 mM phosphate buffer pH 8.0) in the absence and presence of the surfactants 0.1 mM are presented in Figure 3.6. The results clearly showed that the non-ionic surfactants i.e. Tween 20, Triton X-100 and Brij 58 gave greater fluorescence enhancement than the cationic (TTAB, DTAB and HTAB) and anionic (SDS, SDC and SDBS) surfactants. These results agreed well with the lower critical micelle concentration (CMC) of the non-ionic surfactants in comparison with the cationic and anionic surfactants (CMC values of all surfactants [62] are provided in Figure 3.5).

Type of surfactant	Name	Structure	CMC (mM)
Anionic	Sodium dodecyl sulfate (SDS)		8.300
	Sodium dodecanoate (SDC)		27.800
	Dodecylbenzenesulfonic acid, Sodium salt (SDBS)		1.200
Cationic	Trimethyl tetradecylammonium bromide (TTAB)		3.000
	Dodecyltrimethylammonium bromide (DTAB)		15.600
	Hexadecyltrimethylammonium bromide (HTAB)		0.920
Nonionic	Tween 20		0.060
	Triton X-100		0.200
	Brij 58		0.077

Figure 3.5 Table of 9 types of surfactants (3 anionic, 3 cationic and 3 non-ionic) with the structures.

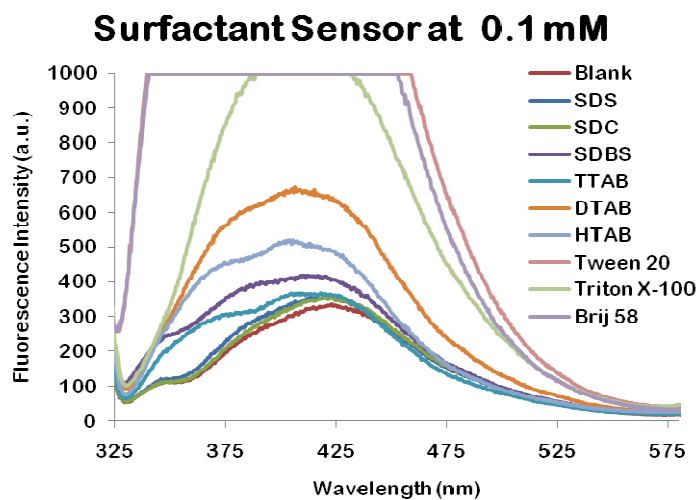


Figure 3.6 Fluorescence intensity of compound **4** ($1 \mu\text{M}$ in 50 mM phosphate buffer pH 8.0) in the presence of 9 surfactants (0.1 mM).

Since the fluorescent signals in the presence of non-ionic surfactants at the above concentration levels were too high to be observed within the instrumental scale, the concentration of **4** and the non-ionic surfactants were reduced by ten times. At this new concentration level, $0.1 \mu\text{M}$ of **4** and 0.01 mM of the surfactants,

the fluorescence signals fit within the instrumental scale that show the enhancement ability order as follows: Brij 58 > Tween 20 > Triton X-100 (Figure 3.7). As Brij 58 exhibited the highest enhancement ability, it was chosen for further investigation.

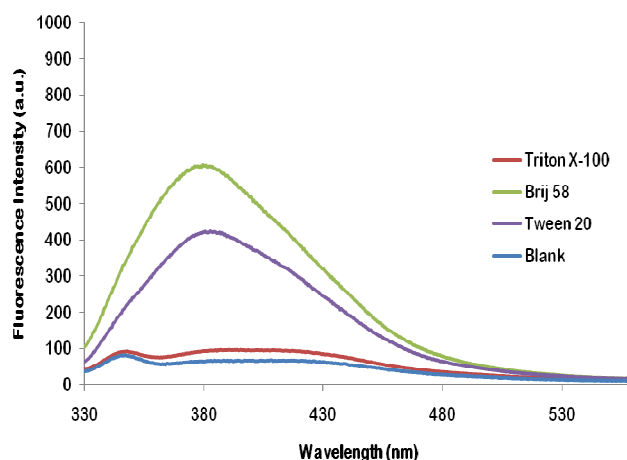


Figure 3.7 Emission spectra of compound **4** (0.1 μM in 50 mM phosphate buffer pH 8.0) with non-ionic surfactants (0.01 mM).

To understand the fluorescence enhancement, the absorption and emission spectra of **4** (1 μM) in the absence and presence of Brij 58 (0.01 mM) are compared as shown in Figure 3.8. The absorption spectra were relatively unchanged while the emission spectra shifted toward shorter wavelength comparing upon the addition of Brij 58. The results suggested that the ICT excited state of **4** within the micelle of the surfactant molecules has higher energy (Figure 3.9a and b) due to less hydrophilic environment. Interestingly, the molar extinction coefficient and quantum yield of **4** in the presence of Brij 58 were $7.5 \times 10^4 \text{ M}^{-1} \text{ cm}^{-1}$ and 0.03, respectively, which were higher than the values measured in the absence of the surfactant (Table 3.3). The increment in the molar extinction coefficient and quantum yield in the presence of Brij 58 is probably associated with reducing hydration process around the fluorophores. The lower hydration level can increase electronic transition dipole moment changes and reduce the stability of the ICT excited state that is in good agreement with the hypsochromic shift of the emission spectrum upon the addition of Brij 58.

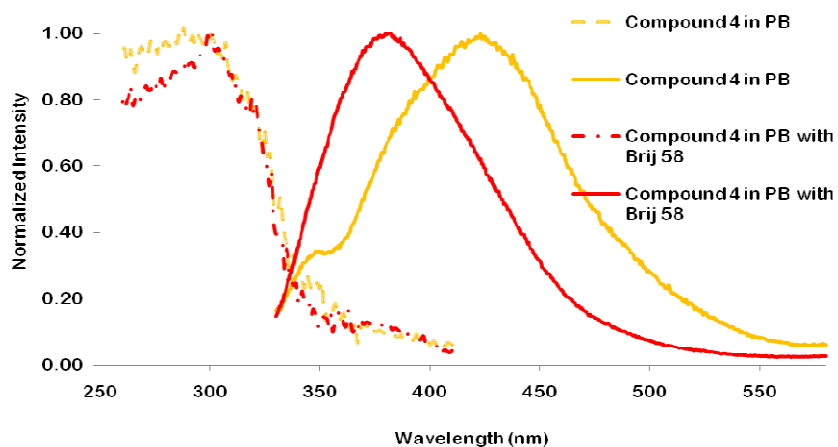


Figure 3.8 Normalized spectral overlap between absorption (dashed line) and emission spectra (solid line) of compound 4.

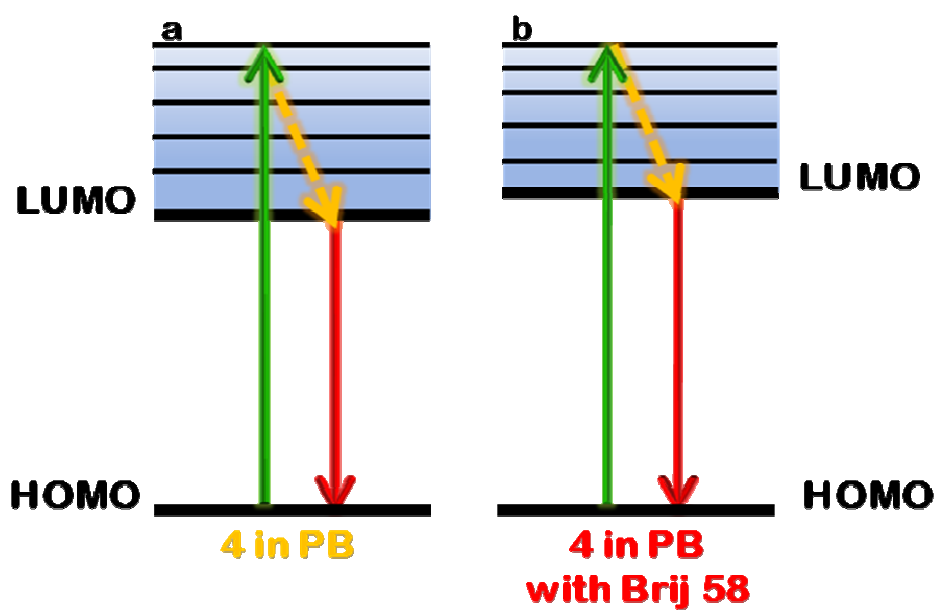


Figure 3.9 Proposed electronic energy levels of compound 4 in phosphate buffer pH 8.0 in the absence and presence of Brij 58.

Table 3.3 Photophysical properties of compound **4** in 50 mM phosphate buffer pH 8.0 in the presence of Brij 58 compared with compound **4** in 50 mM phosphate buffer pH 8.0 in the absence of Brij 58

Compound	Solvent	Absorption		Fluorescence	
		λ_{\max} (nm)	ε ($M^{-1} \text{ cm}^{-1}$)	λ_{\max} (nm)	Φ_F
4	PB	300	5.4×10^4	425	0.006
4	PB with Brij 58	300	7.5×10^4	380	0.03

3.4 Metal ion Sensor

As design, compound **4** in phosphate buffer pH 8.0 was initially tested as a metal ion sensor expecting that its four carboxylate groups can provide metal ion recognition. The fluorogenic responses of **4** (1.0 μM) to 12 metal ions including Ag^+ , Na^+ , Ca^{2+} , Co^{2+} , Cu^{2+} , Fe^{2+} , Hg^{2+} , Mn^{2+} , Ni^{2+} , Pb^{2+} , Zn^{2+} and Fe^{3+} (10 μM) are shown in Figure 3.10. From the spectra, the fluorescence signal of **4** was slightly quenched by the metal ions with no significant selectivity being observed. The low sensitivity and selectivity of the fluorescence quenching is probably due to the strong hydration effect which hinders the coulombic interaction between the fluorophore and metal ions.

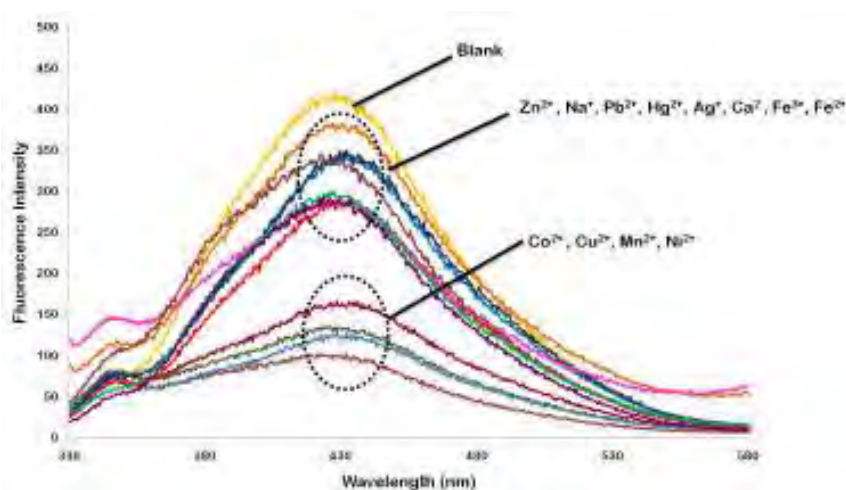


Figure 3.10 Fluorescence spectra of **4** (1 μM in 50 mM phosphate buffer pH 8.0) in the presence of metal ions (100 μM).

As described in the previous section that Brij 58 effectively increased the fluorescent intensity of **4** by the reduction of hydration process, it would be interesting to see if the sensitivity and selectivity of fluorescence quenching of **4** by the metal ions could be enhanced. In the subsequent experiment, the fluorescence quenching of **4** (0.1 μM) buffered solution pH 8.0 in the presence of Brij 58 (10 μM) by the metal ions (100 μM) were investigated. It is important to note that the fluorophore concentration in this experiment was ten times lower than that in the previous experiment in the absence of surfactant due to the high quantum efficiency of the fluorophore/surfactant system. The fluorescence spectra in Figure 3.11 showed that the fluorescence signal of **4** was most effectively quenched by Fe^{2+} and moderately quenched by Fe^{3+} . The quenching mechanism probably involves a selective electrostatic interaction between two carboxylate groups on each calix[4]arene rim of **4** and the iron metal ions. The selectivity is likely to stem from the distance between the two carboxylate groups which governed by the pre-organized calix[4]arene rims [63-64]. The results indicated that **4**/Brij 58 system can be used as a selective sensor for $\text{Fe}^{2+}/\text{Fe}^{3+}$.

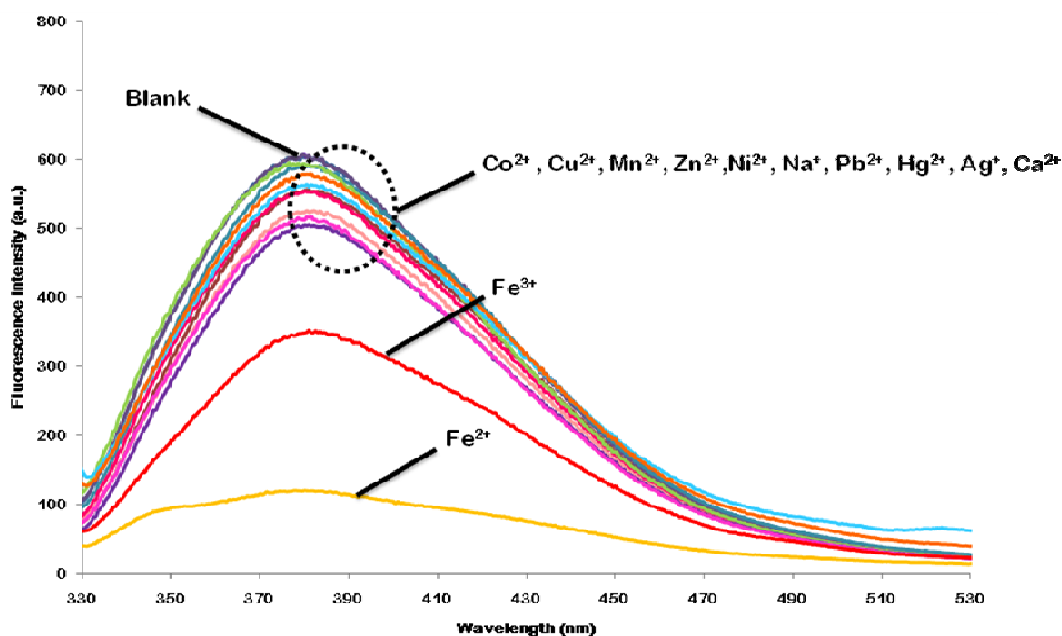


Figure 3.11 Metal ion sensor of **4** (0.1 μM in 50 mM phosphate buffer pH 8.0) with Brij 58 (0.01 mM) and metal ions (100 μM).

In general, the fluorescence quenching signal (I_0/I) can be applied for a quantitative analysis *via* the Stern-Volmer equation:

$$\frac{I_0}{I} = 1 + K_{SV}[Q]$$

In this equation I_0 and I are the fluorescence intensities in the absence and presence of quencher, respectively, Q is the concentration of a quencher. The plot of (I_0/I) against the concentration of Fe^{2+} and Fe^{3+} gave linear lines with the slopes of $3.5 \times 10^4 M^{-1}$ and $8.6 \times 10^3 M^{-1}$ corresponding to the Stern-Volmer constants (K_{SV}) for Fe^{2+} and Fe^{3+} quenchers, respectively (Figure 3.12). These linear relationships between the quenching signals and the concentrations of the metal ions are useful for quantitative determination of Fe^{2+} and Fe^{3+} concentrations in samples containing each corresponding ion species.

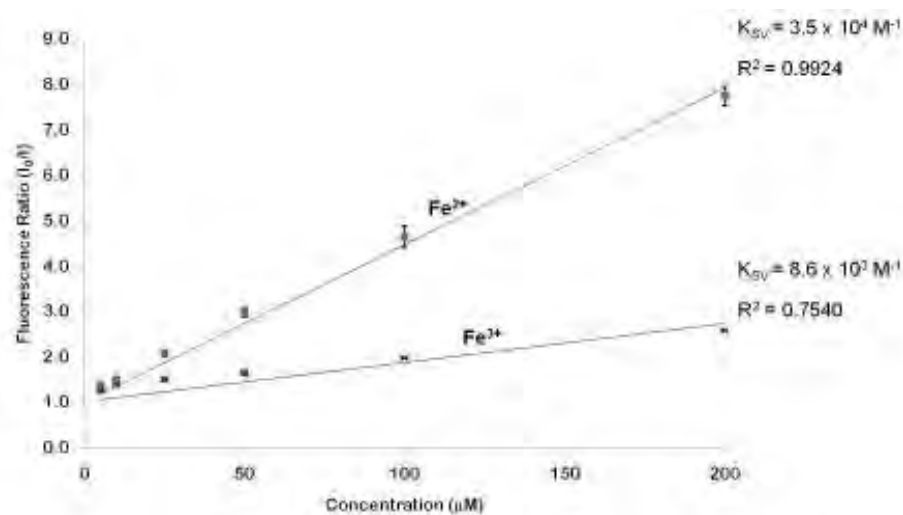
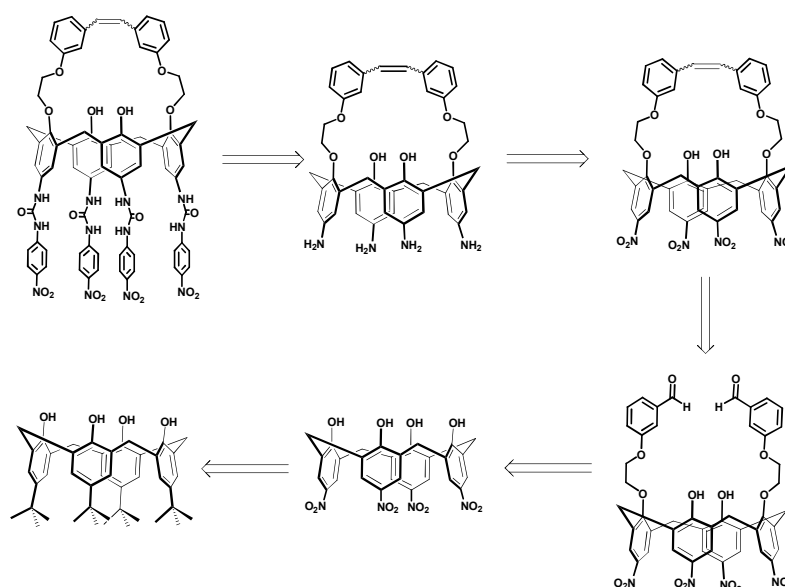


Figure 3.12 Stern-Volmer plots for compound **4** without and with Brij 58 in the presence of Fe^{2+} and Fe^{3+} .

3.5 Synthesis attempt of stilbene-bridged calix[4]arene

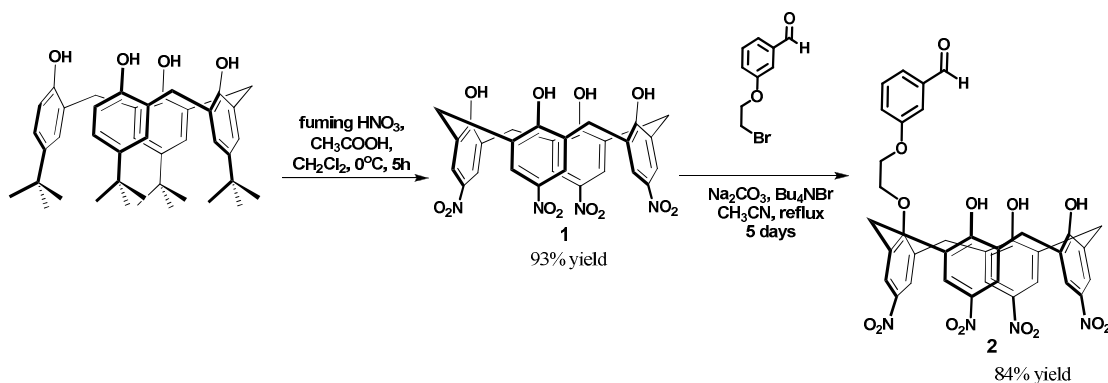
The synthesis of stilbene-bridged calix[4]arene followed the retrosynthesis shown in Scheme 3.2. The synthesis started from the nitration of *p-tert*-butyl calix[4]arene. The reaction of the two equivalents of 3-(2-bromoethoxy)benzaldehyde with two phenol rings of calix[4]arene gave bis-benzaldehyde *p*-nitrocalix[4]arene. The intramolecular reductive coupling of the benzaldehyde moieties of bis-benzaldehyde *p*-nitrocalix[4]arene led to the formation of stilbene-bridged calix[4]arene. The desired product was obtained through the reduction and then substituted with *p*-nitrophenylisocyanate.



Scheme 3.2 Retrosynthesis of stilbene-bridged calix[4]arene.

The attempted synthesis started with nitration of *p-tert*-butyl calix[4]arene with fuming HNO_3 and glacial acetic acid which gave *p*-nitrocalix[4]arene in 93% yield. The nucleophilic substitution reaction of *p*-nitrocalix[4]arene with 3-(2-bromoethoxy)benzaldehyde using Na_2CO_3 as a base in CH_3CN gave a mono-substitution product in 84% yield. Next, the attempt to incorporate two *m*-ethoxybenzaldehyde to tetranitrocalix[4]arene **1** by an *O*-alkylation of *m*-(2-bromoethoxy)benzaldehyde on the calix[4]arene rim using K_2CO_3 gave only the mono-substituted product **2** in 84% yield. Several further attempts to converse this mono-substituted product **2** to the desired di-substituted product using other bases

such as Cs_2CO_3 and NaH were unsuccessful. Hence, the desired stilbene-bridged calix[4]arene could not be synthesized.



Scheme 3.3 Synthesis of mono-substituted *m*-benzaldehyde-*p*-nitrocalix[4]arene.

The $^1\text{H-NMR}$ spectrum of mono-substitution product of *m*-benzaldehyde-*p*-nitrocalix[4]arene in $\text{DMSO-}d_6$ is shown in Figure 3.13. All the signals can be assigned according to their structures. The methylene bridge protons (ArCH_2Ar) of calix[4]arene around 3.4-4.6 ppm represent a mono-substitution product. The ethylene protons ($\text{OCH}_2\text{CH}_2\text{O}$) appeared at 4.4 ppm. Moreover, the proton signals at 7.4-8.2 ppm correspond to aromatic protons and aldehyde proton at 10.0 ppm.

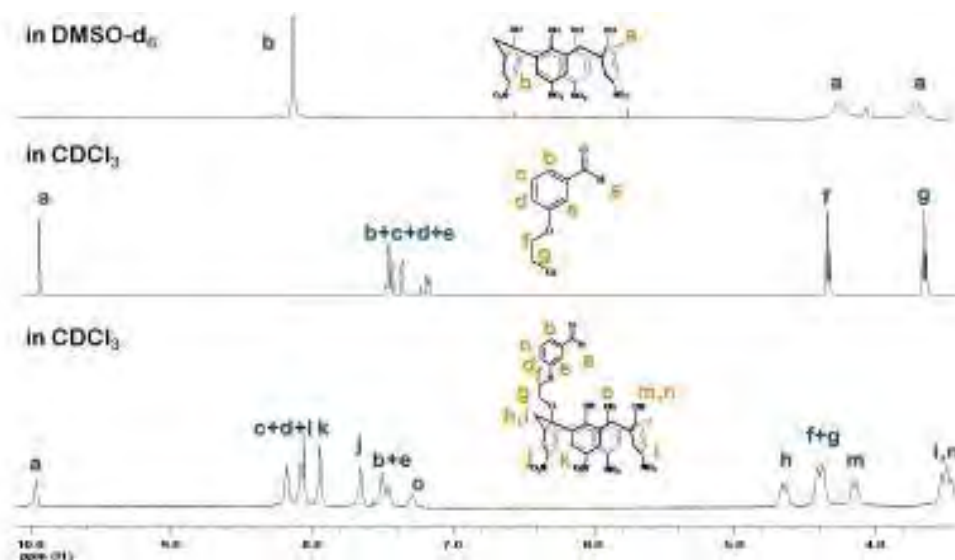
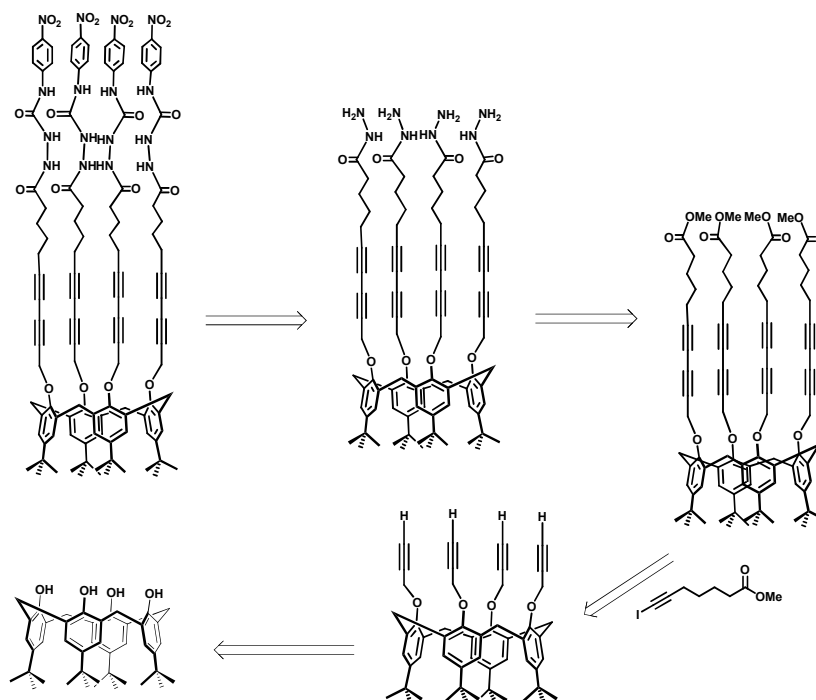


Figure 3.13 $^1\text{H-NMR}$ spectra of mono-substitution product of *m*-benzaldehyde-*p*-nitrocalix[4]arene in $\text{DMSO-}d_6$.

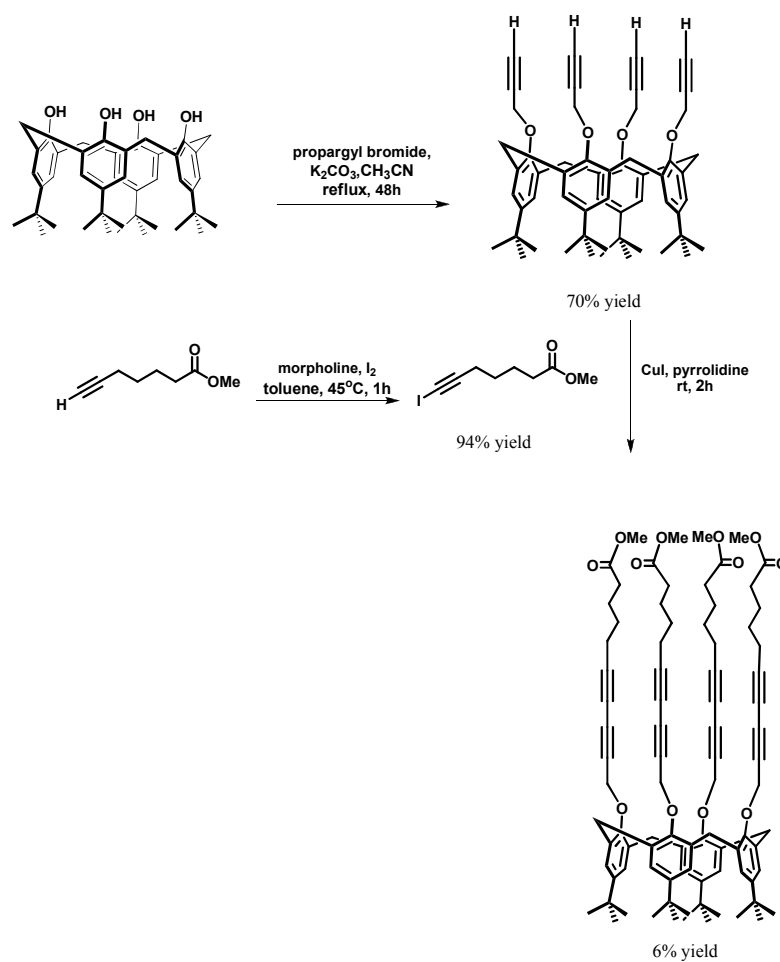
3.6 Synthesis attempt of diacetylene calix[4]arene

The synthesis of diacetylene calix[4]arene followed the retrosynthesis shown in Scheme 3.4. The synthesis began with the alkylation using excess propargyl bromide. The reaction of the four equivalents of iodoalkyne through Cadiot-Chodkiewicz cross-coupling reaction using copper(I)chloride as catalyst gave tetra(methylheptynoate)oxy-*tert*-calix[4]arene. The desired product was obtained through the substitution of hydrazine and *p*-nitrophenylisocyanate, respectively.



Scheme 3.4 Retrosynthesis of diacetylene calix[4]arene.

The synthesis of diacetylene calix[4]arene as shown in Scheme 3.5 started with a nucleophilic substitution reaction on the phenolic proton of calix[4]arene with propargyl bromide in the presence of K_2CO_3 as a base at reflux temperature of acetonitrile in 70% yield. The next step was synthesized from Cadiot-Chodkiewicz cross-coupling reaction with iodoalkyne using copper(I)chloride as catalyst giving the product in low yield (6% yield) and the yield of this product cannot be improved because of the predominant by-products from the homo-coupling and the reactions which resulted in the mono-, di- and tri-substituted mixture which as confirmed by TLC technique and NMR spectra. Hence, diacetylene calix[4]arene (**7**) cannot be synthesized.



Scheme 3.5 Synthesis of 25,26,27,28-tetra(methylheptynoate)oxy-*tert*-calix[4]arene.

The 1H -NMR spectrum of 25,26,27,28-tetra(methylheptynoate)oxy-*tert*-calix[4]arene in $CDCl_3$ is shown in Figure 3.14. All the signals can be assigned according to their structures. The *tert*-butyl protons appeared at 1.0 ppm, the alkyl chain of methylheptynoate appeared around 1.5-1.8 and 2.3 ppm and the methoxy protons at 3.6 ppm. The methylene bridge protons ($ArCH_2Ar$) of calix[4]arene around 3.2 and 4.6 ppm represent a tetra-substitution product in cone formation. The ethylene protons (OCH_2CH_2O) appeared at 4.8 ppm. Moreover, the proton signals at 6.8 ppm correspond to aromatic protons.

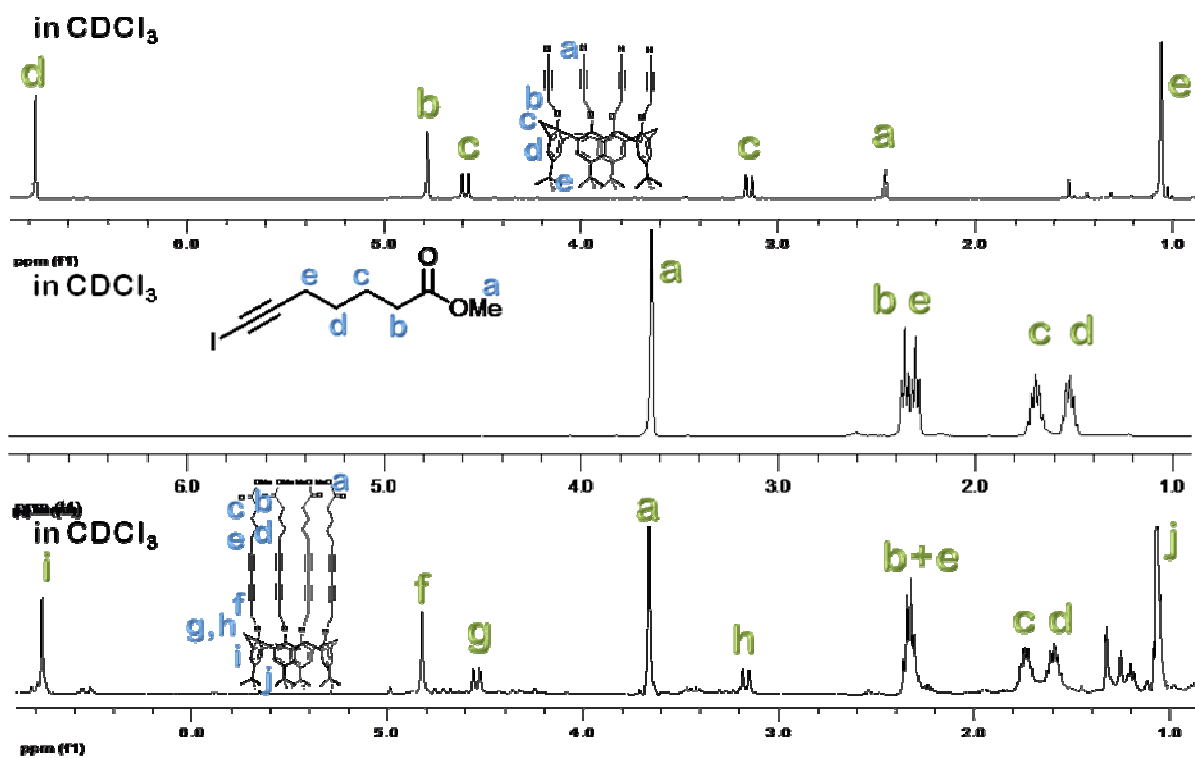


Figure 3.14 $^1\text{H-NMR}$ spectra of 25,26,27,28-tetra(methylheptynoate)oxy-*tert*-calix[4]arene in CDCl_3 .

CHAPTER IV

CONCLUSION

4.1 Conclusion

The water soluble 1,3-alternate calix[4]arene containing ethynylbenzoic acid was successfully synthesized. The comparison of photophysical properties of the compound in dimethylsulfoxide and phosphate buffer indicated that the hydration stabilizing internal charge-transfer (ICT) state was responsible for the low quantum yield observed in the aqueous media. Addition of non-ionic surfactants, especially for Brij 58, to the aqueous solution of the tetracarboxylic calix[4]arene derivative effectively increased the quantum efficiency presumably by the reduction of the hydration process. The fluorophore/Brij 58 system could be developed into Fe^{2+} and Fe^{3+} metal ion sensor through a fluorescent quenching process. The selective quenching effect probably associated with the electrostatic interaction between the iron metal ions and the two carboxylate groups appropriately positioned on each calix[4]arene rim.

4.2 Suggestion for future works

The future work should be focused on

1) Synthesis of water soluble 1,3-alternate calix[4]arenes containing ethynylbenzene with other functionalities i.e. salicylaldehyde and ammonium for sensing applications of other species.

2) Substitution of the oligo(ethyleneglycol) chains on the phenolic hydroxyl groups of the calix[4]arene platform to improve water solubility.

REFERENCES

- [1] Lehn, J. M. Supramolecular chemistry. *Science*. 260 (1993): 1762-1763.
- [2] Rotello, V. M.; Thayumanavan, S. *Molecular recognition and polymers: Control of polymer structure and self-Assembly*; John Wiley & Sons, Inc., Hoboken: New Jersey. 2008.
- [3] Oshovsky, G. V.; Reinhoudt, D. N.; Verboom, W. Supramolecular chemistry in water. *Angew. Chem. Int. Ed.* 46 (2007): 2366-2393.
- [4] Nguyen, S. T.; Gin, D. L.; Hupp, J. T.; Zhang, X. Supramolecular chemistry: Functional structures on the mesoscale. *PNAS*. 98 (2001): 11849-11850.
- [5] Meloen, R.; Timmerman, T.; Langedijk, H. Bioactive peptides based on diversity libraries, supramolecular chemistry and rational design: A new class of peptide drugs. Introduction. *Mol. Divers.* 8 (2004): 57-59.
- [6] Gale, P. A. Supramolecular chemistry, *Annu. Rep. Prog. Chem., Sect. B*. 98 (2002): 581-605.
- [7] Dighe, N. S.; Pattan, S. R.; Musmade, D. S.; Dengale, S. S.; Kalkotwar, R. S.; Gaware, V. M.; Hole, M. B. Supramolecular chemistry: An overview. *RJPBCS*. 1 (2010): 291-301.
- [8] Uhlenheuer, D. A.; Petkau, K.; Brunsveld, Luc. Combining supramolecular chemistry with biology. *Chem. Soc. Rev.* 39 (2010): 2817-2826.
- [9] Schemberg, J.; Schneider, K.; Demmer, U.; Warkentin, E.; Müller, A.; Ermler, U. Towards Biological Supramolecular Chemistry: A variety of pocket-templated, individual metal oxide cluster nucleations in the cavity of a Mo/W-storage protein. *Angew. Chem. Int. Ed.* 46 (2007): 2408-2413.
- [10] Kumar, A.; Ali, A.; Rao, C. P. Photo-physical behavior as chemosensor properties of anthracene-anchored 1,3-di-derivatives of lower rim calix[4]arene towards divalent transition metal ions. *J. Photochem. Photobiol. A*. 177 (2006): 164-169.
- [11] Sun, X. H.; Li, W.; Xia, P. F.; Luo, H. B.; Wei, Y.; Wong, M. S.; Cheng, Y. K.; Shuang, S. Phenyl-calix[4]arene-based fluorescent sensors: cooperative binding for carboxylates. *J. Org. Chem.* 72 (2007): 2419-2426.

- [12] Rashatasakhon, P.; Jaiyu, A.; Rojanathanes, R.; Muangsin, N.; Chaichit, N.; Sukwattanasinitt, M. X-ray guided ^1H NMR analysis of pinched cone calix[4]arenes. *J. Mol. Struct.* 963 (2010): 22-26.
- [13] Cornforth, J. W.; Hart, P. D.; Nicholls, G. A.; Rees, R. J. W.; Stock, J. A. Antituberculous effects of certain surface-active polyoxyethylene ethers. *J. Pharmacol.* 10 (1955): 73-86.
- [14] Cornforth, W. J.; Morgan, E. D.; Potts, K. T. Preparation of antituberculous polyoxyethylene ethers of homogeneous structure. *Tetrahedron.* 29 (1973): 1659-1667.
- [15] Steemers, F. J.; Meuris, H. G.; Verboom, W.; Reinhoudt, D. N.; Van der Tol, E. B. Verhoeven, J. W. Water-Soluble neutral calix[4]arene-lanthanide complexes: Synthesis and luminescence properties. *J. Org. Chem.* 62 (1997): 4229-4235.
- [16] Rostaing, S. P.; Chitry, F.; Spitz, J. A.; Sorin, A.; Re'guillon, A. F.; Lemaire, M. New water-soluble calix[4]arene-bis(benzocrown-6) for caesium-sodium separation by nanofiltration-complexation. *Tetrahedron.* 59 (2003): 10313-10324.
- [17] Liu, Y.; Wang, H.; Wang, L. H.; Zhang, H. Y. Complexation thermodynamics of water-soluble calix[4]arene derivatives with lanthanoid(III)nitrates in acidic aqueous solution. *Thermochim. Acta.* 414 (2004): 65-70.
- [18] Okur, S.; Kuş, M.; Özel, F.; Yılmaz, M. Humidity adsorption kinetics of water soluble calix[4]arene derivatives measured using QCM technique. *Sens. Actuator B.* 145 (2010): 93-97.
- [19] Kim, S. K.; Lee, S. H.; Lee, J. Y.; Lee, J. Y.; Bartsch, R. A.; Kim, J.S. An excimer-based, binuclear, on-off switchable calix[4]crown chemosensor. *J. Am. Chem. Soc.* 126 (2004): 16499-16506.
- [20] Lee, M. H.; Quang, D. T.; Jung, H. S.; Yoon, J.; Lee, H. C.; Kim, J. S. Ion-induced FRET on-off in fluorescent calix[4]arene. *J. Org. Chem.* 72 (2007): 4242-4245.
- [21] Kim, J. S.; Quang, D. T. Calixarene-derived fluorescent probes. *Chem. Rev.* 107 (2007): 3780-3799.

- [22] Kim, S. K.; Kim, S. H.; Kim, H. J.; Lee, S. H.; Lee, S.W.; Ko, J.; Bartsch, R. A.; Kim, J. S. Indium(III)-induced fluorescent excimer formation and extinction in calix[4]arene-fluoroionophores. *Inorg. Chem.* 44 (2005): 7866-7875.
- [23] Choi, J. K.; Kim, S. H.; Yoon, J.; Lee, K. H.; Bartsch, R. A.; Kim, J. S. A PCT-based, pyrene-armed calix[4]crown fluoroionophore. *J. Org. Chem.* 71 (2006): 8011-8015.
- [24] Othman, A. B.; Lee, J. W.; Wu, J. S.; Kim, J. S.; Abidi, R.; Thue'ry, P.; Strub, J. M.; Dorsselaer, A.V.; Vicens, J. Calix[4]arene-based, Hg²⁺-induced intramolecular fluorescence resonance energy transfer chemosensor. *J. Org. Chem.* 72 (2007): 7634-7640.
- [25] Dessingou, J.; Joseph, R.; Rao, C. P. A direct fluorescence-on chemo-sensor for selective recognition of Zn(II) by a lower rim 1,3-di-derivative of calix[4]arene possessing bis-*N*-(2-hydroxynaphthyl-1-methylimine)} pendants. *Tetrahedron Lett.* 46 (2005): 7967-7971.
- [26] Kumar, A.; Ali, A.; Rao, C. P. Photo-physical behavior as chemosensor properties of anthracene-anchored 1,3-di-derivatives of lower rim calix[4]arene towards divalent transition metal ions. *J. Photochem. Photobiol. A.* 177 (2006): 164-169.
- [27] Song, K. C.; Choi, M. G.; Ryu, D. H.; Kim, K. N.; Chang, S. K. Ratiometric chemosensing of Mg²⁺ ions by a calix[4]arene diamide derivative. *Tetrahedron Lett.* 48 (2007): 5397-5400.
- [28] Park, S. Y.; Yoon, J. H.; Hong, C. S.; Souane, R. A Pyrenyl-appended triazole-based calix[4]arene as a fluorescent sensor for Cd²⁺ and Zn²⁺. *J. Org. Chem.* 73 (2008): 8212-8218.
- [29] Joseph, R.; Ramanujam, B.; Acharya, A.; Rao, C. P. Fluorescence switch-on sensor for Cu²⁺ by an amide linked lower rim 1,3-bis(2-picolyl)amine derivative of calix[4]arene in aqueous methanol. *Tetrahedron Lett.* 50 (2009): 2735-2739.

- [30] Wang, H. W.; Feng, Y. Q.; Chen, C.; Xue, J. Q. Two novel fluorescent calix[4]arene derivatives with benzoazole units in 1,3-alternate conformation for selective recognition to Fe^{3+} and Cr^{3+} . *Chin. Chem. Lett.* 20 (2009): 1271-1274.
- [31] Bok, J. H.; Kim, H. J.; Lee, J. Won.; Kim, S. K.; Choi, J. K.; Vicens, J.; Kim, J. S. Selective metal detection in an unsymmetrical 1,3-alternate calix[4]biscrown chemosensor. *Tetrahedron Lett.* 47 (2006): 1237-1240.
- [32] Kim, S. H.; Choi, J. K.; Kim, S. K.; Simb, W.; Kim, J. S. On/off fluorescence switch of a calix[4]arene by metal ion exchange. *Tetrahedron Lett.* 47 (2006): 3737-3741.
- [33] Zhao, Y.; Zhang, X. B.; Han, Z. X.; Qiao, L.; Li, C. Y.; Jian, L. X.; Shen, G. L.; Qin, Yu, R. Q. Highly sensitive and selective colorimetric and off-on fluorescent chemosensor for Cu^{2+} in aqueous solution and living cells. *Anal. Chem.* 81 (2009): 7022-7030.
- [34] Suresh, M.; Mishra, S.; Mishra, S. K.; Suresh, E.; Mandal, A.K.; Shrivastav, A.; Das, A. Resonance energy transfer approach and a new ratiometric probe for Hg^{2+} in aqueous media and living organism. *Org. Lett.* 11 (2009): 2740-2743.
- [35] Hu, Z. Q.; Yang, X. D.; Cui, C.L.; Ding, L.; Lin, C.S.; Lu, H. Y.; Wang, L. 1,8-Anthracene disulfonamide: A simple but highly sensitive and selective fluorescent chemosensor for Hg^{2+} in aqueous media. *Sens. Actuator B.* 145 (2010): 61-65.
- [36] Malhotra, J. D.; Chen, L. Enhanced conjugated polymer fluorescence quenching by dipyridinium-based quenchers in the presence of surfactant. *J. Phys. Chem. B.* 109 (2005): 3873-3878.
- [37] Niamnont, N.; Siripornnoppakhun, W.; Rashatasakhon, P.; Sukwattanasinitt, M. A Polyanionic dendritic fluorophore for selective detection of Hg^{2+} in Triton X-100 aqueous media. *Org. Lett.* 11 (2009): 2768-2771.
- [38] Singh, N.; Kaur, N.; Dunn, J.; MacKay, M.; Callan, J. F. A new fluorescent chemosensor for iron(III) based on the β -aminobisulfonate receptor. *Tetrahedron Lett.* 50 (2009): 953-956.

- [39] Fakih, S.; Podinovskaia, M.; Kong, X.; Collins, H. L.; Schaible, U. E.; Hider, R. C. Targeting the lysosome: Fluorescent iron(III) chelators to selectively monitor endosomal/lysosomal labile iron pools. *J. Med. Chem.* 51 (2008): 4539–4552.
- [40] Que, E. L.; Domaille, D. W.; Chang, C. J. Metals in neurobiology: Probing their chemistry and biology with molecular imaging. *Chem. Rev.* 108 (2008): 1517–1549.
- [41] Lohani, C. R.; Kim, J. M.; Lee, K. H. Facile synthesis of anthracene-appended amino acids as highly selective and sensitive fluorescent Fe^{3+} ion sensors. *Bioorg. Med. Chem. Lett.* 19 (2009): 6069-6073.
- [42] Zhang, X. B.; Cheng, G.; Zhang, W. J.; Shen, G. L.; Yu, R. Q. A fluorescent chemical sensor for Fe^{3+} based on blocking of intramolecular proton transfer of a quinazolinone derivative. *Talanta.* 71 (2007): 171–177.
- [43] Chen, J. L.; Zhuo, S. J.; Wu, Y. Q.; Fang, F.; Li, L.; Zhu, C. Q. High selective determination iron(II) by its enhancement effect on the fluorescence of pyrene-tetramethylpiperidinyl (TEMPO) as a spin fluorescence probe. *Spectroc. Acta Pt. A.* 63 (2006): 438-443.
- [44] Zhang, M.; Gao, Y.; Li, M.; Yu, M.; Li, F.; Li, L.; Zhu, M.; Zhang, J.; Yia, T.; Huang, C. A selective turn-on fluorescent sensor for Fe^{III} and application to bioimaging. *Tetrahedron Lett.* 48 (2007): 3709-3712.
- [45] Oter, O.; Ertekin, K.; Kirilmis, C.; Koca, M.; Ahmedzade, M. Characterization of a newly synthesized fluorescent benzofuran derivative and usage as a selective fiber optic sensor for Fe(III). *Sens. Actuator B.* 122 (2007): 450-456.
- [46] Zhang, L.; Fan, J.; Peng, X. X-ray crystallographic and photophysical properties of rhodamine-based chemosensor for Fe^{3+} . *Spectrochimica Acta Part A.* 73 (2009): 398-402.
- [47] Mitra, A.; Ramanujam, B.; Rao, C. P. 1-(D-Glucopyranosyl-20-deoxy-20-iminomethyl)-2-hydroxynaphthalene as chemo-sensor for Fe^{3+} in aqueous HEPES buffer based on colour changes observable with the naked eye. *Tetrahedron Lett.* 50 (2009): 776-780.

- [48] Noiré, M. H.; Duréault, B. A ferrous ion optical sensor based on fluorescence quenching. *Sens. Actuator B*. 29 (1995): 386-391.
- [49] Hasinoff, B. B. The intracellular iron sensor calcein is catalytically oxidatively degraded by iron(II) in a hydrogen peroxide-dependent reaction. *J. Inorg. Biochem.* 95 (2003): 157-164.
- [50] Chen, J. L.; Zhuo, S. J.; Wu, Y. Q.; Fang, F.; Li, L.; Zhu, C. Q. High selective determination iron(II) by its enhancement effect on the fluorescence of pyrene-tetramethylpiperidinyI (TEMPO) as a spin fluorescence probe. *Spectroc. Acta Pt. A*. 63 (2006): 438-443.
- [51] Wang, S.; Gwon, S. Y.; Kim, S. H. A highly selective and sensitive colorimetric chemosensor for Fe^{2+} based on fluoran dye. *Spectroc. Acta Pt. A*. 76 (2010): 293-296.
- [52] Wu, P.; Li, Y.; Yan, X. P. CdTe quantum dots (QDs) based kinetic discrimination of Fe^{2+} and Fe^{3+} , and CdTe QDs-fenton hybrid system for sensitive photoluminescent detection of Fe^{2+} . *Anal. Chem.* 81 (2009): 6252-6257.
- [53] Gutsche, C. D.; Iqbal, M. *p-tert-Butylcalix[4]arene*. *Organic Syntheses, Coll.* 68 (1990): 234-236.
- [54] Gutsche, C. D.; Levine, J. A.; Sujeeth, P. K. Calixarenes. 17. Functionalized calixarenes: The claisen rearrangement route *J. Org. Chem.* 50 (1985): 5802-5806.
- [55] Pappalardo, S.; Giunta, L.; Foti, M.; Furguson, G.; Gallagher, J. F.; Kaitner, B. Functionalization of calix[4]arenes by alkylation with 2-(Chloromethyl)pyridine hydrochloride. *J. Org. Chem.* 57 (1992): 2611-2624.
- [56] Casnati, A.; Pochini, A.; Ungaro, R.; Ugozzoli, F.; Arnaud, F.; Fanni, S.; Schwing, M. J.; Egberink, R. J. M.; Jong, F. D.; Reinhoudt, D. N. Synthesis, complexation, and membrane transport studies of 1,3-alternate calix[4]arene-crown-6 conformers. *J. Am. Chem. Soc.* 117 (1995): 2767-2777.

- [57] Kim, S.; Kim, J. S.; Shon, O. J.; Lee, S. S.; Park, K. M.; Kang, S. O.; Ko, J. Metallic macrocycle with a 1,3-alternate calix[4]arene phosphorus ligand. *Inorg. Chem.* 43 (2004): 2906-2913.
- [58] Chawla, H. M.; Singh, S. P.; Upreti, S. A facile one-pot access to cone and 1,3-alternate conformers of calix[4]arene-bis(amido)crowns. *Tetrahedron.* 63 (2007): 5636-5642.
- [59] Zhi, Y. G.; Lai, S. W.; Chan, Q. K. W.; Law, Y. C.; Tong, G. S. M.; Che, C. M. Systematic studies on photoluminescence of oligo(arylene-ethynylene)s: Tunability of excited states and derivation as luminescent labeling probes for proteins. *Eur. J. Org. Chem.* (2006): 3125-3139.
- [60] Lavigne, J. J.; Broughton, D. L.; Wilson, J. N.; Erdogan, B.; Bunz, U. H. F. "Surfactochromic" conjugated polymers: surfactant effects on sugar-substituted PPEs. *Macromolecules.* 36 (2003): 7409-7412.
- [61] Attar, H. A. A.; Monkman, A. P. Effect of surfactant on water-soluble conjugated polymer used in biosensor. *J. Phys. Chem. B.* 111 (2007): 12418-12426.
- [62] Nakahara, Y.; Kida, T.; Nakatsuji, Y.; Akashi, M. New fluorescence method for the determination of the critical micelle concentration by photosensitive monoazacryptand derivatives. *Langmuir.* 21 (2005): 6688-6695.
- [63] Park, J. S.; Wilson, J. N.; Hardcastle, K. I.; Bunz, U. H. F.; Srinivasarao, M. Reduced fluorescence quenching of cyclodextrin-acetylene dye rotaxanes. *J. Am. Chem. Soc.* 128 (2006): 7714-7715.
- [64] Rashatasakhon, P.; Jaiyu, A.; Rojanathanes, R.; Muangsinn, N.; Chaichit, N.; Sukwattanasinitt, M. X-ray guided ¹H NMR analysis of pinched cone calix[4]arenes. *J. Mol. Struct.* 963 (2010): 22-26.

APPENDIX

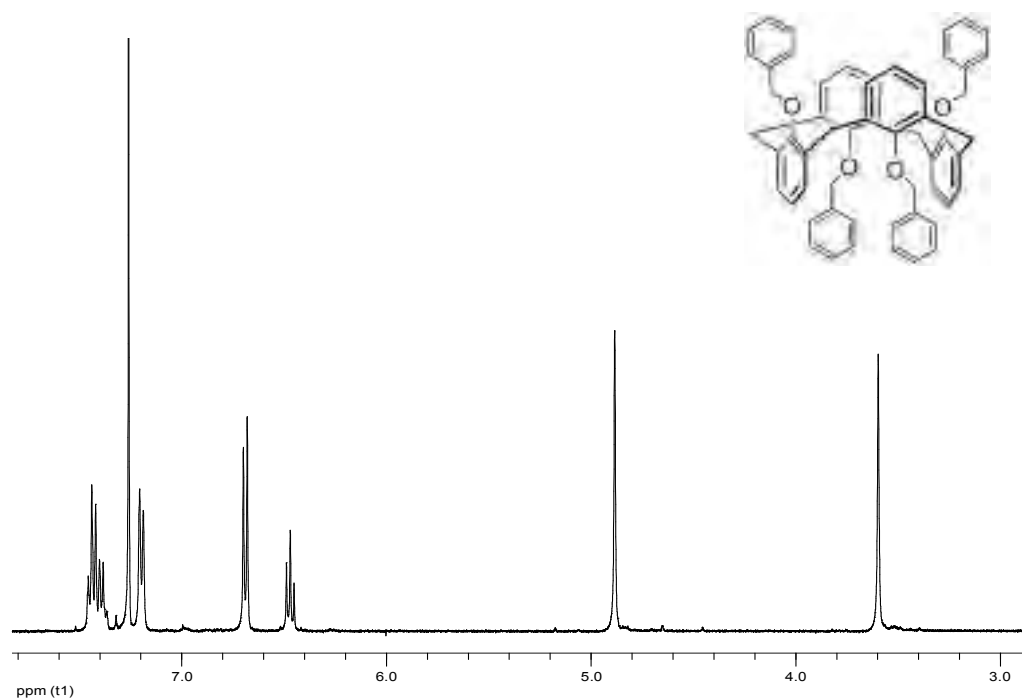


Figure A.1 ^1H NMR of 25,26,27,28-tetrabenzoyloxy-calix[4]arene.

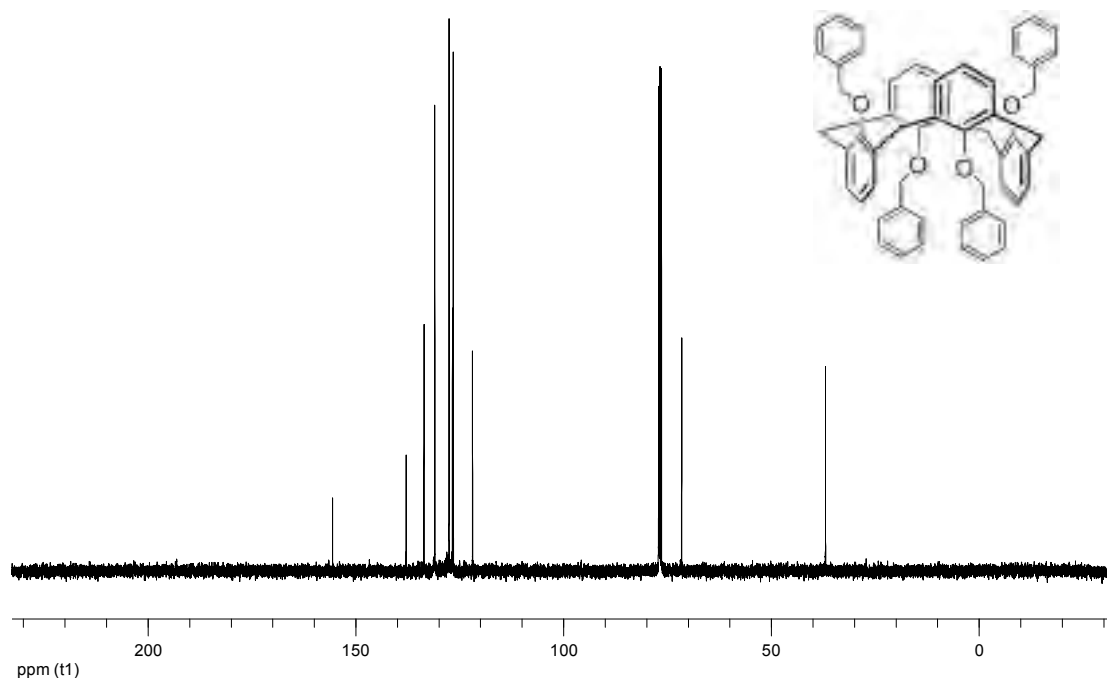


Figure A.2 ^{13}C NMR of 25,26,27,28-tetrabenzoyloxy-calix[4]arene.

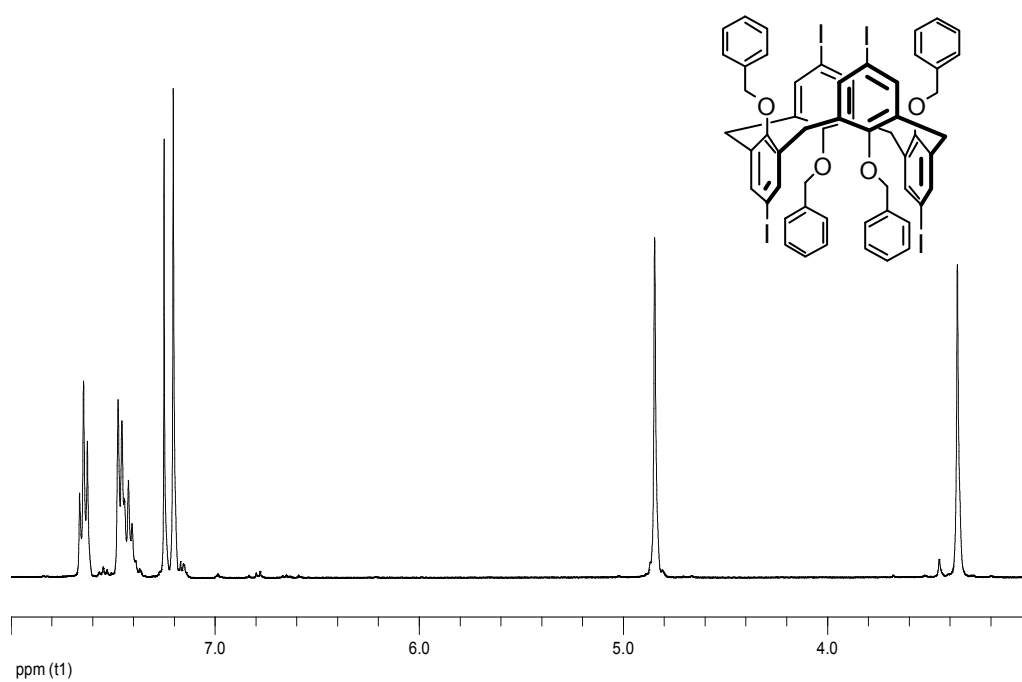


Figure A.3 ^1H NMR of 25,26,27,28-tetrabenzoyloxy-4-iodocalix[4]arene.

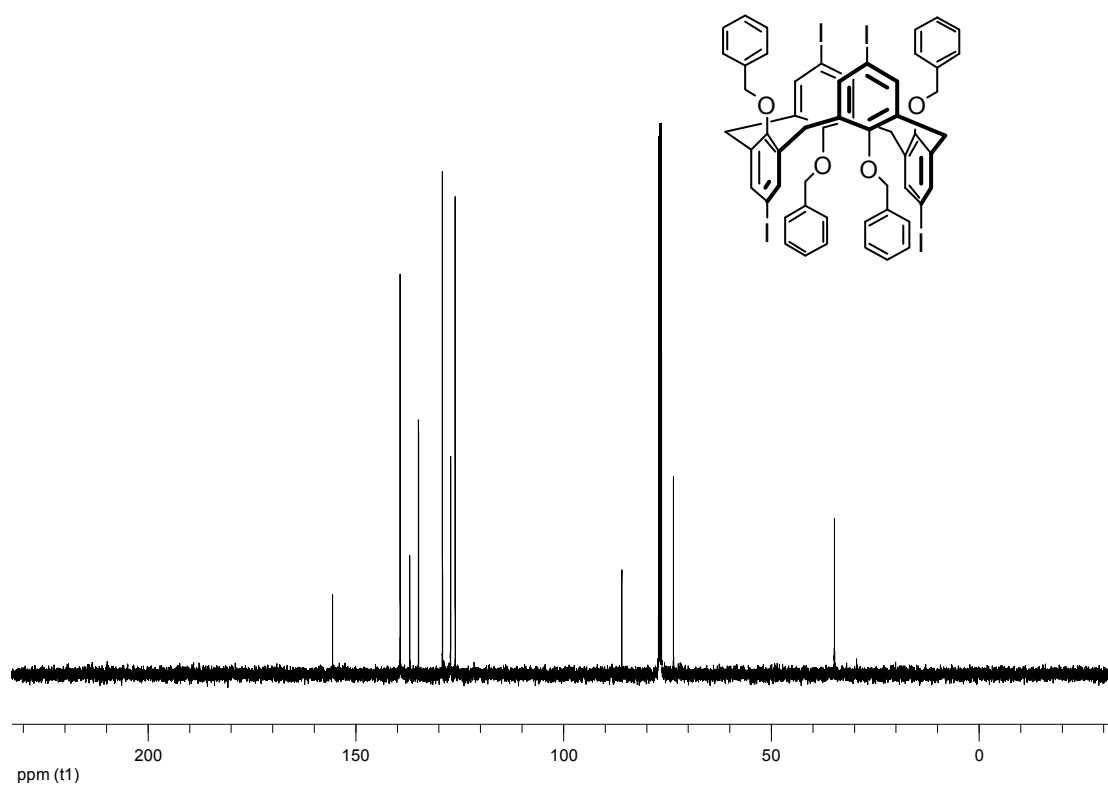


Figure A.4 ^{13}C NMR of 25,26,27,28-tetrabenzoyloxy-4-iodocalix[4]arene.

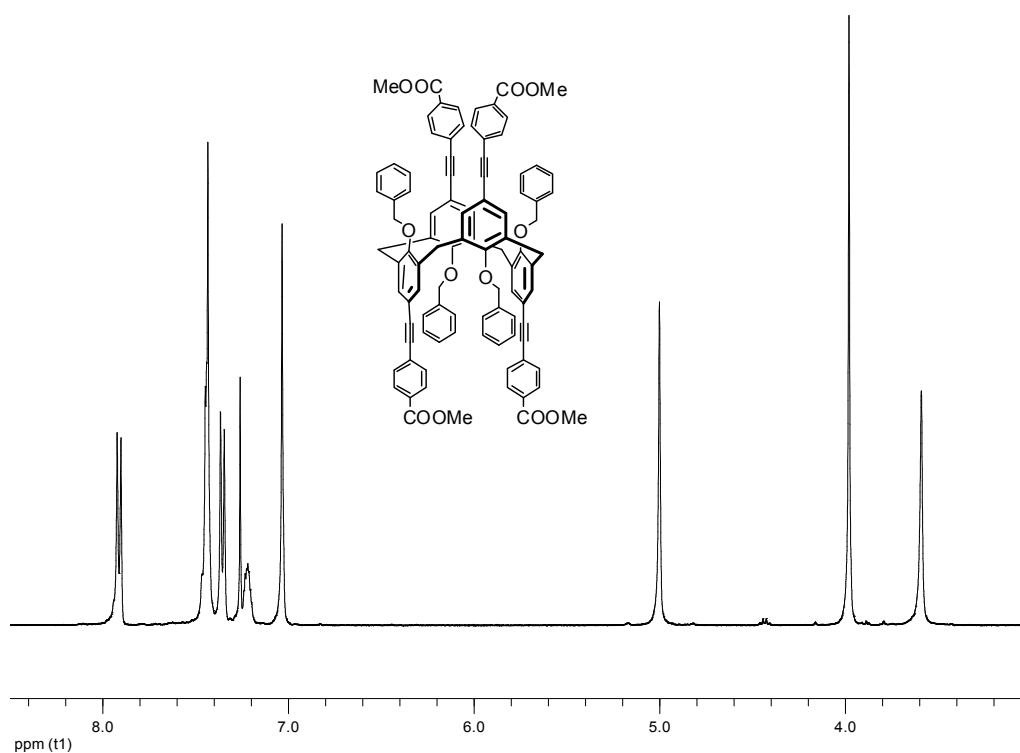


Figure A.5 ^1H NMR of 25,26,27,28-tetrabenzoyloxy-4-ethynylbenzoic methyl ester calix[4]arene.

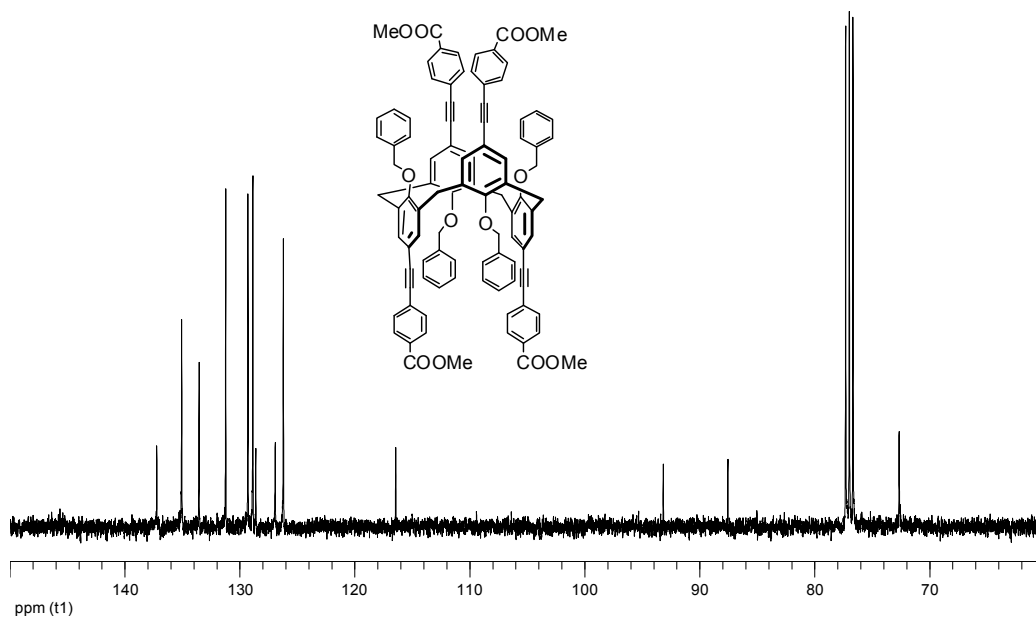


Figure A.6 ^{13}C NMR of 25,26,27,28-tetrabenzoyloxy-4-ethynylbenzoic methyl ester calix[4]arene.

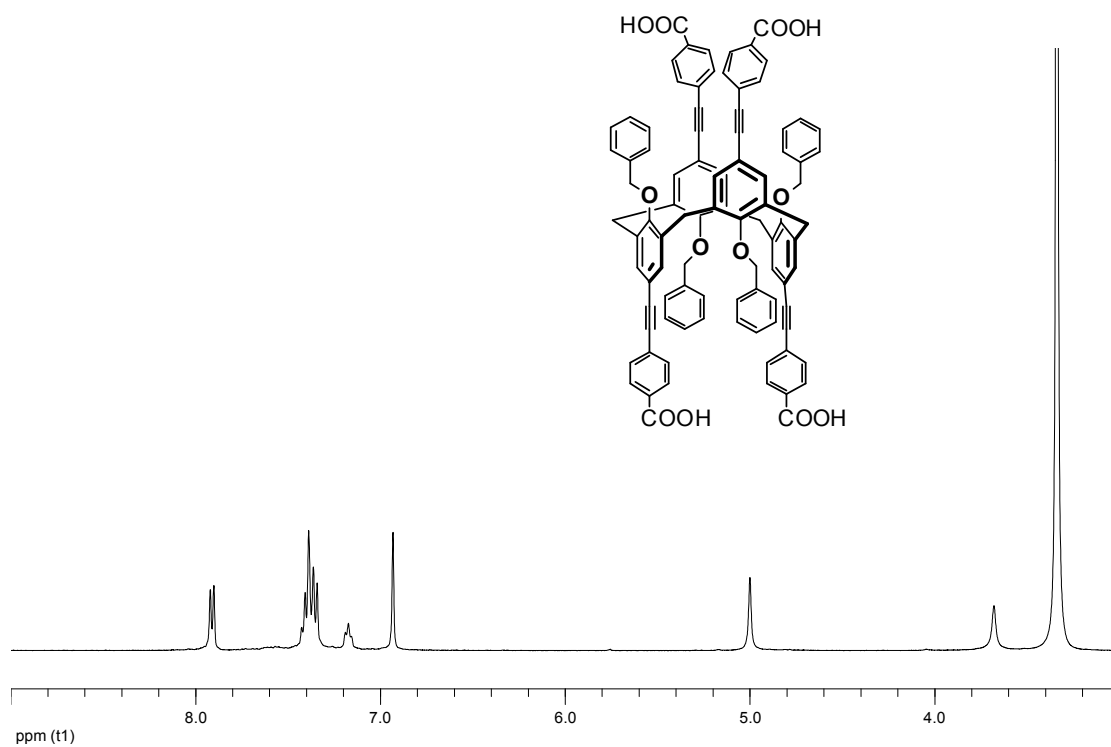


Figure A.7 ^1H NMR of 25,26,27,28-tetrabenzoyloxy-4-ethynylbenzoic acid calix[4]arene.

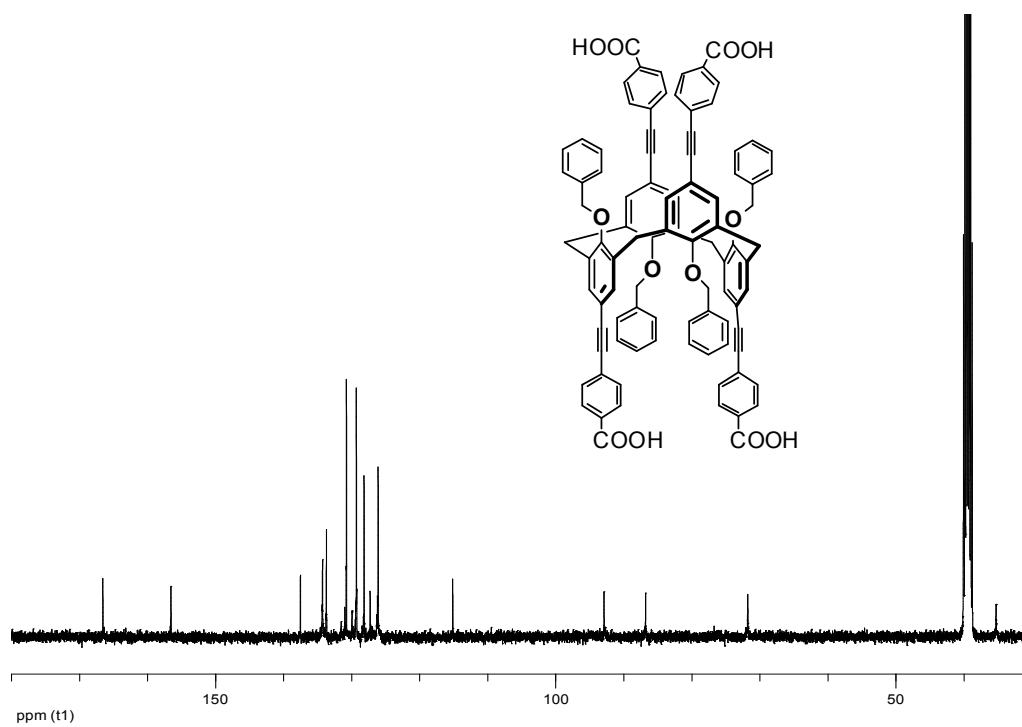


Figure A.8 ^{13}C NMR of 25,26,27,28-tetrabenzoyloxy-4-ethynylbenzoic acid calix[4]arene.

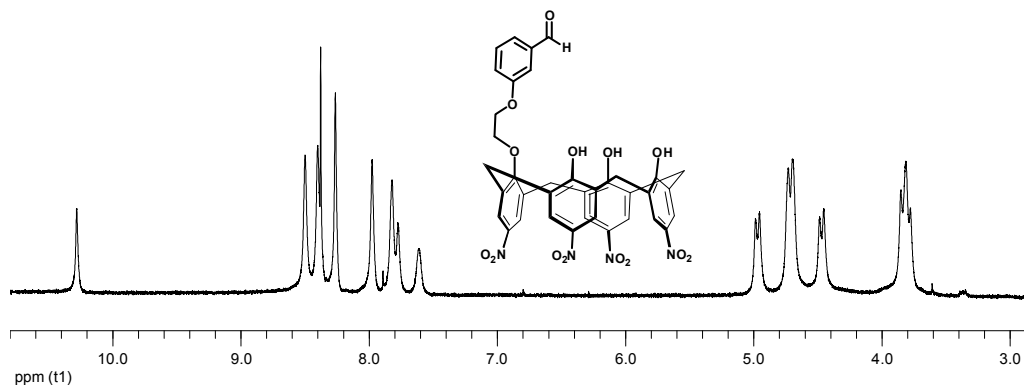


Figure A.9 ^1H NMR of *m*-bisbenzaldehyde-*p*-nitrocalix[4]arene.

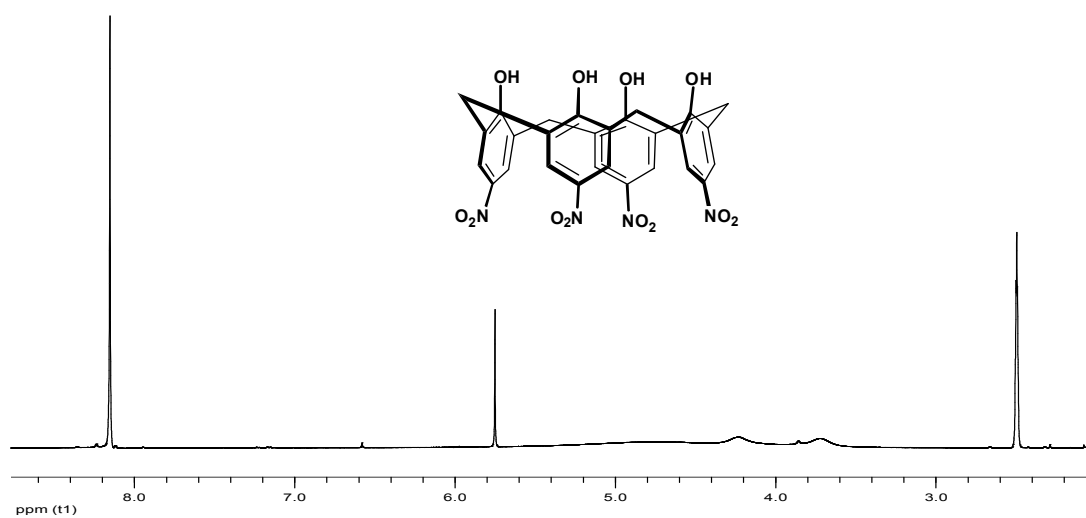


Figure A.10 ^1H NMR of *p*-nitrocalix[4]arene.

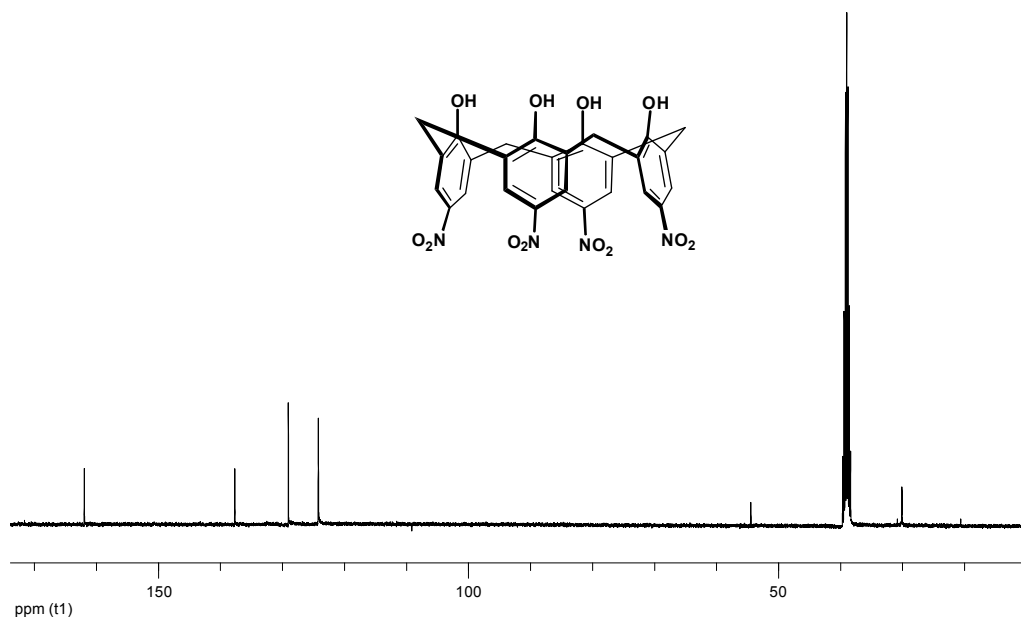


Figure A.11 ^{13}C NMR of *p*-nitrocalix[4]arene.

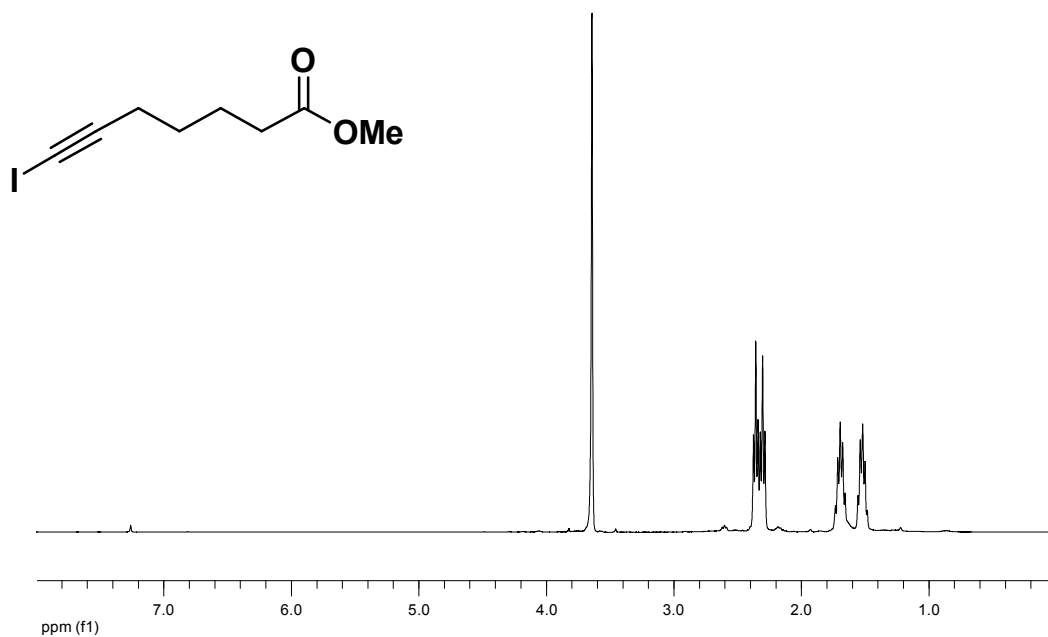


Figure A.12 ^1H NMR of methyl-6-iodoheptynoate.

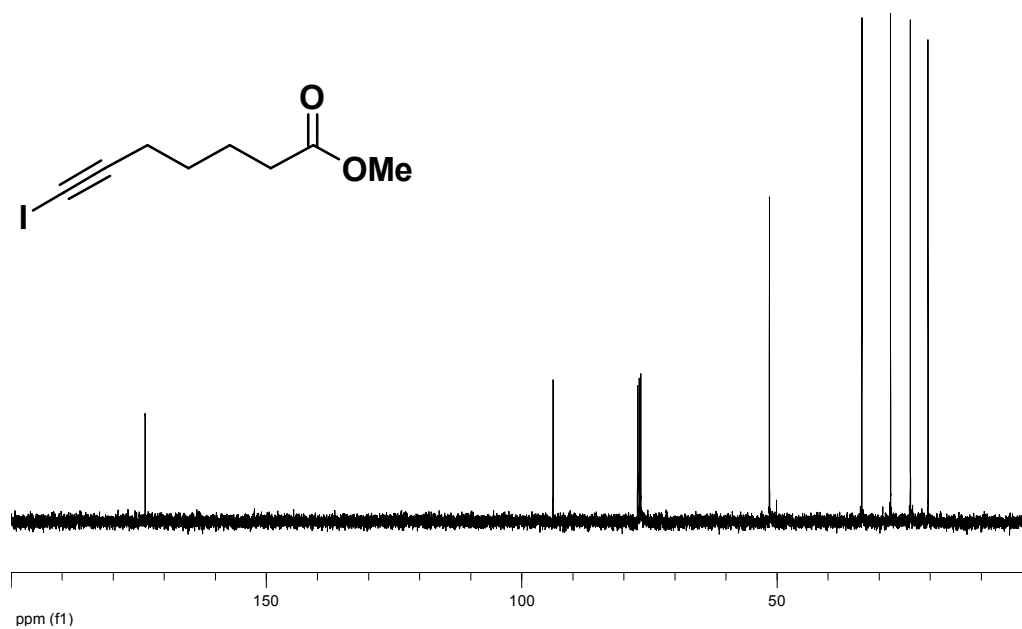


Figure A.13 ^{13}C NMR of methyl-6-iodoheptynoate.

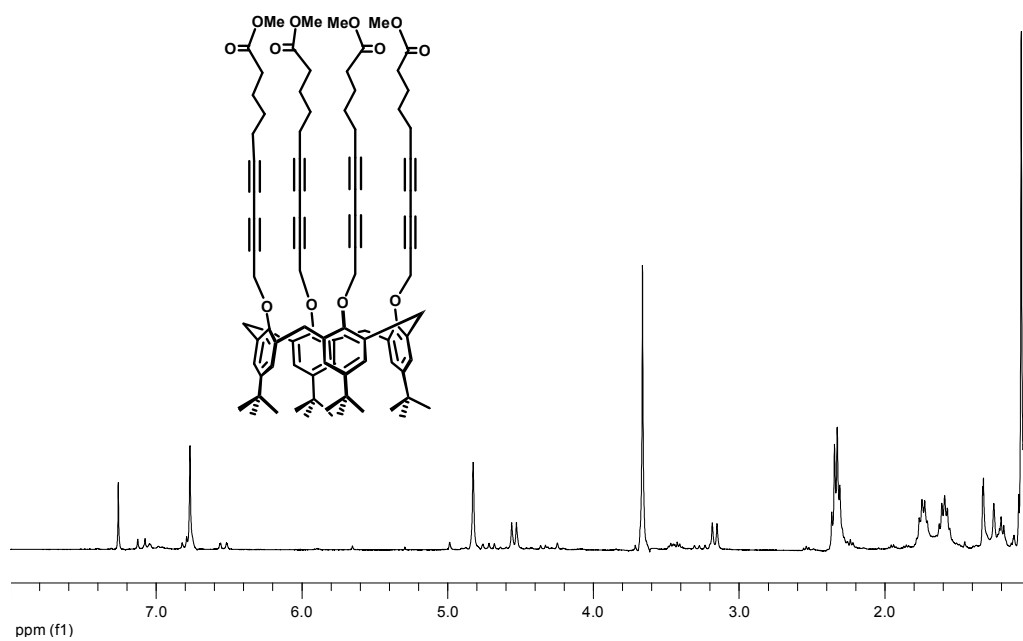


Figure A.14 ^1H NMR of 25,26,27,28-tetra(methylheptynoate)oxy-*tert*-calix[4]arene.

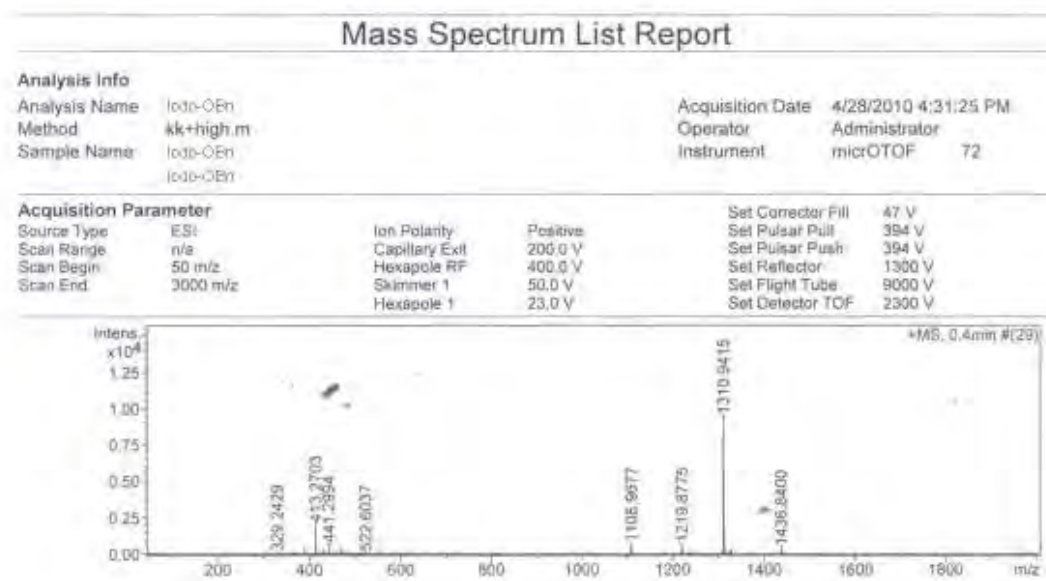


Figure A.15 Mass spectrum (ESI+) of 25,26,27,28-tetrabenzoyloxy-4-iodocalix[4]arene.

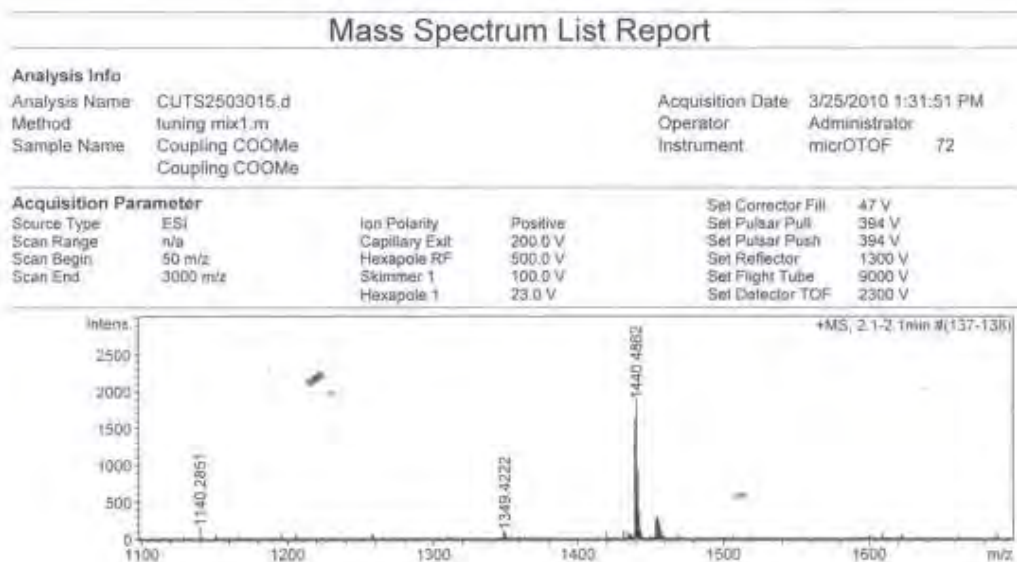


Figure A.16 Mass spectrum (ESI+) of 25,26,27,28-tetrabenzoyloxy-4-ethynylbenzoic methyl ester calix[4]arene.

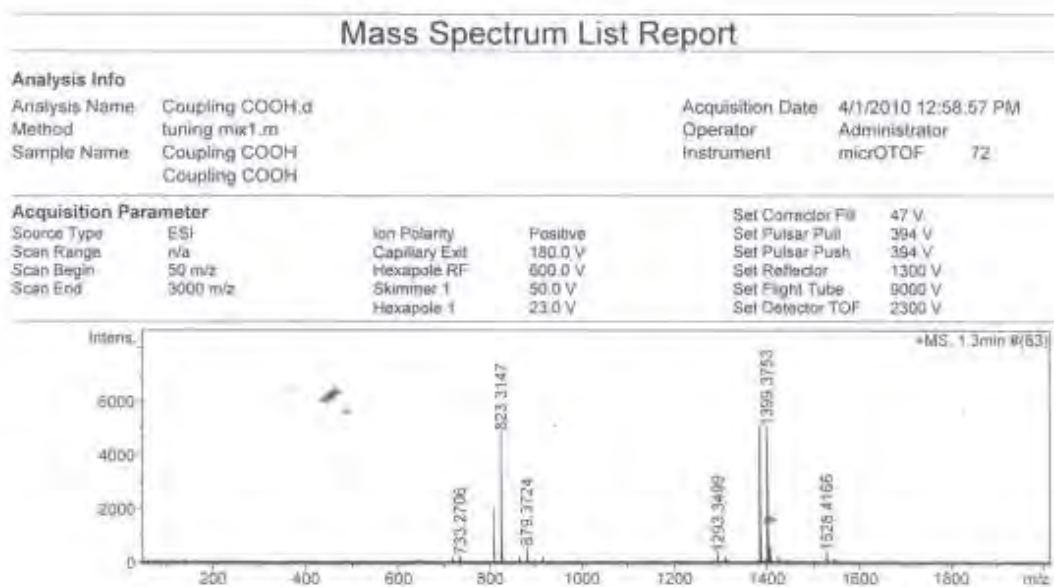


Figure A.17 Mass spectrum (ESI+) of 25,26,27,28-tetrabenzoyloxy-4-ethynylbenzoic acid calix[4]arene.

VITAE

Ms. Yamonporn Yodta was born on January 9th, 1984 in Bangkok, Thailand. She graduated with Bachelor Degree of Science, majoring in Chemistry from Chulalongkorn University in 2006. In 2007, she further received a Master Degree in Department of Chemistry. During the course of study, she received the scholarship from the TRF-Master Research Grants under Thailand Research Fund (TRF), ADB under the Petroleum & Petrochemical Technology Consortium and 90th anniversary of Chulalongkorn University Fund.

Her present address is 43/166 Pakkret Village, Bang Pood, Pakkret, Nonthaburi, Thailand 11120.